"THE ADIABATIC FLOW OF EVAPORATING FLUIDS IN PIPES".

A thesis submitted to the University
of Glasgow for the degree of Ph.D.

by

DAVID L. LINNING, B.Sc.

ProQuest LLC.
789 East Eisenhower Parkway
P.O. Box 1346
Ann Arbor, MI 48106 – 1346

CONTENTS LIST.

PART III. WATER EXPERIMENTS AND ANALYSIS.

Page Number.

.....

ACKNOWLEDGEMENTS.

The work described herein was carried out in the engineering laboratories of the Royal Technical College, Glasgow. In the early stages the work was supervised by Professor Kerr, Ph.D., and following his retiral, by Professor Thomson, D.Sc. For permission to use the facilities of the College laboratories and also for interest taken and advice given during the course of the work, acknowledgement is made to Professors Kerr and Thomson.

I further wish to record my indebtedness to Professor Scott, Ph.D., and to Mr. Laird, B.Sc., for much helpful advice and criticism.

Messrs. L. Sterne and Company Limited, Refrigerating Machinery Manufacturers, Glasgow, kindly supplied a refrigerator test unit.

I offer my sincere thanks to Mrs. William Davidson who so generously undertook the typing of the thesis.

ABSTRACT.

This thesis describes a theoretical and experimental investigation of the adiabatic flow of evaporating fluids in pipes. The theory is developed from the assumptions usually made in the subject of fluid flow, and is tested by experiments with water and also with freon 12.

From a review of previous papers relating to the subject two main points emerge.

(1) An evaporating fluid, depending on the conditions, may conform to any one of a variety of flow mechanisms.

(2) The liquid and vapour components may flow with different mean velocities.

Appropriate theory is developed for three flow forms which are known to occur and which probably cover the majority of practical cases. These modes of flow are characterised as (a) annular, (b) separated and (c) frothing.

In the first two forms relative motion between phases occurs, but in the last is prevented by a liquid network maintained by surface tension forces.

The theory for annular flow shows that the relative velocity factor (ratio of mean vapour to mean liquid velocity) is a function of the thermodynamic properties of the fluid and also of the interface velocity ratio (ratio of mean velocity at interface to mean liquid velocity). This latter is the only empirical quantity influencing the relative velocity factor; its value must be near to, but not less than unity.

In separated flow the relative velocity factor is also affected by the wall shearing force acting on the vapour phase.

Since there is no relative motion between phases with frothing flow, standard thermodynamic theory is applicable provided surface energy may be neglected.

Critical outlet conditions readily occur with evaporating flow because of the high rates of volume increase with pressure drop. The equations which express the relative velocity factor throughout an expansion also provide the criterion for the prediction of critical outlet conditions. For annular and separated flows these are identical.

Critical pressure ratios for frothing flow are much smaller than for a corresponding flow with relative motion.

Critical outlet temperature and pressure charts for water and for freon 12 have been prepared and are given in the text.

The main water tests were made on a tube of 0.1285" bore, a few preliminary tests being carried out on a tube of .060" bore. By measuring fluid momentum at the tube outlet an experimental determination was obtained of the relative velocity factor. Temperature and pressure measurements were made throughout the expansion and the technique adopted for these are fully described. Visual evidence of the flow form was obtained by photographing the fluid as it left the tube.

Both observation and analysis confirm that the flow form adopted by the evaporating water is of the annular type.

The theoretical and measured values of relative velocity factors and critical outlet conditions are in good agreement. Experimental data on critical outlet conditions obtained previously by Burnell on pipes of $\frac{1}{8}$" to $1\frac{1}{8}$" bore, also show agreement with the theory.

Friction factors associated with the annular flow of evaporating water were investigated and a method of correlation is proposed. The wall shearing force is found to be a function of liquid velocity and density, the friction factor being dependent on a Reynold's number.

The freon 12 experiments were carried out on a small refrigerator test unit of a standard type, tests being made on tubes of .042" and .060" bore. Precautions were taken to prevent frosting on the capillary tube.

Critical outlet data showed conclusively that the flow form in this case was of the frothing type. This had been assumed by some previous investigators but had never been proved.

The fact that freon 12 adopts the frothing flow form is consistent with the general theoretical development.

The question of friction factors for frothing flow is discussed but no attempt at a complete investigation could be made because of the extensive nature of the experimental work required.

The factors affecting the occurrence of the various flow mechanisms are given qualitative discussion.

LIST OF SYMBOLS.

A	Cross-sectional area of pipe	ft^2.
a	Cross-sectional area of a phase	ft^2.
B	$= \frac{W}{A}(1 - q)\upsilon_1$	ft/sec.
c	$= \frac{q}{1 - q} \frac{\upsilon_2}{\upsilon_1}$	
D	Diameter of pipe	ft.
E	Internal Energy	BTU/lb.
F_w	Wall shear force	lb.
F_p	Interface shear force	lb.
g	Gravitational acceleration	ft/sec^2.
h	Total heat of liquid	BTU/lb.
H	Total heat of vapour	BTU/lb.
J	Mechanical Equivalent of Heat	
k	Relative velocity factor (V_2/V_1)	
L	Latent heat of evaporation	BTU/lb.
M	Fluid momentum passing a section per unit time	lb.
n	Interface velocity ratio (V_p/V_1)	
p	Pressure	lb/ft^2.
q	Quality of mixture (based on rate of flow past a section)	
T	Temperature	^oF.
V	Velocity	ft/sec.
V_p	Interface velocity	ft/sec.
υ	Specific volume	ft^3/lb.

W	Weight rate of flow	lb/sec.
x	Distance	ft.
τ_o	Wall shearing force per unit area	lb/ft^2.
λ	Stanton friction factor	
μ	Viscosity	$lb.sec/ft^2$.
ϕ	Entropy	$BTU/^oF.lb$.

Subscripts.

1. Refers to liquid at saturated condition.
2. Refers to vapour at saturated condition.
c. Refers to conditions at commencement of evaporation.
o. Refers to conditions at tube outlet.
s. Refers to expansion at saturated condition.

.....

INTRODUCTION.

The present investigation was initiated with the intention of making an examination of the flow of refrigerant fluids through a "capillary tube restrictor". This device is simply a length of small bore copper tubing used for the purpose of metering refrigerant from the high to the low pressure side of a refrigerator. Its advantages in terms of economy and reliability have made its application universal in the modern mass-produced hermetic refrigerator unit.

Figure 1, is a diagrammatic arrangement of the usual set-up of this kind. The capillary tube is in metallic contact with the suction line over a length of four feet or more, the purpose of this being to increase the capacity of the unit. The unattached length of tubing is always at the low-pressure end. Thus, the refrigerant in a balanced circuit enters the capillary tube as a liquid, is cooled externally by the suction vapour returning to the compressor, and commences to evaporate at the point where the fluid pressure becomes equal to the liquid saturation pressure. The subsequent evaporating flow is almost adiabatic, a small amount of heat being supplied from the atmosphere. Figure 2, shows typical pressure and temperature variations of the refrigerant as it flows through a capillary tube restrictor in an actual unit.

From this brief description it is clear that the essential problem consisted of finding or developing an appropriate theory of evaporating fluid flow in uniform pipes

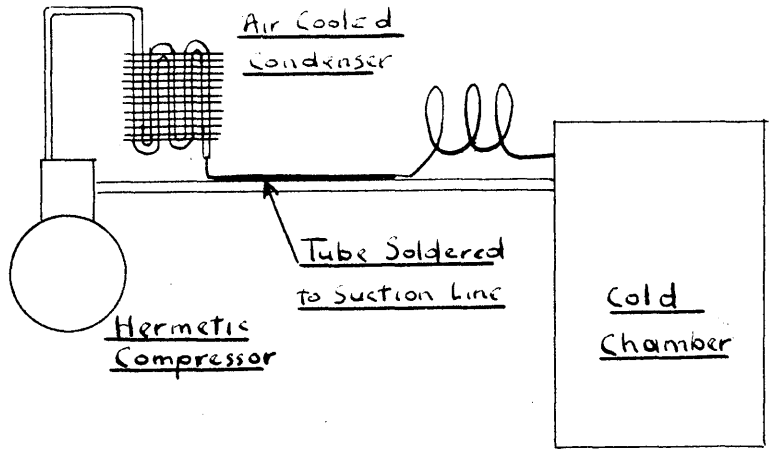

FIGURE 1 Diagrammatic sketch of typical unit employing the capillary tube restrictor

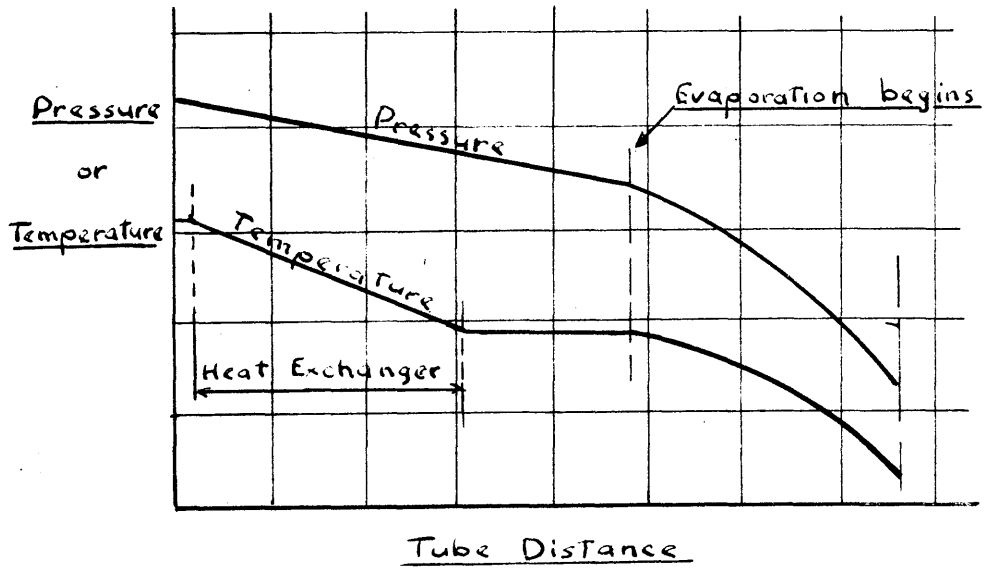

FIGURE 2 Typical pressure and temperature variations in a capillary tube restrictor

and verifying this by suitable experiment.

A general survey of the literature relevant to evaporating fluid flow in pipes revealed that, despite the occurrence of the phenomenon in many fields of engineering, approaches to the problem had hitherto been of an empirical nature and usually of a type appropriate to some particular problem of interest to the individual investigator. This was particularly so in the case of the capillary tube restrictor.

It was decided as a consequence that the present need was for a more fundamental approach and that little purpose could be served by adding to the already excellent empirical data on the subject of capillary tubes. By extending the scope of the investigation to include theory and experiments relevant to the flow through pipes of evaporating fluids in general not only would the value of the work be enhanced, but the problem would be rendered more approachable in that experiments could be designed to suit fundamental requirements rather than to overcome difficulties peculiar to refrigeration units.

The scope of the investigation is therefore adequately described by the title of the thesis as "The Adiabatic Flow of Evaporating Fluids in Pipes".

Whilst the more general non-adiabatic type of flow is of greater practical importance, it was only by limiting the investigation to the adiabatic case that problem could be kept within manageable limits.

PART I.

REVIEW OF PREVIOUS WORK.

REVIEW OF PREVIOUS WORK.

The papers reviewed are divided into three groups

(1) On the capillary tube-restrictor.

(2) On the evaporating flow of water.

(3) On the co-current flow of gas-liquid mixtures.

Subsequent sections of this thesis are relatively independent of existing literature on the subject because of differing methods of approach favoured by previous investigators. A survey of the present sources of knowledge is nevertheless a necessary preliminary to further discussion and it was decided that this object could best be served by summarising all relevant papers in chronological order, rather than by presenting a selective review.

GROUP I. ON THE CAPILLARY TUBE RESTRICTOR.

"Theory and Use of a Capillary Tube for Liquid Refrigerant Control", by L.A. Staebler. (Refrigerating Engineering, January 1948.)

From the point of view of the refrigerator designer this paper is perhaps the most suitable. It provides a lucid description of the aims and technique of design together with useful empirical data relating tube bore and length to compressor horse-power, and condensing and evaporating temperatures. It also emphasises that this data is for guidance only and that each new design must be submitted to extensive practical testing before being accepted as satisfactory. Nothing that has since been published alters this important conclusion. Indeed, the variability of oil circulation and heat exchange with different units under varying conditions makes it seem likely that this will always be so no matter how much detailed information becomes available in the future.

The theory provided is entirely qualitative, dealing in trends rather than in mathematical relationships.

Staebler introduces the idea of the capacity balance characteristic. The restrictor is a non-adjustable metering device and as a consequence condensing and evaporating temperatures are uniquely related for a given unit operating at its fixed speed and containing a specific charge. The characteristic is the curve relating these temperatures. It is obtained

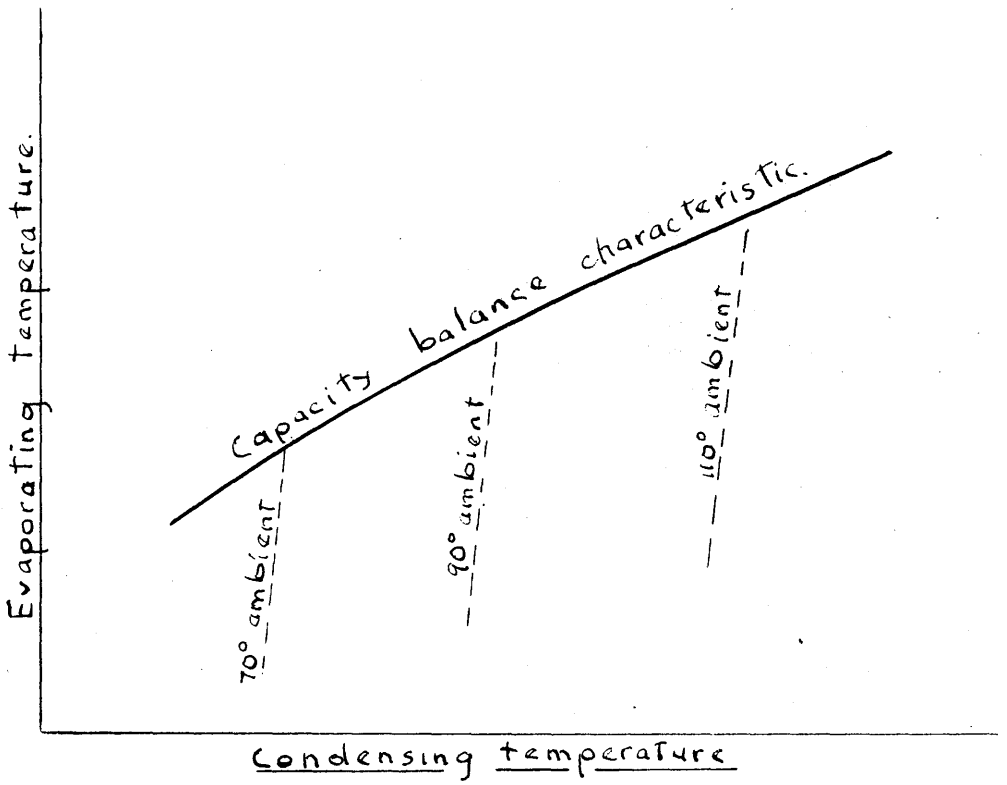

Operation below capacity balance characteristic results in a mixture of liquid and vapour entering the capillary tube.

FIGURE 3. Capacity balance characteristic for a capillary tube refrigerator unit. (ref: L.A. Staebler[10])

experimentally. Figure 3, shows a typical capacity balance characteristic.

"Application and Characteristics of Capillary Tubes", by H. F. Lathrop. (Refrigerating Engineering, August, 1948.)

Lathrop goes over again some of the ground covered by Staebler, devoting a considerable part of his article to explaining in simple terms the purpose and operation of the restrictor.

He introduces the idea of obtaining a characteristic curve for a given unit by plotting compressor circulation capacity and tube circulation capacity to the same base; in his case, suction pressure. The intersection of corresponding lines provides balance points.

As an aid to adjustment of capillary tube length and bore Lathrop proposes the following relationships. If D, L, ΔP represent tube length, bore and overall pressure drop, then mass flow varies as D^3, $(1/L)^{\frac{2}{3}}$, $(\Delta P)^{\frac{2}{3}}$. These relationships are very rough. Lathrop emphasizes the important and at the same time unpredictable effects of heat exchange on circulation rate. The difficulty lies in the estimation of the heat exchange quantity.

"Theory and Use of the Capillary Tube Expansion Device", by M. M. Bolstad and R. C. Jordan. (Refrigerating Engineering, December 1948 and June 1949.)

This paper appeared in two parts. The authors developed standard thermodynamic theory in the first part and applied it to provide a method of calculating tube length and bore for a required set of conditions. Their method is, in effect, that proposed by Fanno in 1904 for compressible fluids flowing in pipes of uniform bore.

Bolstad and Jordan draw attention to the experimentally determined fact that mass circulation in a refrigerator unit employing a restrictor is almost independent of evaporator pressure except in so far as it affects the heat exchange rate between the capillary tube and the suction line. They also found experimentally that using an oil separator in their experimental unit resulted in a reduction in the measured mass circulation.

The second part of this paper showed a marked change in the policy of its authors in that the theoretical approach was discarded as being of little practical value and an empirical approach proposed in its stead.

This empirical approach was based on the idea that the mass flow of freon 12 through a particular capillary tube could be expressed as a function only of inlet pressure and initial evaporator temperature, referred to by them as the bubble point temperature. On this basis they presented a series of graphs

of which Figure 4 is an example, providing guidance to the designers of capillary tube restrictors.

Bolstad and Jordan fail to make it clear that their empirical rationalisation is dependent on their experimental observation that mass flow is largely independent of evaporator pressure. They note that the method is also dependent on the fact that variation in liquid viscosity, and hence in friction factor, over the temperature range encountered, is small.

The chief reasons adduced by these authors for discarding the theoretical approach were tediousness and inaccuracy, the latter resulting from the fact that entropy values quoted in tables are only given to five figures.

It is not desired to go into detail which is irrelevant to the main theme of this report but it is noted that both of these defects could have been alleviated by the construction of a pressure-enthalpy chart with constant entropy lines. The construction of such a chart for the wet field is relatively simple because of the unique relationship between temperature and pressure.

This development would not, of course, have rendered Staebler's conclusion on the necessity for practical testing invalid, a conclusion which is re-iterated by Bolstad and Jordan.

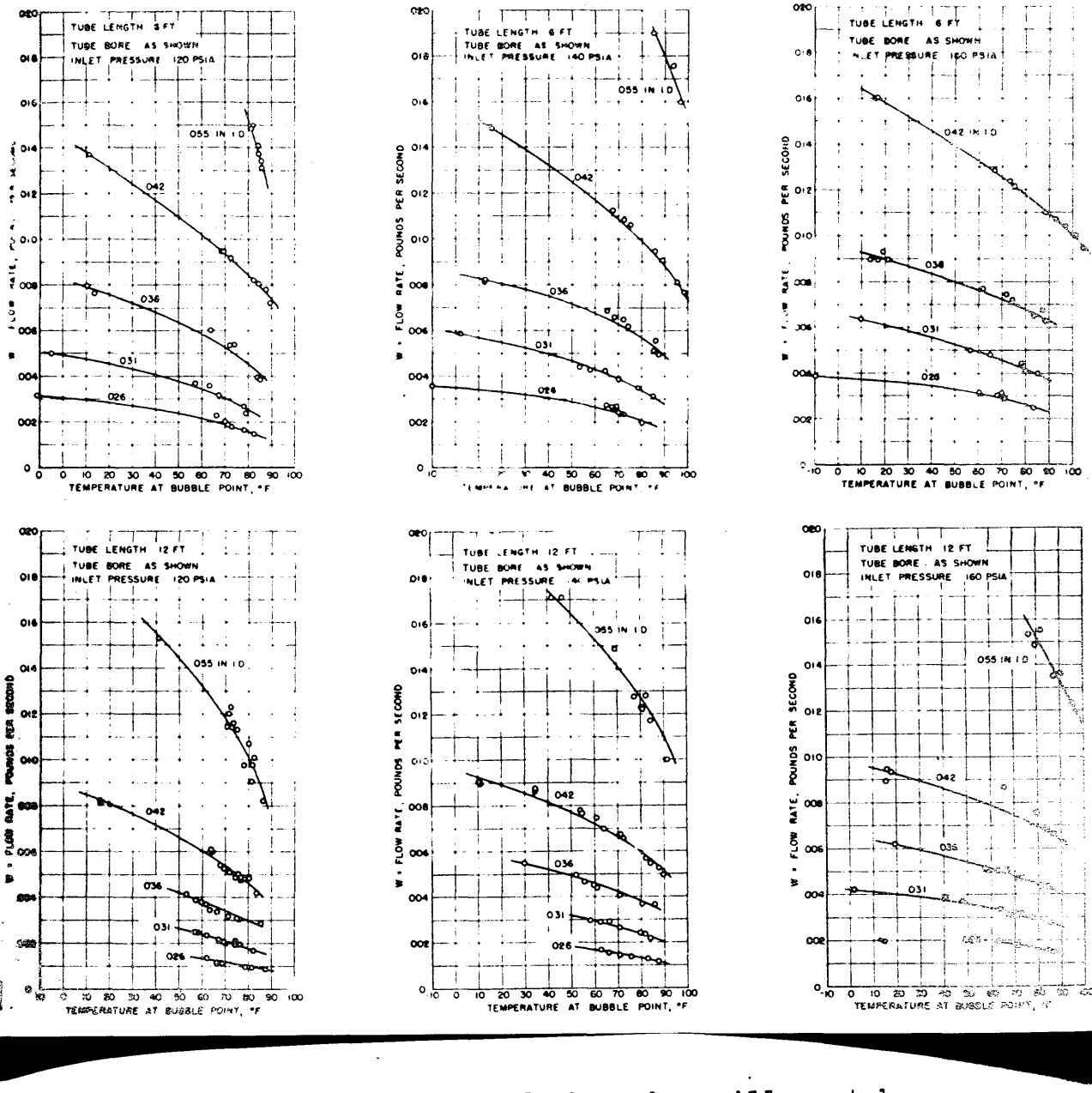

Figure 4. Flow rates of freon 12 through capillary tubes for various conditions. (Reference: Bolstad and Jordan[1]).

"Pressure Drop and Change of Phase in a Capillary Tube", by G. F. Marcy. (Refrigerating Engineering, January 1949.)

Marcy proposes a method of calculating pressure drop during evaporating flow through a capillary tube which is based on the Standard Fanning equation. Friction factors are based on a Reynold's number, the viscosity quantity being that appropriate to the liquid phase. His justification for this is the correlation of a set of four results, two on freon 12, and two on sulphur dioxide.

He ignores the effects of fluid momentum variation during expansion, thereby rendering his paper meaningless.

"Capillary Tubes: A Guide to Their Application on Freon 12 Hermetic Condensing Units", by L. A. Stabler. (Refrigerating Engineering, January, 1950.

This paper is a condensed re-statement of Stabler's earlier paper published in Refrigerating Engineering, January 1948. It was published as a contribution to a series of papers on the design of refrigerators under the general title of "Application Data".

An important criticism of all of the foregoing papers is that none took note of the important and fundamental question of the flow form adopted by the fluid during two phase flow. In the papers proposing some form of relationship between variables it was assumed without question that vapour and liquid flowed with a common velocity at all stages in the expansion.

It will be shown in a later section that this happens to be the case for freon 12 but it will also be shown that this is not a supposition which could be accepted without experimental proof.

GROUP II. ON THE FLOW OF EVAPORATING WATER.

"The Flow of Boiling Water Through Orifices and Pipes" by W.T. Bottomley. (N.E.C. Inst. of E. & S. Vol. LIII 1936-7).

The greater part of Bottomley's paper is concerned with flow through orifices. He shows that in this case the water can exist in the liquid state in a meta-stable condition during expansion through the orifice, thereby allowing a much greater mass flow than predicted by Thermodynamic theory.

In contrast to this he finds that the flow of evaporating water through pipes is in accord with standard theory and the assumption of thermodynamic stability.

His experimental data was obtained by measuring the pressure distribution along a 100 feet length of pipe in Barking B Power Station. The mass flow was 260 lbs/ft.^{2}sec initial pressure 38 lbs/in ^{2}abs and outlet pressure 22 lbs/in ^{2} abs. Using a value for friction factor of .012 he finds that the predicted pressure distribution is in close accord with measured values. The low value friction factor was attributed to the high velocity of flow.

He also draws attention to the existence of a critical outlet pressure at the tube exit and finds that here again experimental data are in accord with standard theory.

These considerations lead Bottomley to assume that the liquid and vapour components of the water flow with a common velocity during expansion in a pipe, and that the fluid is in

thermodynamic equilibrium at all stages.

"Flow of Boiling Water Through Nozzles, Orifices, and Pipes", by J. G. Burnell. (Engineering, December 1947.)

Burnell carried out experiments on the flow of boiling water through nozzles, orifices, pipes and also on nozzles and pipes in series. He re-covered much of Bottomley's work on nozzles and orifices and substantiated his results in this respect.

His experiments on the flow of evaporating water through pipes, however, showed marked divergence from those of Bottomley. Experiments on pipes of diameters .529", .904" and 1.5" revealed that measured critical outlet pressures were very much below those predicted by standard theory based on the assumption of a common liquid-vapour velocity. On the same basis, an assumed friction factor of .018 lead to predicted mass flows very much lower than those obtained experimentally.

To account for this important discrepancy Burnell suggested that the liquid flowed with a smaller velocity than the vapour.

"The Discharge of Saturated Water Through Nozzles", by R.S. Silver and J.A. Mitchell. (Trans N.E.C. Inst. of E. & S. Vol. LXII, Dec. 1945.)

Silver and Mitchell carried out experiments on the flow of evaporating water through convergent-parallel nozzles, finding that the measured mass flow was much in excess of that predicted by standard thermodynamic theory. They attributed this to delayed evaporation and proposed a quantitative theory based on the idea that this delay was due to the finite time required for heat flow within the fluid. In constructing the theory they assumed that the liquid flowed in a central core and the vapour in the remaining annular area, the liquid and vapour having a common velocity.

Experiment showed that critical outlet pressure was dependent to some extent on the back pressure. In one test, reduction of the back pressure from 25 to 0 lbs/in^2 guage resulted in a reduction of the critical outlet pressure from 25.5 to 20.5 lbs/in^2 guage. This feature was attributed by Silver and Mitchell to increased heat loss to the environment.

"The Circulation of Water and Steam in Water Tube Boilers, and the Rational Simplification of Boiler Design", by W. T. Lewis and S.A. Robertson. (Proc., I. Mech. E. Vol. CXLIII, 1940).

This paper covers a wide field, its chief interest to the present purpose being a description of the flow mechanism as water, flowing upwards in a heated vertical tube, evaporates. This description is based on the experimental work of Barbet; Brooks and Badger; Boarts, Badger and Meisenburg; Stroebe, Baker, and Badger; Lewis and Robertson. Figure 5, which is copied from the paper being reviewed, shows diagrammatically the changes taking place.

Evaporation commences with the formation of a large number of small bubbles which subsequently coalesce to cause slugs of alternate steam and water. These soon break up to form an inner core of steam and an outer annulus of liquid, the latter travelling more slowly than the steam core. Finally the thin film of liquid on the tube wall disperses and the fluid flows as a decreasingly wet mixture until it eventually becomes superheated. The length of the tube occupied by the different stages depends on the intensity of heating and on the rate of water supply to the tube.

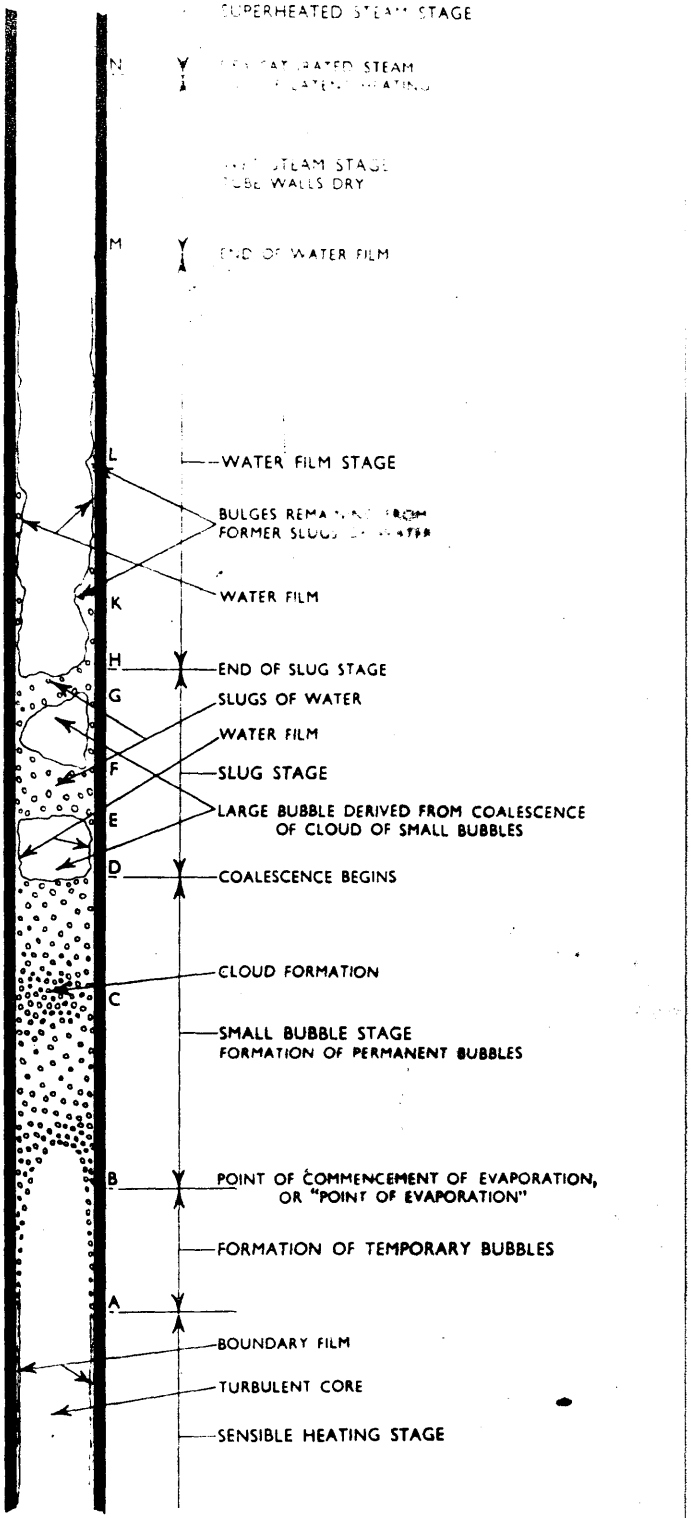

Fig. 3. Change from Water to Steam in a Vertical Tube

The vertical scale is much smaller than the horizontal scale.

Figure 5. Change from water to steam in a heated vertical tube. (Reference: Lewis and Robertson[6]).

GROUP III. ON THE FLOW OF GAS - LIQUID MIXTURES IN PIPES.

"Isothermal Pressure Drop for Two-Phase Two-Component Flow in a Horizontal Pipe", by R. C. Martinelli, L. M. K. Boelter, T. H. M. Taylor, E. G. Thomsen and E. H. Morrin. (Trans. A.S.M.E. Vol. LXVI, 1944.)

This paper reports measurements of the static pressure drop accompanying the two-component flow of air and a variety of liquids, including water, benzene and oil. The experiments were carried out on a $\frac{1}{2}$" galvanized iron pipe and in a 1" glass pipe, flow conditions varying from 100% air to 100% liquid. In addition, flow patterns existing at various flow rates were studied visually and an empirical analysis, based on various non-dimensional parameters, was presented. The subject is very complex and the analysis correspondingly approximate. Their extensive experimental data shows a correlation of $\pm$ 30% with predicted values.

Figure 6, a reflex of a figure given in the paper being reviewed, shows the flow patterns observed in air-water flow under varying conditions. The patterns are divided into two groups corresponding to turbulent and viscous liquid flow respectively. The air flow was stated to be turbulent in all cases although this would appear to be misleading in respect to bubbling flow. Table 1, quoted from the paper in question, provides qualitative information relative to the occurrence of the various flow forms. These forms can be listed under the

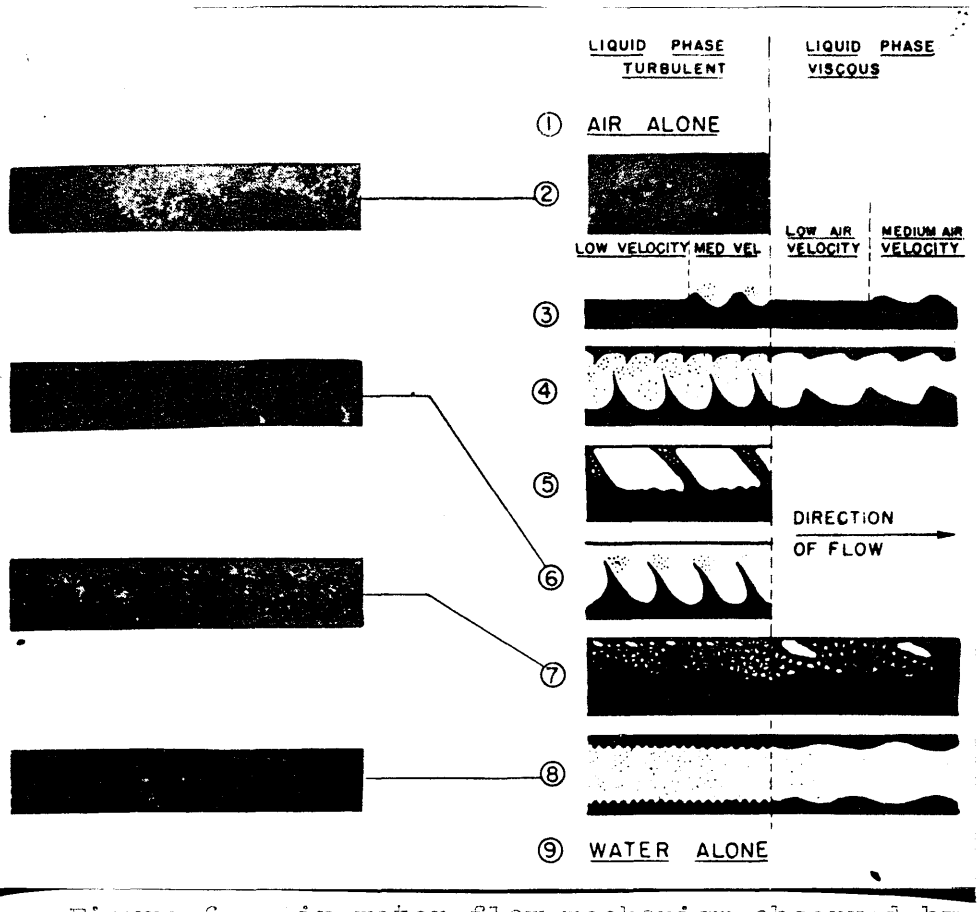

Figure 6. Air-water flow mechanism observed by Martinelli and co-workers.[8]

	Low Air Rate		Medium Air Rate		High Air Rate	
	Liquid Turbulent	Liquid Viscous	Liquid Turbulent	Liquid Viscous	Liquid Turbulent	Liquid Viscous
Very low liquid rate	3	3	3	3	8	8
Low liquid rate	5	3	6	3	8	8
Medium liquid rate	7	7	4	4	4	4
High liquid rate	2		2		2	

Table 1. Observations on flow mechanisms for air-water mixtures Martinelli and co-workers.

self-explanatory titles of frothing, bubbling, separated and annular. It is not clear from the Authors' description whether type 4 would best be described as annular or separated.

"Co-current Gas - Liquid Flow". (Published by A.S.M.E. for Heat Transfer and Fluid Mechanics Institute 1949.)

1. "Flow in Horizontal Tubes", by O. P. Bergelin and C. Gazley.

This paper continues the examination of the gas-liquid flow problem on the lines developed by Martnelli and his co-workers, concentrating attention on, what is termed, the 'stratified' flow form. Stratified flow is described as a flow in which the vapour occupies an upper segmental area in the tube and is separated from the liquid by a smooth interface.

They show that Martnelli's empirical analysis requires modification to render it applicable in this instance.

The various types of flow are re-examined visually and some relevant quantitative data given in a chart which is reproduced here in figure 7. The following description of the possible flow mechanisms is quoted.

"If one introduces increasing amounts of gas to a pipe flowing full of liquid, the following types of flow successively occur (a) bubbling flow in which the gas flows along the top of the pipe in the form of bubbles (b) stratified flow in which the liquid flows along the bottom of the pipe with a smooth

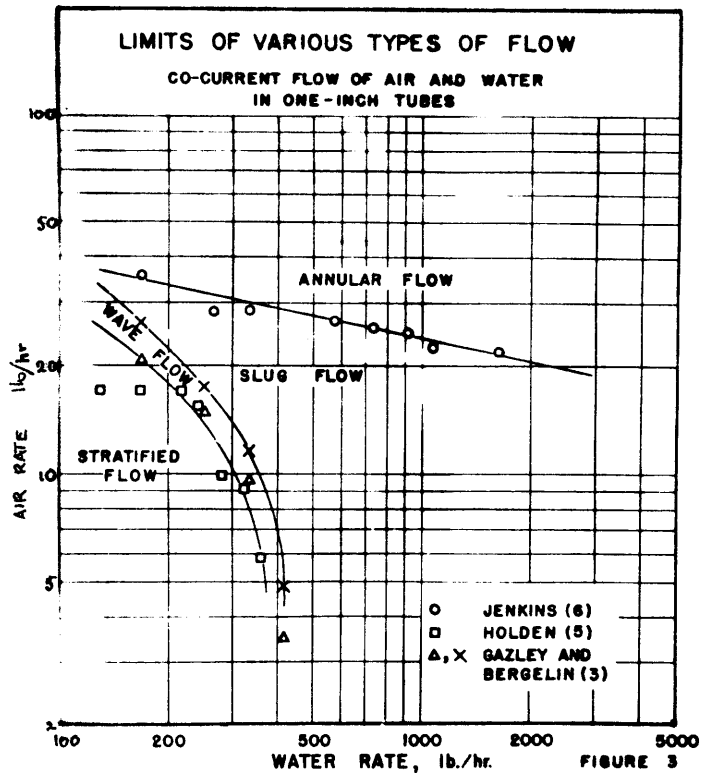

Figure 7. Co-current flow of air and water in a horizontal one-inch tube. (Reference: Bergelin and Gazley[12])

surface and the gas flows above (c) wave flow which is similar to stratified flow except that the interface is disturbed by waves (d) slugging flow in which occasional frothy slugs pass rapidly through the pipe; and (e) annular flow in which the liquid flows along the pipe wall while the gas flows through a central core. At very low liquid rates the type of flow changes directly from wave to annular, with no intermediate region of slug flow".

They also state that bubbling, wave and slugging flow are of an unsteady type whereas annular and stratified flows are steady.

2. "Flow in Vertical Tubes", by O. P. Bergelin; P. K. Kegal; F. G. Carpenter; C. Gazley.

In this paper an experimental study is reported of the downward annular flow of air and water through a vertical one inch tube. The results were found to agree with previous data obtained by Martinelli and his co-workers.

By calculating the velocity of the gas phase on the rather artificial assumption that it occupied the whole of the flow area, friction factors were determined. The values thus obtained were much in excess of those appropriate to the corresponding flow of air in a smooth pipe, this being attributed to irregularities on the surface of the water film flowing along the tube wall. This data was applied to predict pressure

drops occurring during the condensing flow in a vertical tube, of the vapours of water, alcohol, toluene, and trichlorethylene. Measured and predicted results correlated very approximately.

3. "Interfacial Shear and Stability", by C. Gazley.

The data reported in the earlier paper of this series, "Flow in Horizontal Tubes", is used to assess energy transfer between the two components during air-water stratified flow in a horizontal tube. Energy balance equations enabled the Author of the paper to assess the energy quantity lost by the air and that gained by the liquid at the interface between the two fluids.

For a stable interface these two quantities were found to be equal, but above a certain relative velocity the interface became unstable and the energy lost by the air was found to be in excess of that gained by the liquid. This latter feature was attributed to the irreversible work done by the gas in forming unstable waves at the interface.

Selective Summary of the Preceding Review.

The features emerging from previous papers which are directly relevant to the present work may be summarised as below:

1. The investigations of Bottomley[2] and Burnell[3] yield conflicting results in relation to the evaporating flow of water in pipes, the former finding support for his contention that liquid and vapour flow with a common velocity, the latter demonstrating very conclusively the existence of relative motion.

The discrepancy between the two sets of data may possibly be accountable to unobserved or unnoted factors such as a detergent additive in the water used by Bottomley.

Burnell's experiments on pipes, in contrast to those of Bottomley, were carried out under laboratory conditions and in consequence may be accepted with greater reliance as representing the true behaviour of evaporating water.

To account for his results, Burnell postulated, but did not develop, the idea that relative motion exists between the two phases during the evaporating flow of water in pipes.

2. Previous investigations indicate the occurrence of several possible flow forms with two phase flow. Using the terminology adopted by Bergelin and Gazley[12], these are (a) bubbling, (b) slugging, (c) stratified, (d) wave, (e) annular, (f) frothing.

PART II.

THEORY.

THEORY.

The specific problem discussed in succeeding sections of this thesis is the behaviour of a fluid entering a horizontal pipe of uniform bore at a temperature just below its boiling point, and subsequently evaporating whilst flowing adiabatically through the pipe. Evaporation commences within the pipe when the pressure of the fluid has been reduced by wall friction to the saturation value corresponding with fluid inlet temperature. Throughout the subsequent expansion the fluid mass is mainly associated with the liquid, whereas, except during a very small initial pressure drop, the volume is mainly associated with the vapour.

Figure 8, illustrates the change of mass and volume ratios for the two phases with temperature and pressure during a typical adiabatic expansion of water.

Flow Forms.

The simultaneous flow of two phases in a pipe renders possible the occurrence of a variety of flow mechanisms, as has been shown by previous investigators, and it is necessary to consider these qualitatively before going on to develop appropriate theory.

In Britain, Lewis and Robertson, and in America, Martinelli and co-workers and also Bergelin and Gazley have devoted considerable attention to this aspect of the problem, their findings being mutually consistent.

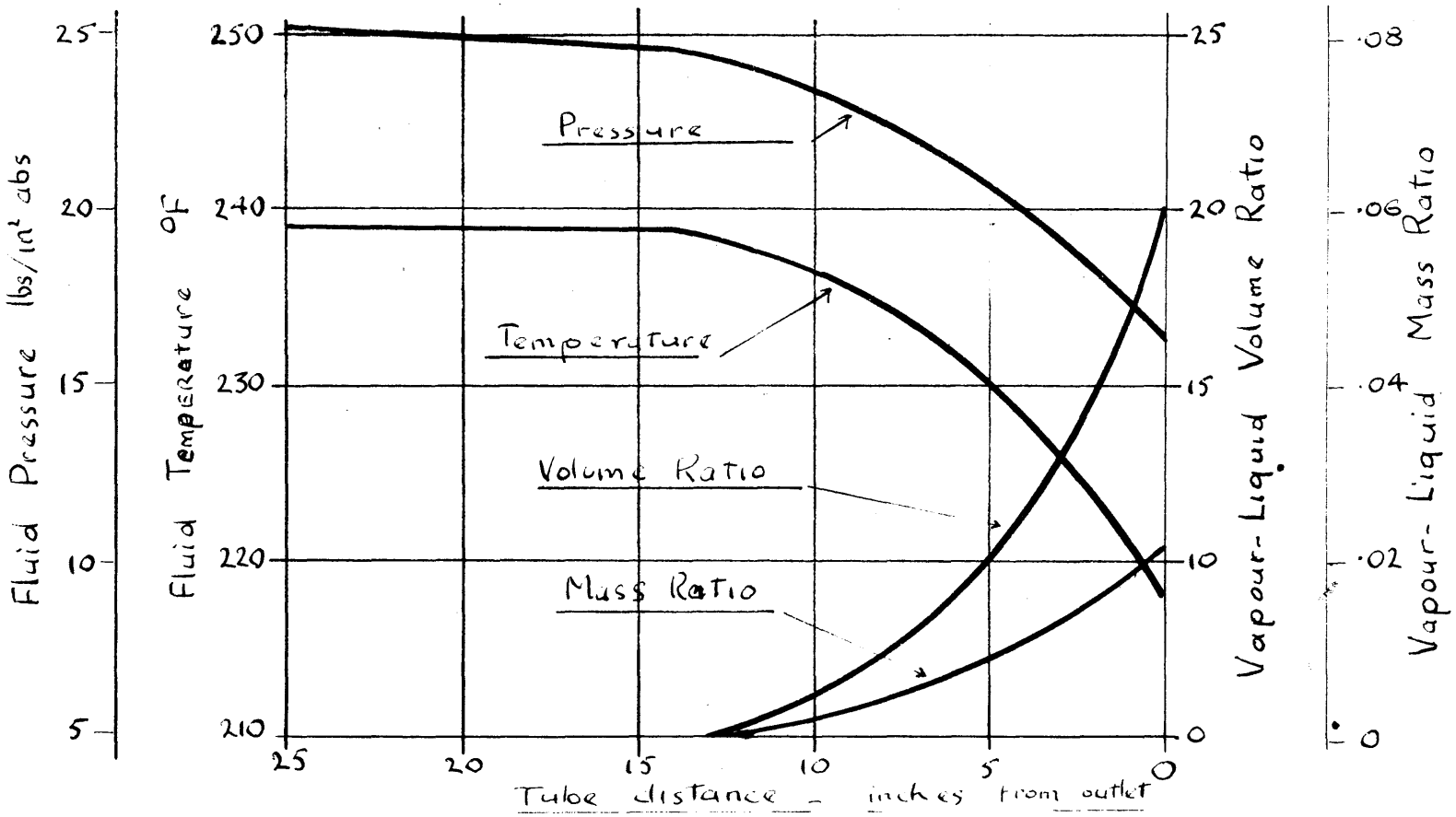

FIGURE 8

Variation of temperature and pressure, and vapour-liquid volume and mass ratios for a typical expansion with water in a small bore tube.

Taking the work of Bergelin and Gazley[12] as being typical and referring to the quotation from their paper given in the foregoing review, the observed flow mechanisms are classified under the headings (a) bubbling, (b) stratified, (c) wave, (d) slugging, (e) annular.

These observations were made on air - water mixtures flowing through a 1" bore horizontal glass tube.

An incidental advantage attaching to the gas - liquid flow as a medium for observation as opposed to the evaporating fluid, is that volume ratios and relative flow rates remain fairly constant along the length of the pipe. A major difference between the two sets of phenomena which is likely to affect flow forms lies in the respective fluid accelerations incurred during flow. Consequently, any data on gas - liquid flow must be applied with caution to evaporating flow, although the summary given by Lewis and Robertson[6] of flow forms occurring in a water - tube boiler, shows qualitative consistency with those observed by Bergelin and Gazley.

Considering the published information with reference to the present discussion the following observations are made. Bubbling flow will not occur when the vapour volume is greater than the liquid volume, which is, except during a very small initial pressure drop, the case with adiabatic evaporating flow. Stratified and wave flows can come under the common heading, separated flow, and whether it be stratified or wave is not relevant to the subsequent theoretical development.

Slugging flow is not expected to be a stable form of flow, since small slugs of liquid dependent on the agency of surface tension are not likely to withstand the disruptive forces involved in the high accelerations of the fluid. Annular flow is believed to be of frequent occurrence, particularly at the higher mass flow rates, and as will be shown is the form obtaining for water flowing through small bore tubes. Frothing flow was not observed by Bergelin and Gazley although Martinelli and his co-workers reported its occurrence in experiments of a similar nature. Under certain conditions, described later, it is a likely flow form.

The foregoing provides a basis for the following postulate.

A particular evaporating flow will conform to one of the three types described below:

(1) Annular flow, in which the liquid phase is confined to the wall of the pipe, the vapour flowing in an inner core. The essential feature of this type of flow is the existence of a continuous layer of liquid flowing along and covering the complete wall surface. The vapour need be neither regular in form, nor co-axial with the pipe.

(2) Separated flow, in which the phases occupy segmental areas of the cross-section, the vapour flowing above the liquid and being subject to wall friction forces.

(3) Frothing flow, in which a network of liquid encloses

the vapour phase, the two phases flowing with a common velocity.

Introductory Note on the Development of Annular and Separated Flow Equations.

Frothing flow is amenable to standard thermodynamic theory and requires no introductory treatment. It is considered, however, that a few explanatory comments on the development of the theory for annular and separated flow forms will not be redundant.

In evaporating flow the high rate of volume increase with pressure drop demands proportionate fluid accelerations, the forces for this deriving originally from pressure variation in the pipe. Since the acceleration of a fluid element is, for a given force intensity, inversely proportional to its density, it is clear that in annular and separated types of flow the vapour will tend to flow with a higher velocity than the liquid. This relative motion will generate an important shearing action between the phases, subsequently referred to as the "interface shear force".

Interphase forces are also induced as a result of mass transfer and relative movement.

In evaporating flow, the force actions which must be considered are consequently due to (1) pressure drop, (2) wall shear, (3) interface shear, (4) mass acceleration, (5) mass transfer between phases.

The mass forces can only be assessed when the separate

velocities of the two phases are known and it is clear that this feature is of fundamental importance.

A convenient variable to which phase velocities and mass forces are related in a simple manner is the "relative velocity factor", defined as the ratio of the mean vapour velocity to the mean liquid velocity.

Since liquid and vapour phases must flow in such a manner as separately to satisfy the three fundamental concepts of continuity, momentum, and energy, six independent equations may be obtained to relate the variables concerned. Combining these equations yields an expression which defines the relative velocity factor in terms of the thermodynamic properties of the fluid, and one empirical coefficient. It may further be shown by rational consideration that the empirical coefficient referred to will have a value close to and not less than unity.

It is noted that, in expressing the three fundamental conditions, account must be taken of mass, momentum and energy transfer between phases, and also of the reversible shear work done by the vapour on the liquid. Heat conduction and radiation are not involved in the energy transfer, the liquid and vapour having a common temperature at all stages during expansion.

A critical outlet condition occurs when a further expansion of the fluid within the pipe would render the laws of continuity, momentum and energy, mutually incompatible. The equations expressing these laws will, therefore be expected to provide a criterion for the prediction of critical outlet conditions, as is found to be the case.

Assumptions.

The following assumptions are made:-

(1) The pressure and temperature are constant across any section normal to the flow.

(2) The fluid is in thermodynamic equilibrium at all stages of an expansion.

(3) The mean velocities on the bases of continuity, momentum and energy, are equal.

Annular Flow Equations.

Although the problem dealt with is classified as adiabatic, there was in the experimental tests carried out, a small amount of unavoidable heat loss to the environment. In order that this feature might be taken into consideration in the analysis of experimental data, the annular flow theory is developed to cover the more general non - adiabatic case.

Considering a normal section of the flow at any stage in the steady state evaporating expansion of a fluid through a uniform pipe and expressing the condition of continuity for the two phases in turn,

$$a_1 V_1 = W(1-q)v_1 \qquad (1a)$$

$$a_2 V_2 = Wqv_2 \qquad (1b)$$

From these, putting $V_2/V_1 = k$ and $\frac{q}{1-q} \cdot \frac{v_2}{v_1} = C$

$$a_1 = \frac{a_1 + a_2}{1 + C/k} = \frac{A}{1 + C/k} \qquad (1c)$$

From (1a) and (1c)

$$V_1 = B(1 + C/k). \qquad (1)$$

Where

$$B = \frac{W}{A}(1-q)v_1$$

Applying the principle of energy conservation to the complete fluid between the stage at which evaporation commences and any later stage of the expansion, and taking into account the heat Q supplied from the environment,

$$JH_c + (K.E)_c + JQ = JH + (K.E). \qquad (2a)$$

where all quantities refer to one pound of fluid, (K.E) is the kinetic energy of the fluid, and the suffix 'c' denotes conditions at the commencement of evaporation.

Now,

$$H_c = h_c \qquad \text{since} \quad q = 0$$

$$(K.E)_c = \frac{1}{2g} V_c^2$$

$$H = h + qL$$

$$(K.E) = \frac{1-q}{2g} V_1^2 + \frac{q}{2g} k^2 V_1^2$$

$$= \frac{V_1^2}{2g} \left[1 + q(k^2-1) \right]$$

Substituting in equation

$$2gJ(h_c - h - qL + Q) = V_1^2 \left[1 + q(k^2-1) \right] - V_c^2 \qquad (2b)$$

For a given value of k, equation (2b) specifies the quality of the fluid. It is clear that q must be within the extreme values corresponding to ideal frictionless and full throttling flow. In the adiabatic case these two conditions correspond to isentropic and constant total heat expansion respectively.

It is shown in Appendix 1, that for a reasonable range of expansion in the wet field at normal or higher temperatures the values of quality corresponding to these two conditions are very nearly equal, and consequently little sacrifice of accuracy is involved in assuming quality to correspond to one or other. That is, for the purpose of calculating q, kinetic energy terms may be neglected in equation (2b), and

$$q = \frac{h_c - h + Q}{L} \qquad (2)$$

This simplification, although not essential to a solution, greatly reduces the amount of arithmetical work involved.

At this point it is perhaps worth noting that the quality of the mixture as here defined is the vapour to fluid mass ratio passing the section during a given period of time, and that, provided k is not unity, this differs from the vapour to fluid mass ratio for the fluid enclosed in an elementary volume at the section.

Equations (1) and (2) refer to relations between variables at a fixed section of the expansion. The remaining equations to be developed prescribe the changes which can take place during a small pressure or temperature increment during unit time. Second and higher order quantities will be neglected. Reference will be made to Figure 9, which is a diagrammatic sketch of an elementary volume of the fluid enclosed between two transverse planes δx feet apart.

Applying the momentum law to the complete fluid,

$$-A\delta p - \delta F_w - \delta M = 0 \qquad (3a)$$

where δM is the change in fluid momentum across the element during unit time, and δF_w is the total wall shear force acting on the element.

Yoga missed out.

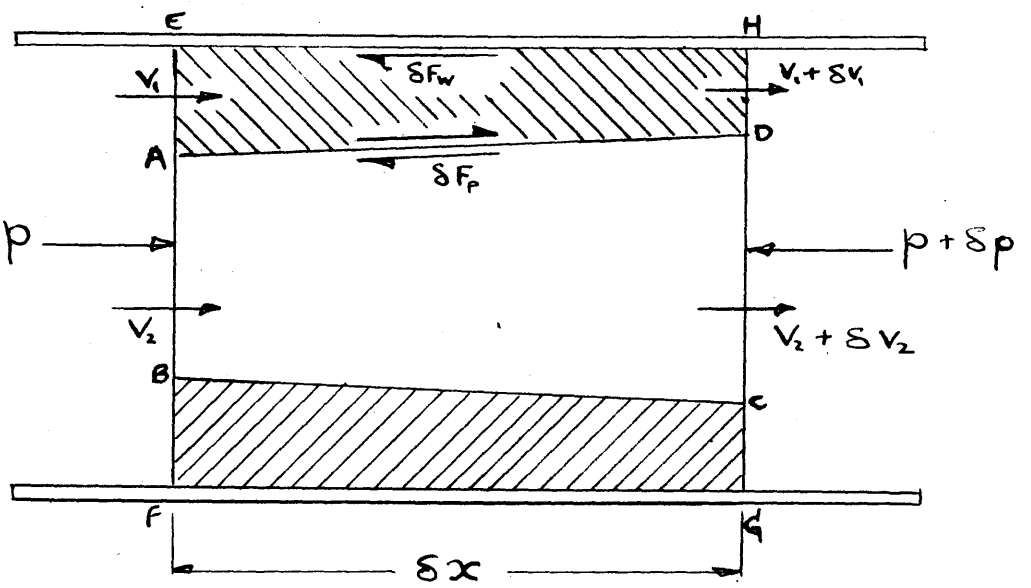

FIGURE 9. Diagrammatic sketch of a section of fluid during annular flow.

Now, $$M = \frac{W}{g}(1-q)V_1 + \frac{W}{g}qkV_1$$
$$= \frac{W}{g}V_1\left[1 + q(k-1)\right]$$

Differentiating,
$$\delta M = \frac{W}{g}\left\{\left[1 + q(k-1)\right]\delta V_1 + \left[(k-1)\delta q + q\,\delta k\right]V_1\right\}$$

Substituting in (3a)

$$-A\delta p - \delta F_w - \frac{W}{g}\left\{\left[1+q(k-1)\right]\delta V_1 + \left[(k-1)\delta q + q\,\delta k\right]V_1\right\} = 0 \qquad (3)$$

The momentum law applied to the liquid phase alone yields,

$$-a_1\delta p - \delta F_w + \delta F_p - \delta M_1 = 0 \qquad (4a)$$

where δF_p is the total interface shear, on the element, and δM_1 is the gain in liquid momentum per unit time. In assessing δM_1 account must be taken of the momentum lost by mass transfer to the vapour phase.

Considering the gain of momentum to the liquid element, at the faces EF, GH, and AC in turn.

Gain of momentum:-

At $EF = \frac{W}{g}(1-q)V_1$;

At $GH = -\frac{W}{g}\left[(1-q)V_1 + (1-q)\delta V_1 - V_1\delta q\right]$;

At $AC = -\frac{W}{g}\delta q\left(V_1 + \delta V_1/2\right)$
$$= -\frac{W}{g}V_1\delta q.$$

Adding these together to obtain the total momentum gain by the liquid element, and substituting in (4a),

$$a_1 \delta p - \delta F_w + \delta F_p - \frac{W}{g}(1-q)\,\delta V_1 = 0 \qquad (4)$$

The final independent equation is obtained by applying the principle of energy conservation to the vapour phase. The control element chosen for the purpose is the vapour volume enclosed between two adjacent sections normal to the flow, represented diagrammatically in Figure 9, as a truncated cone A B C D. It is not essential to the theory, however, that this control surface be regular in any way.

In expressing the law symbolically, the pressure work and shear work done by the fluid at the control surface, and the kinetic and internal energy carried across the surface per unit time will be considered in turn. For steady state flow and a fixed control volume the sum of these items is zero. All terms are expressed on the basis of unit time.

Pressure work done by the fluid on:-

$$AB = -Wq p v_2 \;;$$

$$CD = W(q p v_2 + q p \delta v_2 + p v_2 \delta q + v q \delta p) \;;$$

$$BD = -W p v_2 \delta q .$$

Summing these terms the total pressure work done by the fluid element in unit time is:-

$$Wq(p \delta v_2 + v_2 \delta p) \qquad (5a)$$

Shear work done by the fluid element on:-

$$AB = 0 \ ;$$

$$CD = 0 \ ;$$

$$BD = V_p \, \delta F_p .$$

The total shear work done by the fluid element per unit time is:-

$$V_p \, \delta F_p . \qquad (5b)$$

where V_p is the 'interface velocity', defined as the mean velocity of the fluid particles lying on the line traced by the liquid - vapour interface periphery on a transverse plane.

The kinetic energy carried out of the control volume across:-

$$AB = -\frac{W}{2g} q V_2^2 \ ;$$

$$CD = \frac{W}{2g} (q V_2^2 + 2 q V_2 \delta V_2 + V_2^2 \delta q) .$$

$$BD = -\frac{W}{2g} V_1^2 \delta q$$

Adding these together and putting $V_2 = k V_1$ and $\delta V_2 = k \delta V_1 + V_1 \delta k$, the total outflow of kinetic energy per unit time is,

$$\frac{W}{2g} \left\{ 2 q k^2 V_1 \delta V_1 + (k^2 - 1) V_1^2 \delta q + 2 q V_1^2 k \delta k \right\} \qquad (5c)$$

The internal energy carried out of the control volume across:-

$$AB = -JWq E_2 \ ;$$

$$CD = JW(q E_2 + q \delta E_2 + E_2 \delta q) \ ;$$

$$BD = -JW E_2 \delta q .$$

The total outflow of internal energy per unit time is therefore:-

$$JWq \, \delta E_2 . \qquad (5d)$$

Adding together the terms (5a), (5b), (5c), (5d), and equating to zero, the energy equation for the vapour phase is obtained.

$$W_q(p\delta v_2 + v_2\delta p) + V_p\delta F_p + JW_q\delta E_2 + \frac{W}{2g}\left[2q k^2 V_1 \delta V_1 + (k^2-1)V_1^2\delta q + 2q V_1^2 k\,\delta k\right] = 0 \qquad (5e)$$

Noting that $J\delta H_s = J\delta E_2 + p\delta v_2 + v_2\delta p$, the equation may be reduced to:-

$$J_q W\delta H_s + V_p\delta F_p + \frac{W}{2g}\left[2q k^2 V_1 \delta V_1 + (k^2-1)V_1^2\delta q + 2q V_1^2 k\,\delta k\right] = 0. \qquad (5)$$

It is noted that there is no energy transfer by heat conduction or radiation since the two phases have a common temperature at all stages in the expansion.

The foregoing equations (1), (1c), (2), (3), (4) and (5), can be solved if the interface velocity V_p, is known in terms of the liquid velocity V_1, The relationship between these variables is of necessity empirical and requires to be determined by experiment. Meantime, it is expressed in the form,

$$V_p/V_1 = n \qquad (6)$$

'n' being termed the interface velocity ratio.

This ratio clearly cnnot be less than unity and in the usual case of turbulent liquid flow it might be expected that it will not greatly exceed unity.

The main equations referring to the annular type

of flow listed below for convenience.

Continuity:

$$V_1 = B(1 + c/k) \tag{1}$$

Continuity:

$$a_1 = \frac{A}{1 + c/k} \tag{1c}$$

Overall Energy:

$$q = \frac{h_c - h + Q}{L} \tag{2}$$

Overall Momentum:

$$-A\delta p - \delta F_w - \frac{w}{g}\left\{[1 + q(k-1)]\delta V_1 + [(k-1)\delta q + q\,\delta k]V_1\right\} = 0 \tag{3}$$

Liquid Momentum:

$$-a_1\delta p - \delta F_w + \delta F_p - \frac{w}{g}(1-q)\delta V_1 = 0 \tag{4}$$

Vapour Energy:

$$Jq_l W \delta H_s + V_p \delta F_p + \frac{w}{2g}\left[2q_l k^2 V_1 \delta V_1 + (k^2-1)V_1^2 \delta q_l + 2q_l V_1^2 k\,\delta k\right] = 0 \tag{5}$$

Interface Velocity ratio:

$$n = V_p / V_1 \tag{6}$$

These equations can be combined to yield a single equation expressing the relative velocity factor, k in terms of thermodynamic properties, mass flow per unit area, and the interface velocity ratio. Eliminating δF_w and δF_p between (3), (4) and (5),

$$\frac{Jq_l W \delta H_s}{n V_1} - (A - a_1)\delta p + \frac{w}{2g}\left\{2q_l\left(\frac{k}{n} - 1\right)(k\,\delta V_1 + V_1\,\delta k) + V_1\left[\frac{1}{n}(k^2-1) - 2(k-1)\right]\delta q_l\right\} = 0 \tag{7d}$$

Now, $$k\,\delta V_1 + V_1\,\delta k = \delta(k V_1)$$

and $$k V_1 = B(c + k)$$

The total variation of B over a typical evaporating expansion is of the order of 2 per cent. It will therefore be in order to assume B constant during an elementary change and,

$$\delta(k V_1) = B(\delta c + \delta k) \qquad (7e)$$

Substituting for $(k\,\delta V_1 + V_1\,\delta k)$ and, V_1 and further re-arranging terms in equation (7d),

$$\frac{k J \delta H_s}{n v_2} - \delta p + \left(\frac{W}{A}\right)^2\left(1+\frac{k}{c}\right)\frac{v_1(1-q)}{2g}\left\{2q\left(\frac{k}{n}-1\right)(\delta c+\delta k) + \left(1+\frac{c}{k}\right)\left[\frac{1}{n}(k^2-1) - 2(k-1)\right]\delta q\right\} = 0 \qquad (7)$$

For a given fluid, a knowledge of mass flow per unit area, initial condition, and interface velocity ratio suffice to determine the relative velocity factors during annular flow expansion as expressed in equation (7).

It is shown in appendix 6, by considering the signs of coefficients, that equation (7), which is a bi-quadratic, has only two positive roots. That is, there are two values of 'k' which satisfy the conditions. This result may be

compared with that obtained by an analysis of the similar phenomenon of flow in an open channel, where two liquid depths satisfy the conditions.

Critical Outlet Conditions for Annular Flow.

The criterion by which the critical outlet pressure for a given fluid flow is determined is usually stated as that condition at which the rate of supply of energy is just equal to the rate of increase of kinetic energy. This may be more explicitly stated as that stage in an expansion beyond which the equations based on continuity, momentum and energy are mutually incompatible.

For annular flow, equation (7) supplies the means of expressing the above condition numerically, the three basic requirements being incompatible when the roots of (7) are imaginary.

In Appendix 5, a description is given of the method adopted in the construction of a critical outlet pressure chart for water on the basis of equation (7).

Separated Flow Equations.

Figure 10, is a diagrammatic sketch representing separated flow. δF_1 and δF_2 are respectively the wall shearing forces on the liquid and vapour components of the fluid element. The step by step development of the equations for separated flow so closely resembles that for annular flow that it will suffice to quote them in their final form.

The equations quoted refer to adiabatic flow in a straight horizontal pipe.

Continuity: As for annular flow. (1) and (1c)

Overall Energy: As for annular flow. (2) where $Q = 0$

Overall Momentum:

$$-\delta F_1 - \delta F_2 - \frac{W}{g}\left\{\left[1 + q(k-1)\right]\delta V_1 + \left[(k-1)\delta q + q\,\delta k\right]V_1\right\} = 0 \qquad (8)$$

Vapour Energy: As for annular flow, (5)

Interface Velocity Ratio: $n = V_p/V_1$ (6)

Combination of these equations yields,

$$\frac{k\,J\,\delta H_s}{n\,v_2} - \delta p - \frac{(c+k)\,\delta F_2}{c\,A}$$

$$+\left(\frac{W}{A}\right)^2\left(1+\frac{k}{c}\right)\frac{v_1(1-q)}{2g}\left\{2q\left(\frac{k}{n}-1\right)(\delta c+\delta k) + \left(1+\frac{c}{k}\right)\left[\frac{1}{n}\left(k^2-1\right) - 2(k-1)\right]\delta q\right\} = 0 \qquad (9)$$

Except for the additional term involving the wall shearing force acting on the vapour phase, this equation is identical to that for annular flow.

Critical Outlet Conditions for Separated Flow.

A compressible fluid approaching a pipe exit at

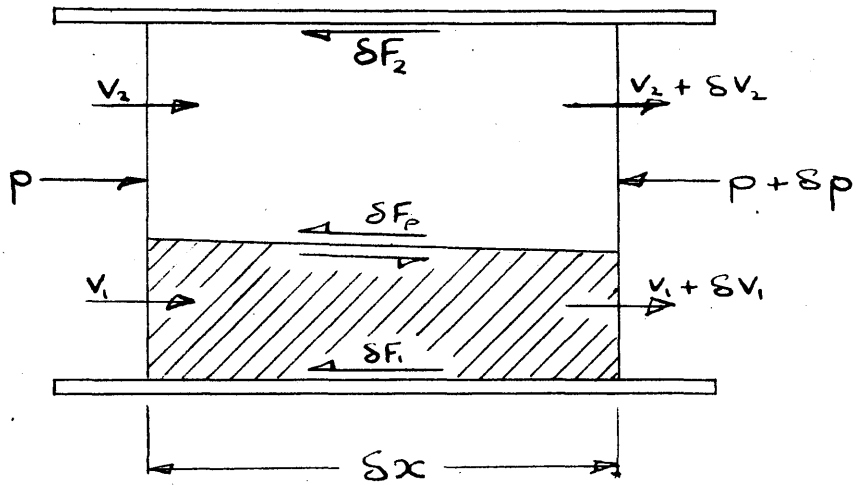

FIGURE 10. Diagrammatic sketch of a section of fluid during separated flow.

which a critical condition exists tends towards ideal frictionless flow. Hence δF_2 tends to zero at a critical outlet condition involving the separated flow of an evaporating fluid, and equation (9) reduces to equation (7), indicating that critical outlet pressures for annular and separated flow forms are identical.

Frothing Flow.

In this type of flow a network of liquid is maintained by surface tension and relative motion between phases is prevented. If surface energy may be neglected, the standard theory for compressible fluid flow is applicable. The method outlined below for dealing with steady state adiabatic expansion of a compressible fluid through a horizontal uniform pipe was first suggested by Fanno.

The continuity equation is:-

$$AV = W\upsilon \qquad (10)$$

The energy equation may be written as:-

$$J(H_c - H) + \frac{1}{2g}(V_c^2 - V^2) = 0 \qquad (11)$$

where the subscript 'c' refers to the section at which evaporation commences.

For a specified mass flow per unit area, and initial condition, H_c and V_c are known constants.

Thus, during any such expansion

$$\upsilon = f(H)$$

Since both these quantities are thermodynamic properties of state, and since any two properties of state suffice to determine completely the condition of a fluid, υ and H may be found for any chosen pressure in the range of expansion. This calculation invloves a trial and error process and a more convenient approach may be used if a pressure - enthalpy

chart having constant volume lines in the wet field is available. By choosing a velocity value, compatible values of v and H may be calculated from equations (10) and (11). Pressure may then be read directly from the chart.

To calculate wall shearing force for a given pressure drop, the momentum equation is required. Considering the forces acting on an element of fluid enclosed between two normal sections δx feet apart,

$$-A\delta p - \delta F_w - \frac{1}{g}\delta V = 0 \qquad (12)$$

An approximate but more convenient method of analysis is to assume that the specific volume, during an adiabatic expansion, is the mean of the volumes corresponding to isentropic and constant total heat expansions respectively; Appendix 1, provides justification for this procedure.

Critical Outlet Conditions for Frothing Flow.

By the methods of the previous section, entropy may calculated for any stage in an expansion. The point of maximum entropy is the critical outlet condition since a decrease in entropy is contrary to the second law and consequently indicates an unrealisable type of flow.

An alternative and more usual approach is to use the concept that, since at the critical outlet condition the fluid tends towards ideal frictionless flow, the rate of supply of energy is equal to the rate of increase of kinetic energy,

obtaining the equation,

$$\left(\frac{W}{A}\right)^2 = -g\left(\frac{dp}{dv}\right)_\phi \qquad (13)$$

The construction of a critical outlet chart for freon 12 on the basis of (13) is outlined in Appendix 8.

The foregoing theory implicitly relates pressure, temperature, specific volume and phase velocity for the three postulated types of expansion and in addition allows the calculation of wall shearing force on the fluid during a specified pressure or temperature change.

Whilst from the thermodynamic viewpoint this is a complete solution, the prediction of pressure or temperature distribution in a pipe requires additional data relevant to friction factors.

The correlation of friction factor with other variables is an empirical process and as such may be approached in a variety of ways, the ultimate relationships adopted requiring the sanction of experiment over the whole of the range covered. It will therefore be more convenient to deal with this question in conjunction with the acquired data and accordingly its consideration is left over to a later section of the thesis.

PART III.

WATER EXPERIMENTS AND ANALYSIS.

AIM AND SCOPE OF EXPERIMENTS ON WATER.

The essential purpose of the experimental work described in this section was to test the practical validity of the proposed thermodynamic theory for evaporating fluid flow. In addition it was desired to obtain some empirical data on wall friction factors and interface velocity ratios.

Water was chosen as the experimental medium because it combined three fundamental requirements; (1) it was known from Burnell[3]'s data on critical outlet pressures that the two-phases of evaporating water flowed with different velocities; (2) the thermodynamic properties of water are accurately known and readily available in suitable form; (3) the saturation temperature-pressure relationship is such that experiments could be carried out on an open circuit.

The proposed theory predicts relative velocity factors and critical outlet pressures and accordingly the experimental test rests on a measurement of these two quantities. The former was achieved by measuring the momentum of the fluid as it emerged from the tube, the latter by concentrating a series of thermocouples near the tube exit.

In order to obtain data for the calculation of friction factors the temperature distribution of the fluid was measured over the whole length of the tube.

Visual data relative to the flow form was obtained by photographing the fluid leaving the tube.

The main experiments were made on a tube of 12 feet length and 1/8" bore, the choice of dimensions being to a certain extent determined by available apparatus in the form of two centrifugal pumps and two electric heaters. This choice of bore had the added advantage of extending Burnell's critical outlet data, his work being done on pipes between $\frac{1}{2}$" and $1\frac{1}{2}$" bore.

The test range covered initial evaporation temperature between 230°F and 250°F, and mass flow between 250 and 500 lbs/ft^{2}sec. As the mass flow increases beyond this value in the quoted temperature range, expansion takes place over a decreasing length of pipe, and theoretical considerations indicate an upper limit at which evaporation within the tube is completely suppressed.

A few preliminary tests were carried out on a tube of .06" bore with the purpose of investigating experimental technique. In these experiments slightly sub-cooled water was supplied from a main boiler via a condenser, initial evaporation temperatures between 280°F and 300°F being obtained.

Temperatures were measured at tube inlet and outlet, providing data on critical flow conditions.

In these preliminary tests trouble was experienced in maintaining steady conditions and in removing dissolved air from the water supply. These difficulties made it necessary to carry out the main tests on a self-contained unit.

APPARATUS.

Figures 11 and 12 show a photograph and general arrangement of the apparatus respectively. The water flows in continuous circuit and the apparatus is entirely self-contained except for the power supply to the pumps. The advantages of this are ease in maintaining steady conditions and freedom from dissolved air in the water. The temperature of the latter never falls below 180°F. at any point in the circuit during a test.

Preliminary tests on an apparatus supplied with hot water from a main heating boiler via a condenser indicated that the latter difficulty was one which could not be readily overcome by other means.

The circulating fluid, on leaving the reservoir passes through two centrifugal pumps in series in which the pressure is raised to about 35 lbs/in^{2}abs. The centrifugal pump characteristic is ideal for this purpose since developed head at low mass flows is almost independent of quantity. The fluid then passes through two electric heaters which are controlled by variac and rheostat and is, in this way, supplied to the tube with a controlled amount of sub-cooling.

On emerging from the tube the fluid mixture impinges on the momentum balance from which it drains back to the reservoir.

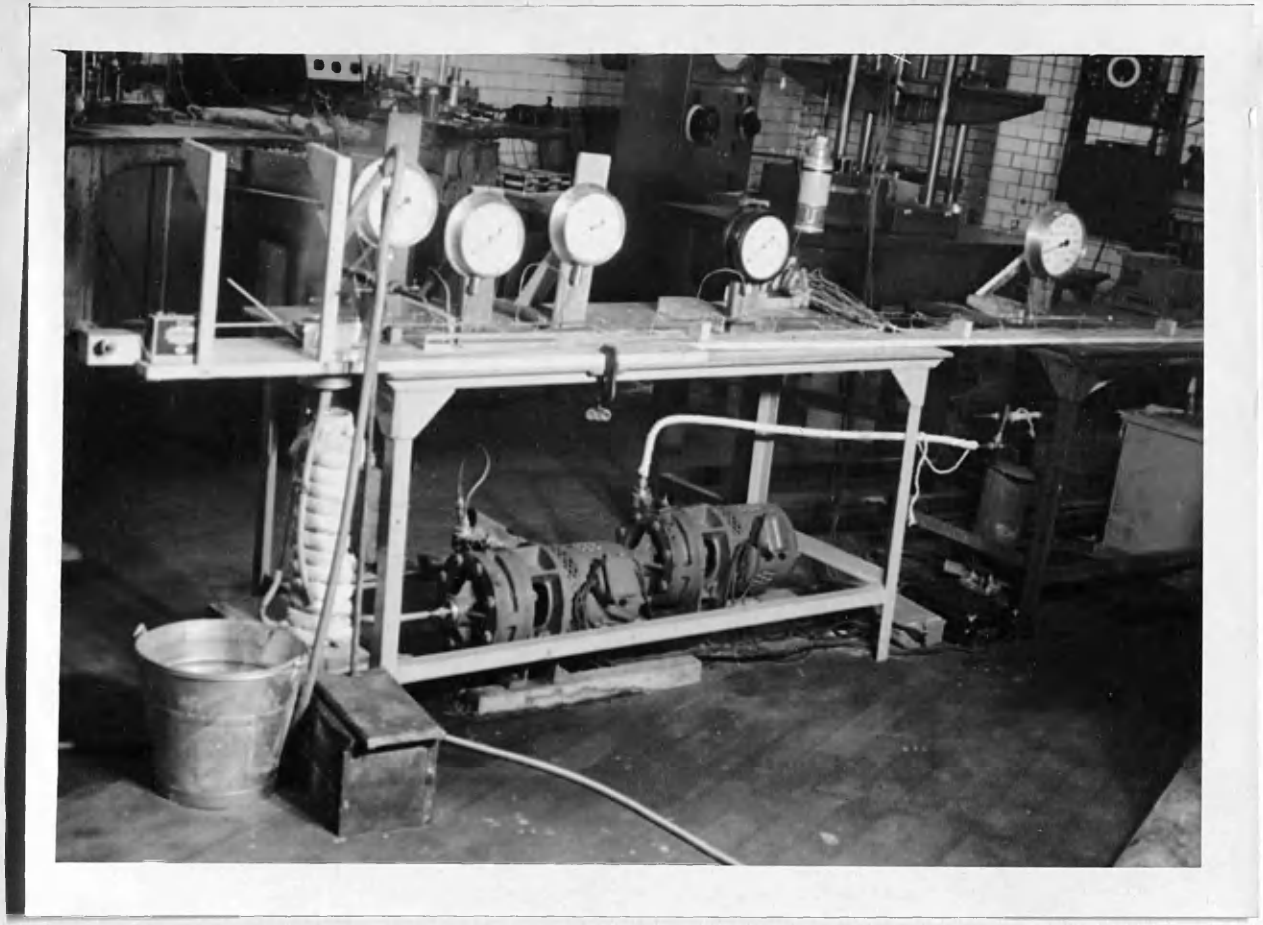

Figure 11. General view of water apparatus.

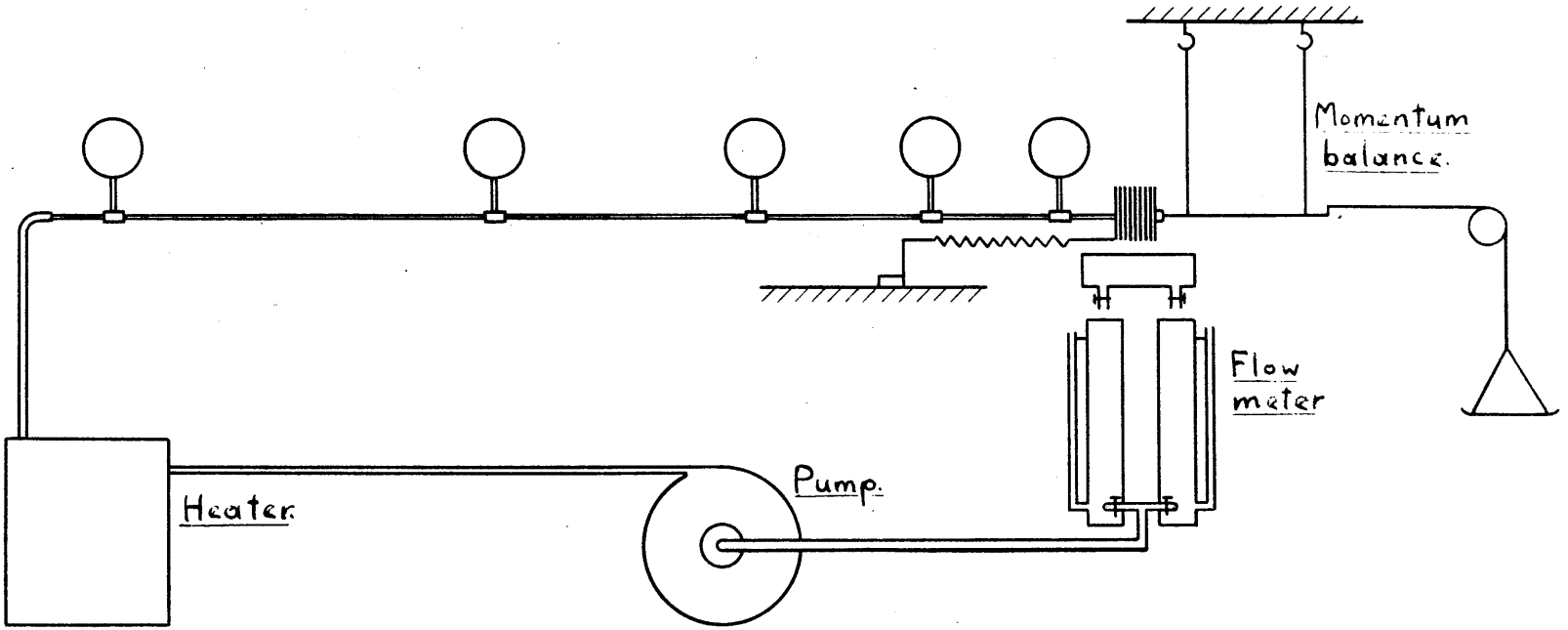

FIGURE 12. General arrangement of water apparatus.

During a test, measurement was made of mass flow, fluid pressures and temperatures, and momentum at the tube outlet.

Mass Flow.

The mass flow meter, as indicated in the general arrangement, consisted of two calibrated reservoirs in parallel. The time taken for one of these to empty could be measured without interfering with the steadiness of flow. The estimated accuracy of measurement is ± 2%.

Temperatures.

It would appear to be physically impossible to make a direct temperature measurement of the fluid in a small bore tube without interfering seriously with the flow. Consequently it was necessary to find a reliable method of measuring the external surface temperature of the tube and relating this to fluid temperature.

Dealing with the latter first, theoretical analysis, confirmed by experiment, showed that the difference between the fluid temperature and that of the tube surface never exceeded 0.2 degrees fahrenheit. The experimental check is given in Table 2, and the theoretical analysis in Appendix 4.

In the latter it is shown that the effects of axial heat flow in the tube metal may be ignored and that a conservative estimate of the ratio of equivalent heat conductances, fluid to tube surface and tube surface to atmosphere, is 880.

Thermocouples (Numbered from tube exit).	E.M.F. mv. (R.J. 32°F)	Tube Surface Temperature °F.
1	3.874	190.7
2	3.878	190.8
3	3.882	191.0
4	3.889	191.2
5	3.890	191.3
6	3.888	191.2
7	3.895	191.4
8	3.885	191.1
9	3.889	191.2
10	3.880	191.2
11	3.892	191.3
12	3.895	191.4
13	3.900	191.7
14	3.900	191.7
15	3.902	191.7
16	3.902	191.7
17	3.907	191.9
18	3.920	192.0
19	3.927	192.7
20	3.929	192.8
21	3.922	192.5
22	3.940	193.2
23	3.945	193.4

Temperature of water at inlet by mercury thermometer - 193.5°F
" " " " outlet " " " - 191.0°F

Table 2. Check on thermocouple temperature measurements on the .01285" tube for water tests.

Thus, for an overall temperature drop of 170 deg.F., the external surface of the tube is within 0.2 deg.F. of the fluid temperature.

In a symposium on "Temperatures", compiled by the American Institute of Physics, Houghten and Olsen discuss the problem of measuring surface temperatures, and a method to which they draw attention was adopted in principle for the present purpose.

28 S.W.G. copper-constantan thermocouples were used, the two leads being wrapped round the polished copper tube at adjacent sections as shown in Figure 13. This incorporates the tube metal in the thermocouple circuit ensuring that the electromotive force is generated at the contact area between the tube and the constantan lead. The method is feasable because of the high purity of commercial copper.

In order to obviate possible error due to stray electric currents during a test, each constantan lead was provided with an adjacent copper lead in the actual set up.

The thermocouples were finally checked in position by passing water through the tube and measuring the temperature at inlet and outlet by mercury thermometers, E.M.F. being measured by means of a Cambridge Potentiometer. The result of this test is given in Table 2.

The copper-constantan thermocouples were calibrated using the ice point and the boiling point with standard apparatus. The final conversion curve was obtained on the principle that differences in e.m.f. between any two thermocouples of the same

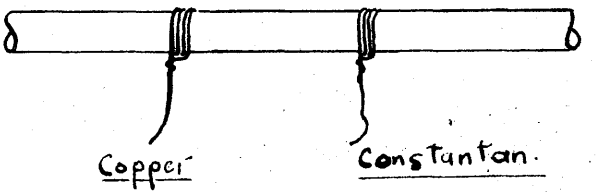

FIGURE 13 Thermocouple attachment to tube.

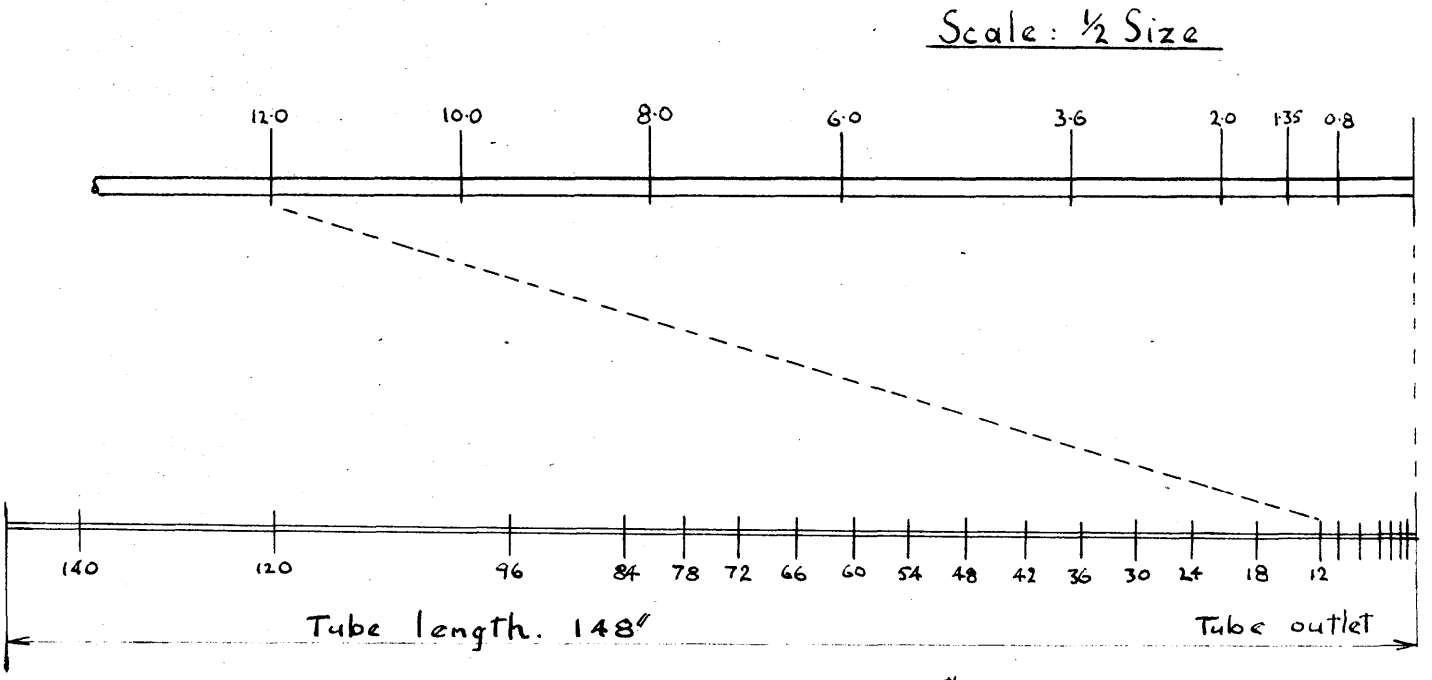

FIGURE 14 Distribution of thermocouples on 0·1285″ tube for water tests.

material are proportional to the temperature range between the reference point and the measured temperature. Adam's table for copper-constantan as quoted in the Temperature Symposium of the American Institute of Physics was used as a reference. In this symposium, the accuracy of the method adopted is quoted as $\pm$ 0.4F°.

Figure 14 shows the distribution of thermocouples on the tube.

Pressures.

Pressure measurements were made at a few points in the tube to check, in as direct a manner as possible, the assumption regarding thermodynamic equilibrium during expansion.

The chief difficulty to be over-come in this aim was the possible occurrence of rags on the unburred tap holes. It was decided to make these holes with a .030" drill rotating at the highest available speed of 9000 r.p.m., and check for rags by measuring the pressure drop accompanying the flow of a homogeneous fluid through the tube. The pressures were recorded on 6" dial close range Bourdon gauges and the method proved adequate.

Figure 15, shows a detail of the pressure lead connection and Figure 16, the distribution of pressure taps on the tube.

The gauges were calibrated in position by connecting a mercury manometer to the tube outlet and supplying air under pressure.

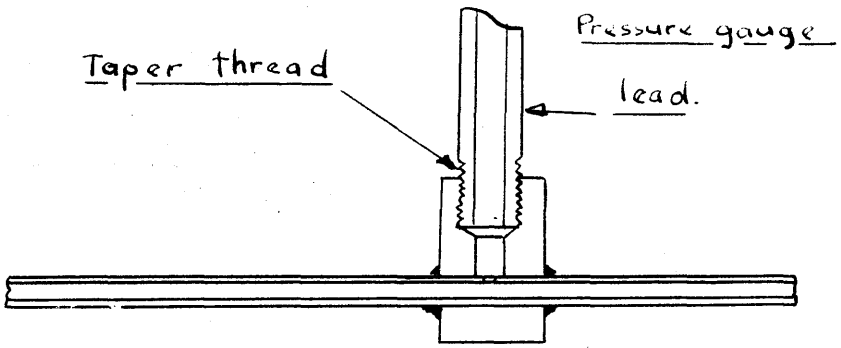

FIGURE 15. Detail of pressure lead adaptor.

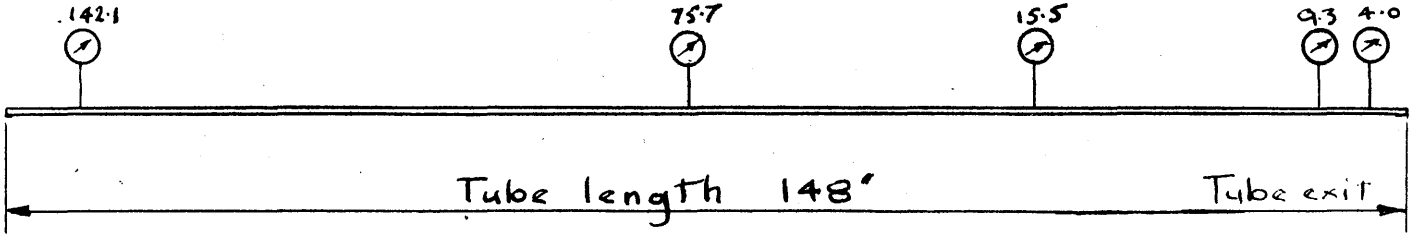

Numbers show distance in inches from Tube exit.

FIGURE 16 Distribution of pressure Taps on 0·1285" Tube for water tests.

Because of the rapid rate of change of pressure with distance the accuracy of pressure measurement was dependent on the accuracy with which the position of the tap holes was known. Since these tap holes could not be made until the adaptor had been soldered to the tube their exact position was subject to some doubt.

A conservative estimate of the accuracy of pressure measurement is ± 1 lbs/in^2.

Momentum Measurement.

A preliminary calculation indicated that the average momentum force would be about 0.01 lbs. This force is of the same order as that measured by Giffen and Crang[5] in their experiments on small steam nozzles, reported in Proc. of I.M.E. 1946, and accordingly the principle feature of their apparatus were incorporated in the balance constructed for the present purpose.

As shown in Figure 17, the balance consists of a carrier rod R, with an impulse cage, C, fixed to one end and a balance weight, B, at the other, the whole being supported by two fine guage wires 18" long. A sensitive helical spring, S, attached to a sliding block, D, balances the carrier during test, the spring being subsequently balanced against weights in pan, P. This method of force measurement eliminates errors due to a possible wrong setting of the electrical contact, E, or deviations from linearity in the spring, S.

The momentum cage, C, consists of an impulse plate

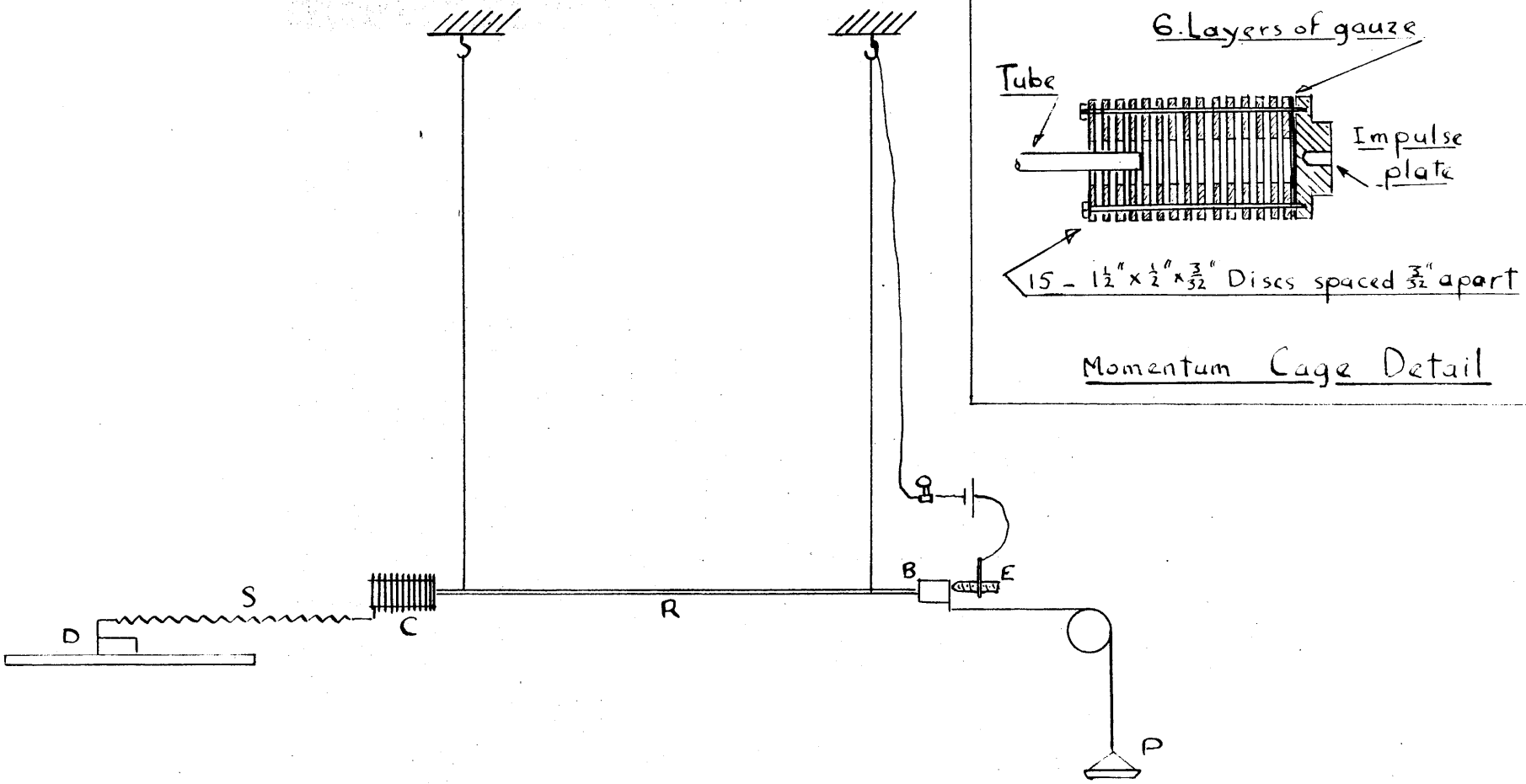

Momentum Cage Detail

FIGURE 17 Momentum Balance

covered by several layers of fine mesh gauze and prefixed by a series of 15 annular discs whose purpose is to ensure complete destruction of the fluid momentum and to avoid induced currents in the adjacent atmosphere.

The dimensions of the cage are given in the detail of figure 17.

Giffen and Crang tested their momentum cage in a specially designed apparatus employing a null-deflection method. It was therefore considered adequate in this instance to check the apparatus in place by passing water through the tube and calculating the momentum from a measurement of mass flow and tube bore. The test indicated an accuracy of ± 5%.

PROCEDURE.

Tests were carried out over the range available to the apparatus covering initial evaporation temperatures of 230 to 250°F. and mass flows of 250 to 500 lbs/ft^{2}sec.

Conditions were presumed to be steady if the temperature measurements remained constant over a period of about 30 minutes. Gross variations in condition could be most readily observed on the pressure guages.

The maintenance of steady conditions was found to be impossible in the sub-cooling range within about 5 degrees of saturated conditions. Silver and Mitchell[9] experienced the same difficulty in their experiments on the flow of saturated water through nozzles.

Temperatures and pressures were taken and the setting of the momentum balance checked at frequent intervals during a test, mass flow being measured just before shutting off the pumps and heaters. The spring force on the balance was measured against dead weight at the end of each test.

TEST RESULTS.

The complete data obtained from the tests on water are presented in Graphs 1 to 12, Table 3 and Figure 18.

Graphs 1 to 12, present the temperature distribution obtained for each test, mass flow and fluid momentum at tube outlet being noted on each graph.

Table 3, shows a comparison between measured pressure and saturation pressure corresponding to measured temperature.

Figure 18, is a photograph of the evaporating fluid leaving the tube.

Test No.	Gauge No.1 lbs/in²abs Sat.ⁿ press.	Meas. press.	Gauge No. 2. lbs/in²abs. Sat.ⁿ press.	Meas. press.
1	18.6	17.9	21.1	20.6
2	20.2	20.1	23.2	23.9
3	22.8	22.6	26.6	25.8
4	21.0	21.0	22.0	22.3
5	17.9	17.6	19.9	20.1
6	18.4	18.0	20.5	20.1
7	18.9	18.5	21.6	21.3
8	22.5	22.0	24.0	23.8
9	23.6	23.7	27.9	27.0
10	20.7	20.2	22.9	22.6
11	19.9	19.2		
12	23.0	22.1		

Pressure gauge distance from tube outlet:-

No. 1 - 40" No. 2 - 9.3"

Table 3. Water Tests.

Comparison of measured pressures with saturation pressures corresponding to measured temperatures.

Figure 18. Appearance of evaporating water leaving the 0.1285" tube.

ANALYSIS TEST RESULTS.

The appearance of the fluid jet leaving the tube (Figure 18) before it is dispersed as a result of free pressure drop, is that of full bore flow. Bearing in mind that the volume of vapour present is about 30 times that of the water, and that vapour velocity is about 8 times greater, it would appear on the basis of this evidence alone that the flow form could be assumed to be annular, a step which is subsequently justified by the correlation obtained between experiment and theory.

In all subsequent calculations the basic variable is temperature and the basic incremental change is 1 fahronheit degree. This is sufficiently small to reduce second order quantities to a negligible amount and is at the same time convenient for calculation. Tables compiled by Keenan and Keyes (1936) were used.

Interface Velocity Ratios and Friction Factors.

The annular flow equations inter-relate friction factors and interface velocity ratios via the temperature distribution curve, so that it is only necessary to obtain an independent determination of one or other to solve this aspect of the problem.

Both quantities can be estimated at the tube outlet from momentum and critical outlet measurements and preliminary calculation on this basis indicated that the following

assumption regarding wall friction forces might be tentatively made. The wall shearing force developed by the liquid annulus is the same as that for full bore liquid flow at the same mean velocity.

Expressing this statement symbolically, the wall shear force per unit area,

$$\tau_o = \frac{\lambda V_1^2}{8 g v_1} \qquad (14)$$

where λ is the standard friction factor for pipe flow and Reynold's number is defined by equation (15)

$$R_D = \frac{D V_1}{g v_1 \mu_1} \qquad (15)$$

A further basis for presuming that this assumption is at worst likely to be a good approximation is given below.

In full bore liquid flow the outer elements of fluid are propelled by the dual forces due to pressure drop and shear transmitted from the faster flowing inner core.

In annular evaporating flow the liquid core is replaced by a vapour core of lower density but much greater velocity. The wall shear force will be unaffected if the distribution of turbulence intensity is unaltered by this change.

Making use of this a ssumption to determine relative velocity factors and interface velocity ratios, the wall shear force may be written:

$$\delta F_w = \frac{\lambda \pi D}{8 g v_1} V_1^2 \delta x \qquad (16)$$

where δx is obtained from the experimental temperature distribu-

tion curve.

Substituting in the overall momentum equation, (5)

$$-\frac{\lambda \pi D}{8 g v_1} V_1^2 \delta x - A \delta p - \frac{W}{g}\left\{(1-q)\delta V_1 + (k-1) V_1 \delta q + q k \delta(k V_1)\right\} = 0 \qquad (17)$$

From equation (1)

$$\delta V_1 = \frac{B}{k^2}(k \delta c - c \delta k) \quad , \qquad (18)$$

B being assumed constant across the element. For any selected stage in the expansion equations (17) and (18) relate compatible values of k and δk.

Considering now two adjacent stages in the expansion which will be referred to as A and B, and assuming that over this range k is a linear function of T,

$$k_B = k_A + \left(\frac{\delta k}{\delta T}\right)_{A\text{-}B} (T_B - T_A) \qquad (19)$$

Equation (19) supplies the condition for selecting unique values of k and δk at stages A and B. By repeating the process for several stages, k is obtained over the complete expansion.

It is now possible to calculate interface velocity ratios by means of equations (5) and (6).

Appendix 2 provides a sample calculation of test 1, on the foregoing basis and also gives the calculation of outlet relative velocity factor from measured fluid momentum. Graphs 13 to 17 show results of the analysis of tests 1 to 4, and Table 4 compares measured and predicted outlet relative velocity factors on this basis.

It is found that the interface velocity ratio in each test varies from 1 at the commencement of evaporation, to about 1.2 at the critical outlet condition and that this may be

Test No.	Mass flow W/A lb/ft^2. sec.	Initial Temp. T_c °F.	Outlet Temp. T_o °F.	Measured outlet values			Predicted outlet values.		
				k	V_1 ft/sec.	V_2 ft/sec	k	V_1 ft/sec.	V_2 ft/sec.
1.	278	240.5	212	7.6	33.5	255	8.4	30.5	256
2.	369	239	218	8.2	28.8	236	8.1	29	235
3.	412	246.7	222	10.5	30	314	8.6	35	301
4.	485	234.2	221.5	7.7	25.7	198	7.6	26	197

Table 4. Water tests on 0.1285" tube. Comparison of measured relative velocity factors with those calculated as shown in Appendix 2.

expressed with reasonable accuracy in the form :

$$n = 1 + a(T_c - T)^2 \qquad (20)$$

where 'a' is a constant calculated from the condition that $n = 1.2$ when $T = T_o$, the critical outlet temperature.

It is emphasised that this is not claimed as a general law, but is simply designed to cover the present range of tests.

Critical Outlet Temperatures and Interface Velocity Ratios.

A critical outlet temperature chart, shown in Figure 19, was constructed to cover the range of results. The methods of calculation are described in Appendix 5, the interface velocity ratio at outlet being assumed equal to 1.2.

Table 5, compares measured and predicted values, the agreement supporting the finding of the previous section that $n = 1.2$ at the critical outlet condition.

Figure 20, shows a critical outlet pressure chart covering an initial pressure range of 8 to 100 lbs/in^{2}abs, and a mass flow of 200 to 700 lbs/ft^{2}sec.

Table 6, compares Burnell's critical outlet data with values taken from Figure 20.

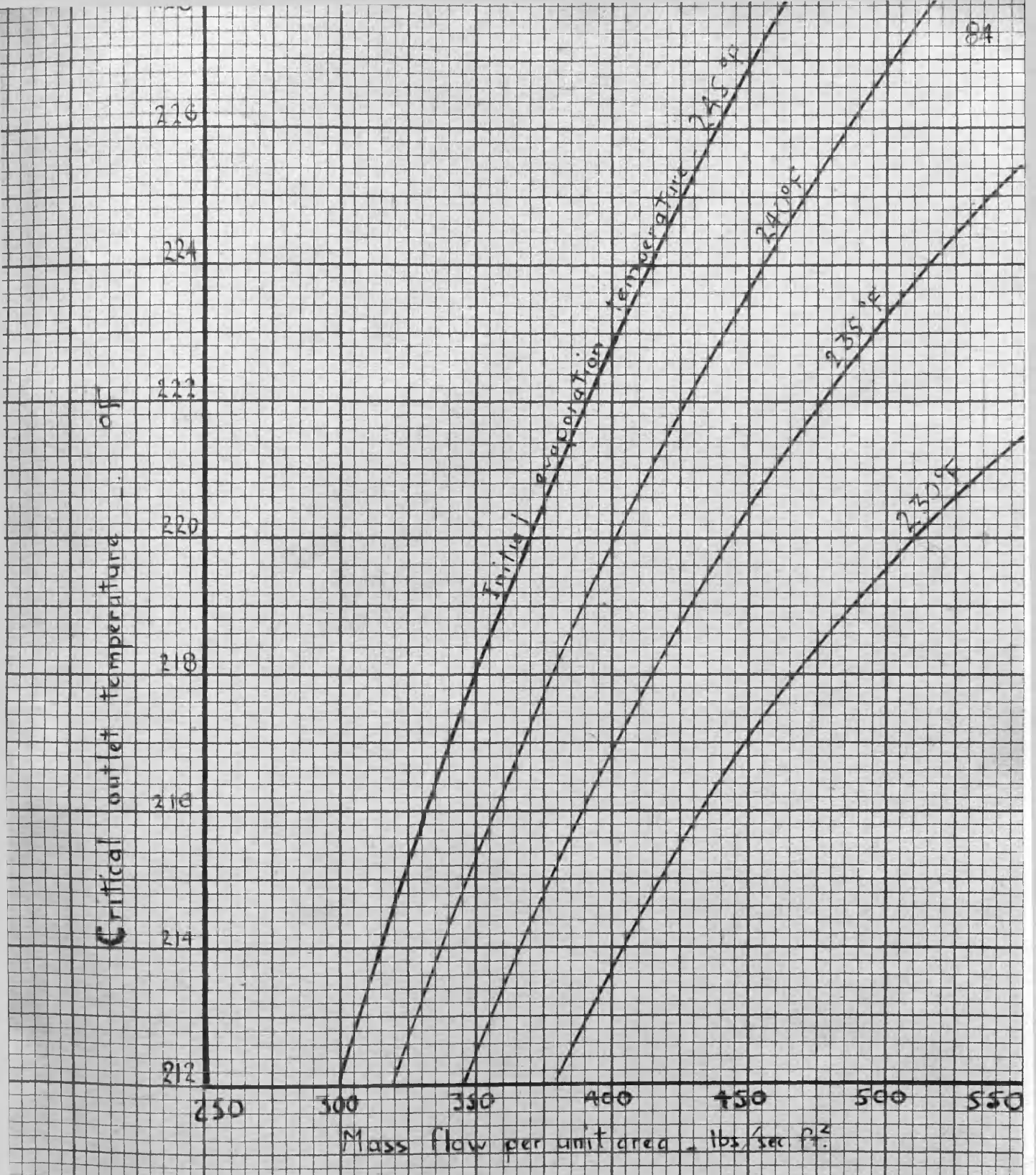

FIGURE 19 Critical outlet temperature chart for evaporating water flowing adiabatically in horizontal pipes.

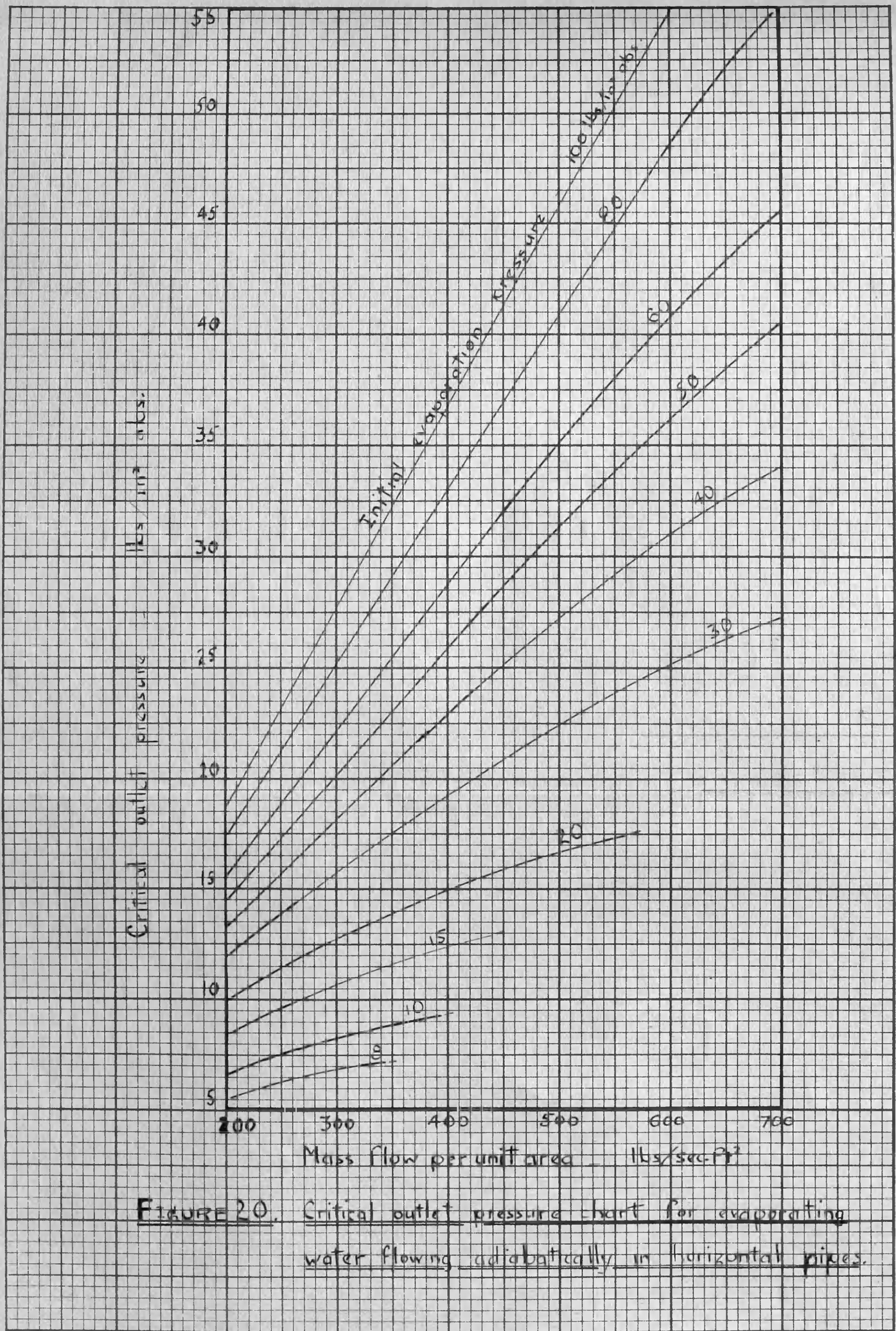

FIGURE 20. Critical outlet pressure chart for evaporating water flowing adiabatically in horizontal pipes.

FIGURE 20.
Critical outlet pressure chart for water.

Test No.	Measured			Predicted	Predicted
	$\frac{W}{A}$ lb/ft²sec	T_c °F	T_o °F	T_o °F (n_o = 1.2)	T_o °F (k = 1)
1.	278	240.5	212	< 212	230
2.	369	239	218	217	$T_o = T_c$
3.	412	246.7	222	224	$T_o = T_c$
4.	485	234.2	221.5	221	$T_o = T_c$
5.	366	235	212	< 212	223
6.	282	235.4	212	< 212	230
7.	333	233.5	214	211	$T_o = T_c$
8.	469	238	224	223	$T_o = T_c$
9.	384	250	223	223.5	$T_o = T_c$
10.	397	237	219.5	218	$T_o = T_c$
11.	410	230	217	214	$T_o = T_c$
12.	429	240.6	222	222	$T_o = T_c$
13.	280	283	230	227	244
14.	337	300	243	242	256
15.	414	283	243	244	263

Table 5. Water Tests.

Comparison between outlet temperatures as (a) Measured; (b) predicted on assumption of relative motion; (c) predicted on assumption of no relative motion.

Tube bore; in tests 1 - 12 0.1285"

in tests 13 - 15 0.060"

Tube. Bore. Inches	Measured. W/A $lb/ft^2 sec.$	Measured. p_c $lb/in^2 abs.$	Measured. p_o $lb/in^2 abs.$	Predicted. p_o $lb/in^2 abs.$ (n_o = 1.2)	Predicted. p_o $lb/in^2 abs.$ (k = 1)
.529	410	24	14.8	16.5	$p_c = p_o$
.529	353	14.3	10.2	10.9	$p_c = p_o$
.529	190	8.8	5.1	5.6	$p_c = p_o$
.529	225	14.3	7.0	7.6	$p_c = p_o$
.904	313	14.3	8.7	10.2	$p_c = p_o$
.904	260	14.3	8.35	9.1	$p_c = p_o$
.904	175	14.3	6.2	6.8	11.4
1.5	500	52.4	25.4	31.6	43.0

Table 6. Comparison of measured critical outlet pressures, as obtained by Burnell[3], with values predicted (a) on the assumption of relative motion; (b) on the assumption of zero relative motion.

Prediction of Temperature Distribution Curve for a given mass flow, initial evaporation Temperature and Tube Diameter.

With the information acquired on wall shearing forces and interface velocity ratios it becomes possible to predict, for a particular mass flow and initial condition, the temperature and pressure variations in a tube carrying evaporating water. The procedure is outlined briefly below, a full development being given in the sample calculation in Appendix 3.

By means of equation (7), values of k and δk may be calculated for any number of selected temperatures in the expansion. It is found that for water, k is almost independent of δk. This greatly simplifies the arithmetical work since the chief difficulty in differential equations not susceptible to mathmatical operations, other than numerical integration, is the determination of compatible values of a variable and its differential.

Equations (1) and (18) provide corresponding values of V_1 and δV_1 which may be substituted in (17) to find $\delta x/\delta T$ at the selected temperature.

The summation,

$$\sum_{A}^{B}\left(\frac{\delta x}{\delta T}\right)\delta T = x\Big]_{A}^{B} \qquad (21)$$

provides the required information.

Graphs 22 to 25 show the comparison between measured temperatures and predicted curves for tests 5 to 8. In each

case the summation was begun at the tube outlet temperature

Table 7, compares predicted and measured outlet relative velocity factors.

Test No.	Mass Flow W/A lb/ft^2 sec.	Initial Temp T_c °F.	Outlet Temp T_o °F.	Measured outlet values			Predicted outlet values		
				k	V_1 ft/sec	V_2 ft/sec	k	V_1 ft/sec	V_2 ft/sec
5.	266	235v	212	5.1	35.8	182	5.8	32	186
6.	282	235.5	212	6.0	36.6	220	7.0	32	224
7.	333	233.5	214	6.4	32.1	205	7.1	29.5	210
8.	469	238	224	9.5	23.2	220	7.4	27.5	203

Table 7. Water tests on 0.1285" tube. Comparison of measured relative velocity factors with those predicted by equation (7).

GRAPH N° 1

GRAPH Nº 1

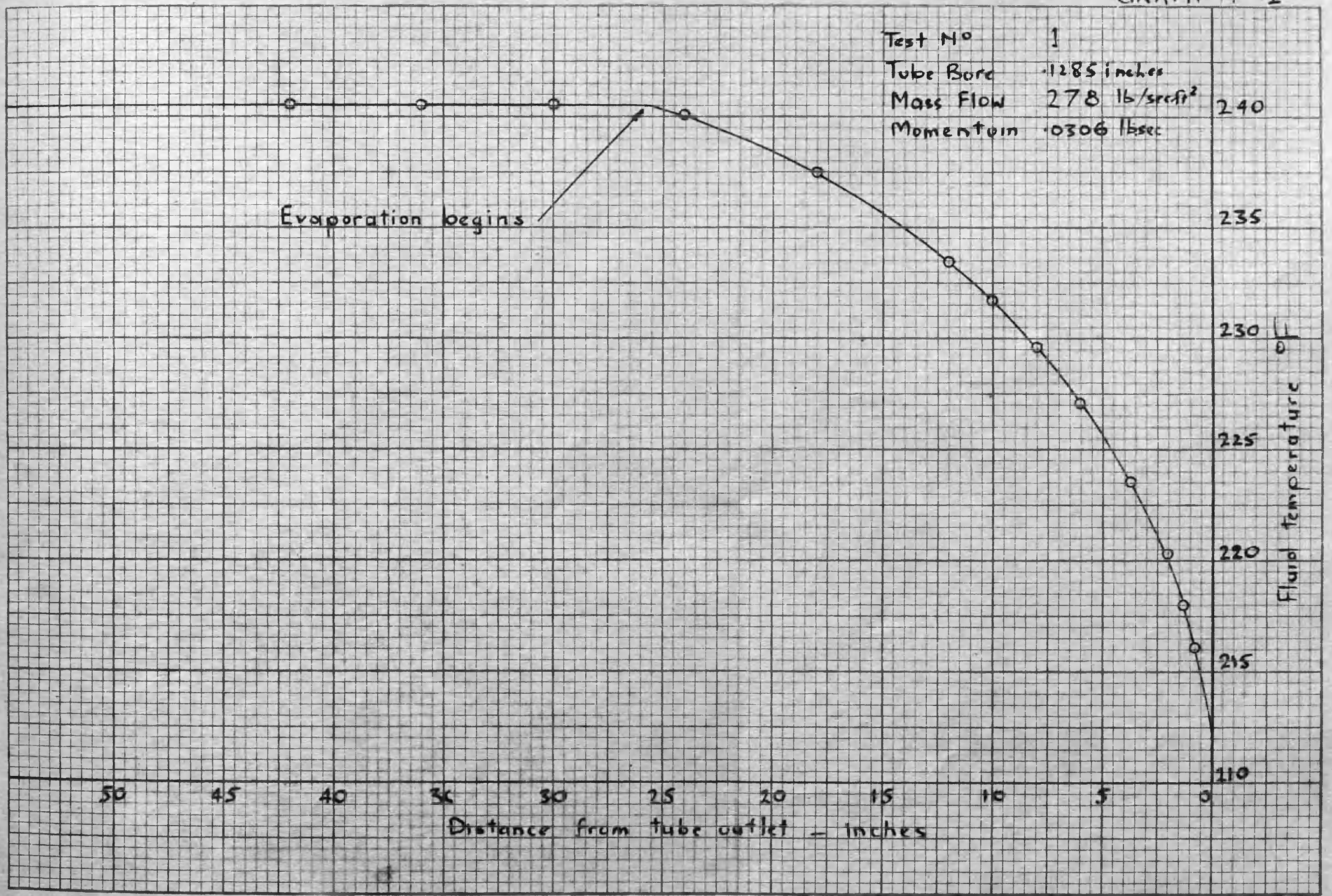
Test Nº 1
Tube Bore .1285 inches
Mass Flow 278 lb/sec ft²
Momentum .0306 lb sec
Evaporation begins
240
235
230
225
220
215
210
Fluid temperature
50
45
40
35
30
25
20
15
10
5
0
Distance from tube outlet – inches

GRAPH N°2.

GRAPH N°2

Test N° 2
Tube Bore .1285 inches
Mass Flow 369 lb/sec. ft²
Momentum .0584 lbsec

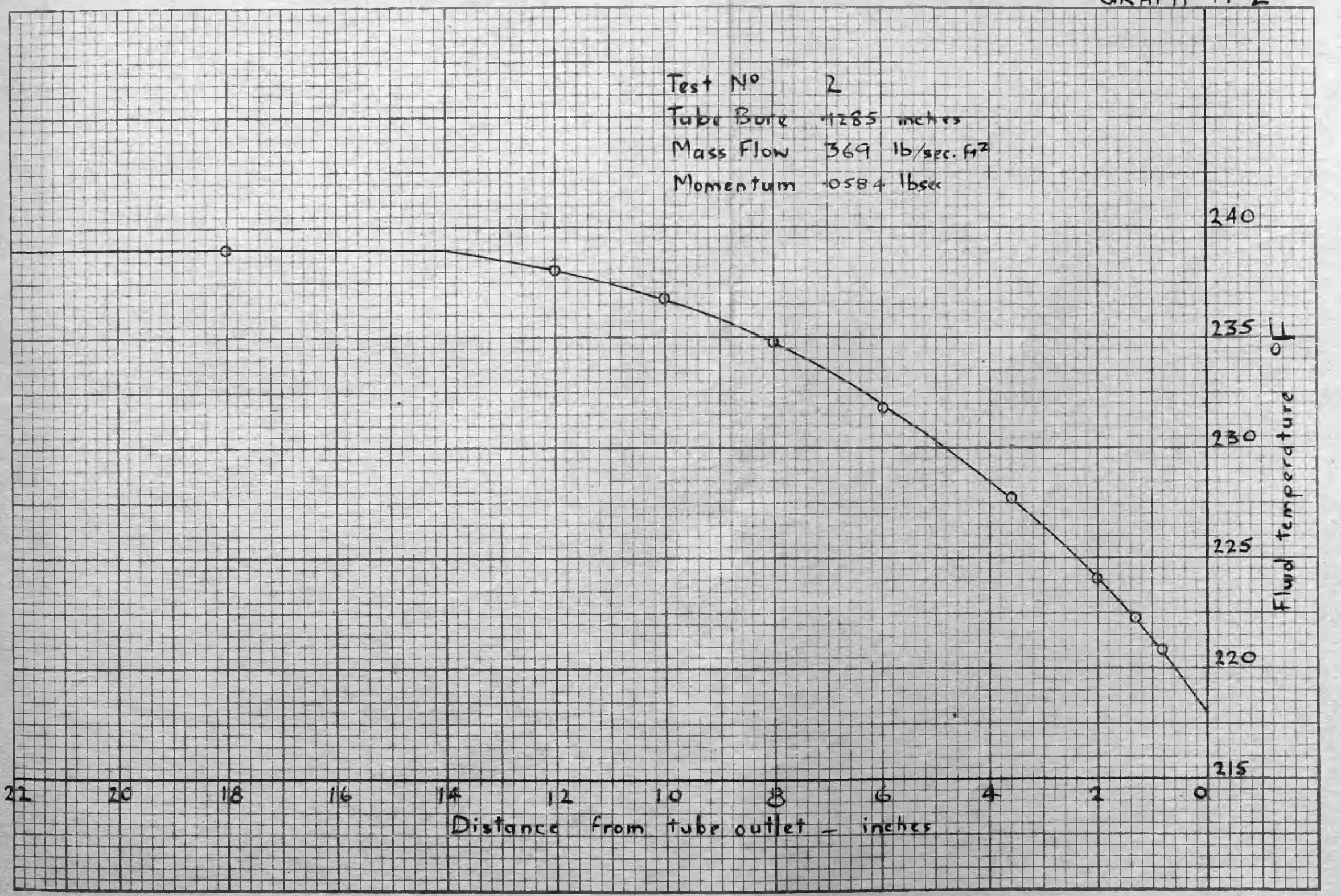

GRAPH 11°3

GRAPH Nº 3

Test Nº 3
Tube Bore .1285 inches
Mass Flow .412 lb/sec.ft²
Momentum .0838 lbsec

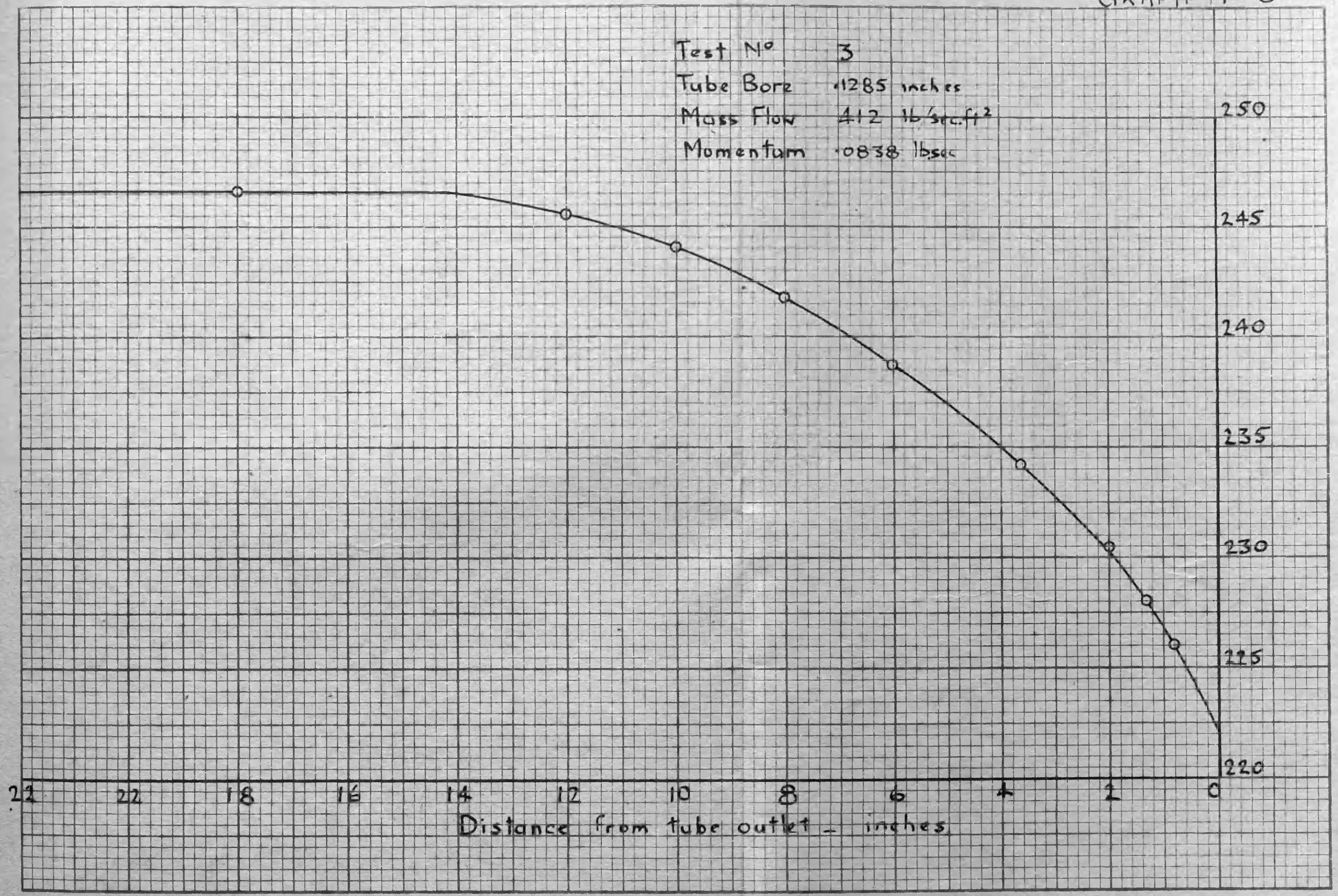

GRAPH N° 4.

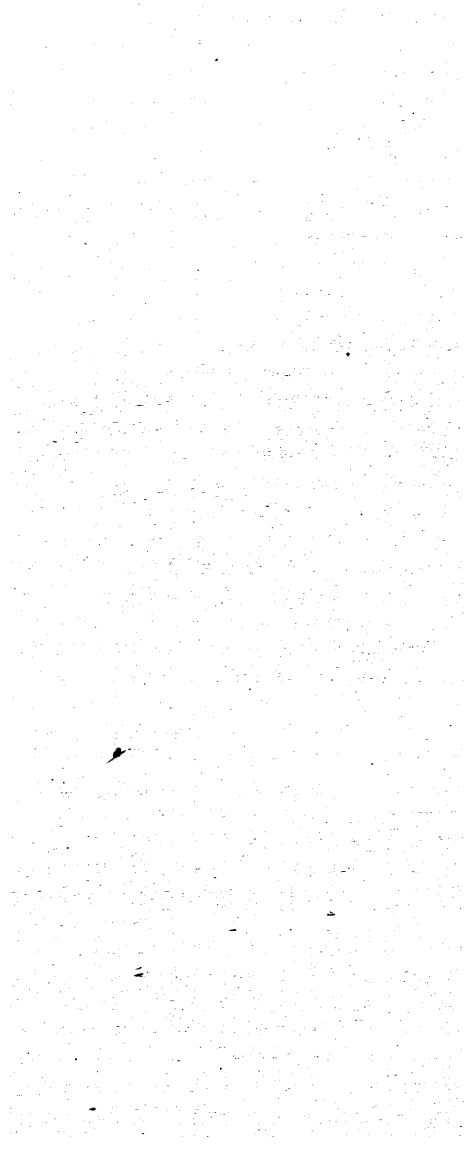

GRAPH No 4

Test No 4
Tube Bore 0·185 inches
Mass flow 4·85 lb/sec.ft²
Momentum 0·172 lbsec

240
235
230
225
220
215

Fluid Temperature °F

20 18 16 14 12 10 8 6 4 2 0

Distance from tube outlet – inches

GRAPH N 5

GRAPH Nº 5

Test Nº 5
Tube Bore .1285 inches
Mass Flow 266 lb/sec. ft²
Momentum .033 lbsec

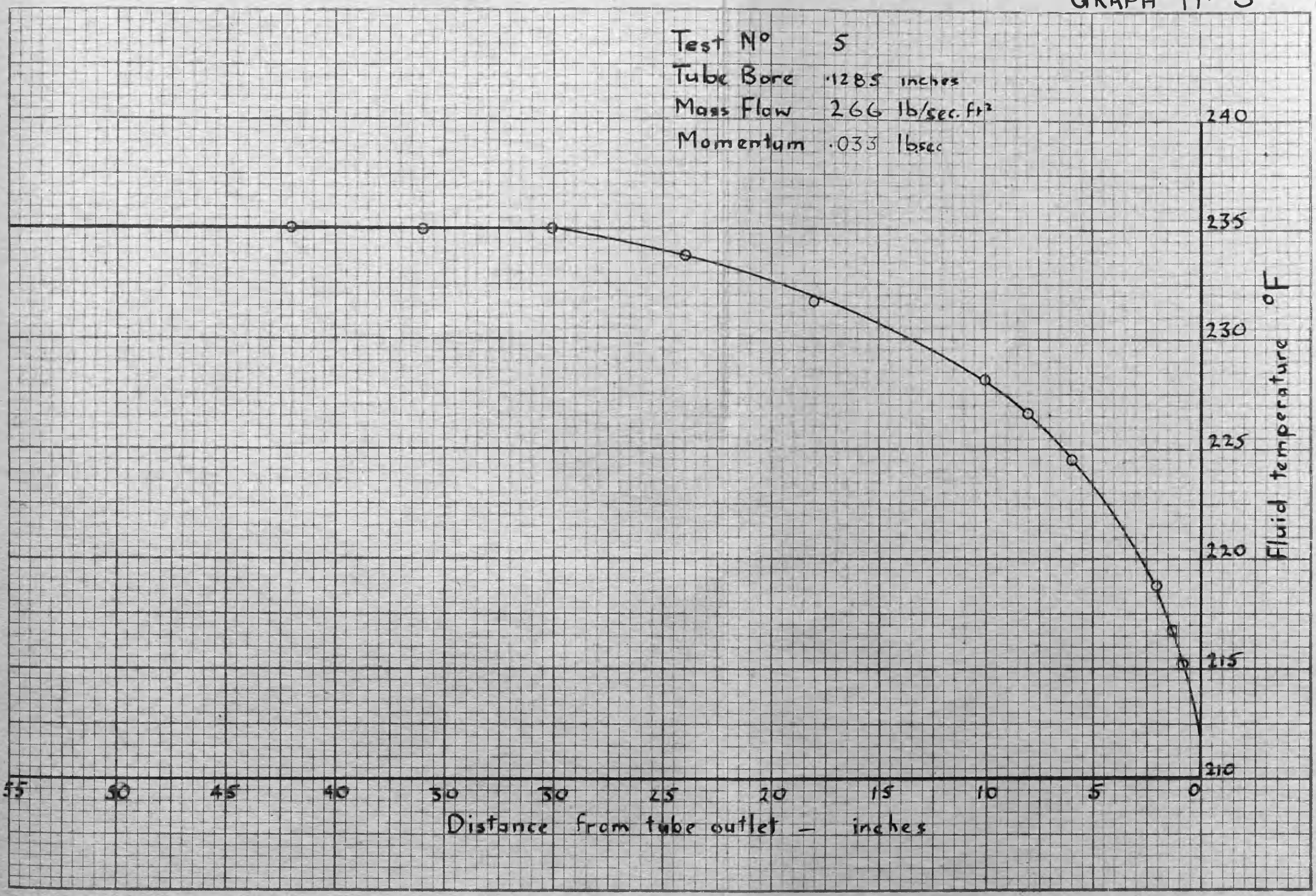

GRAPH N° 6

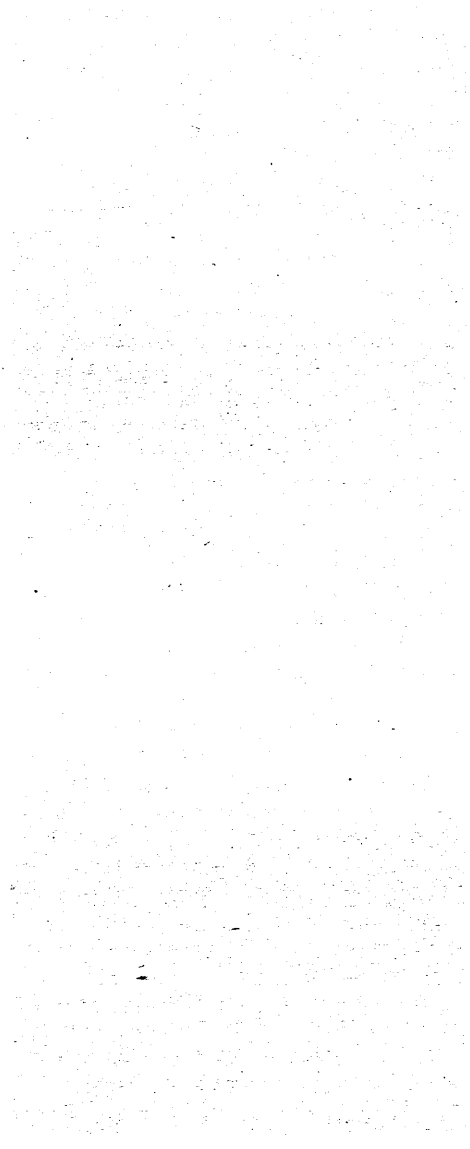

GRAPH Nº 6

Test Nº 6
Tube Bore ·1285 inches
Mass Flow 282 lb/sec.ft²
Momentum ·0353 lbsec

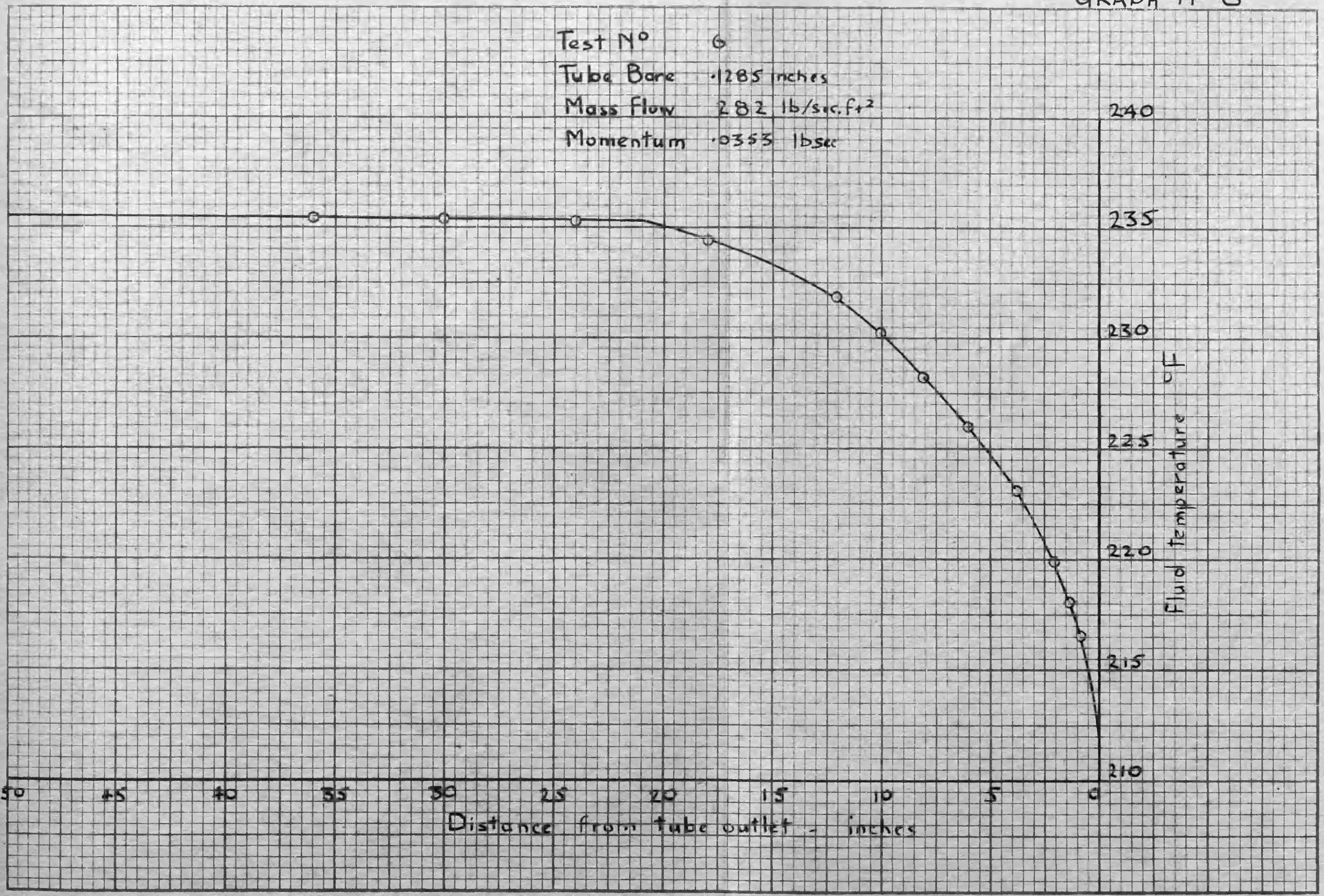

GRAPH N° 7.

GRAPH Nº7

Test Nº 7
Tube Bore .1285 inches
Mass Flow 3,73 lb/sec.ft²
Momentum .0584 lbsec

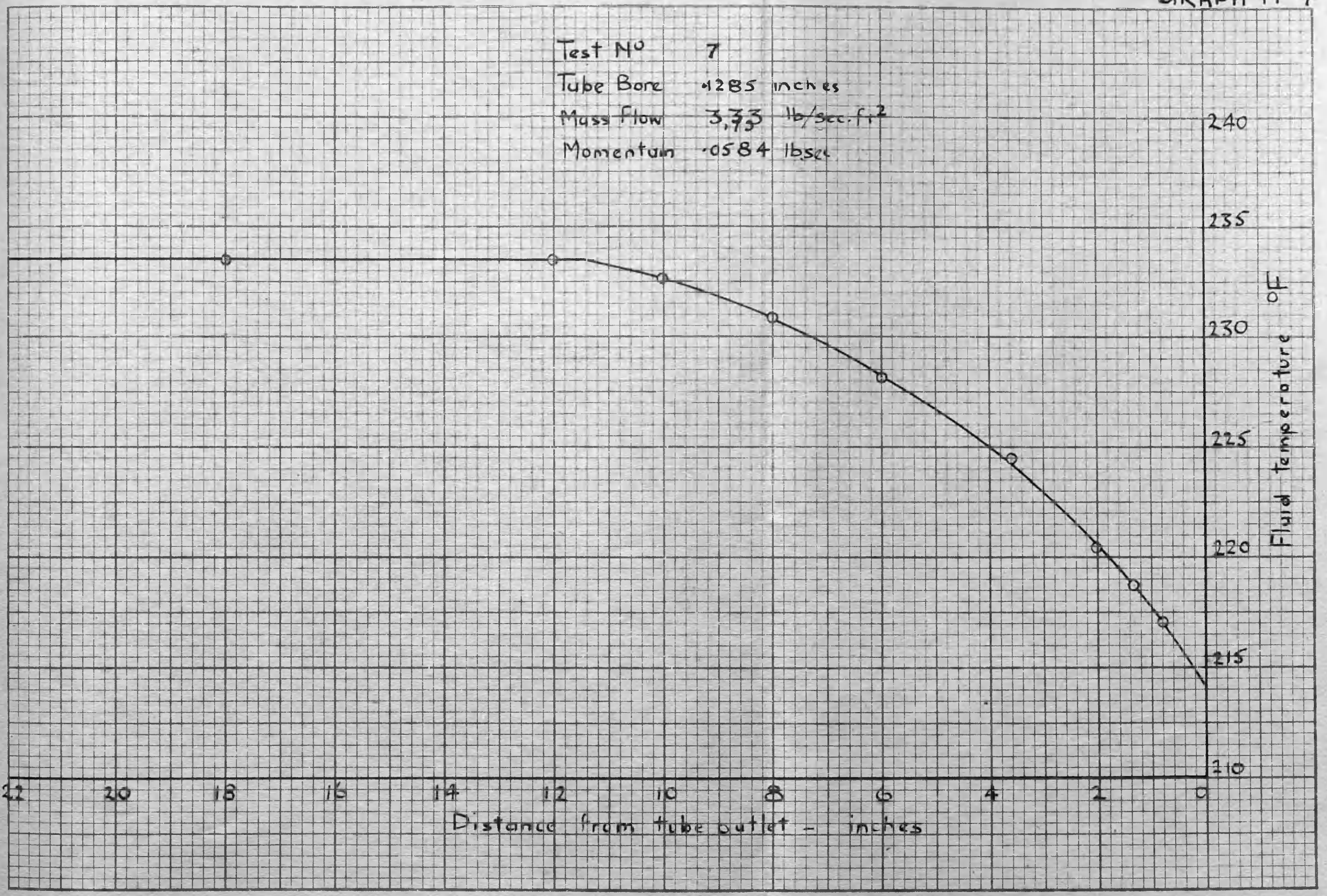

GRAPH N° 8

GRAPH Nº 8

Test Nº 8
Tube Bore .1285 inches
Mass Flow 467 lb/sec. ft²
Momentum .075 lbs/sec

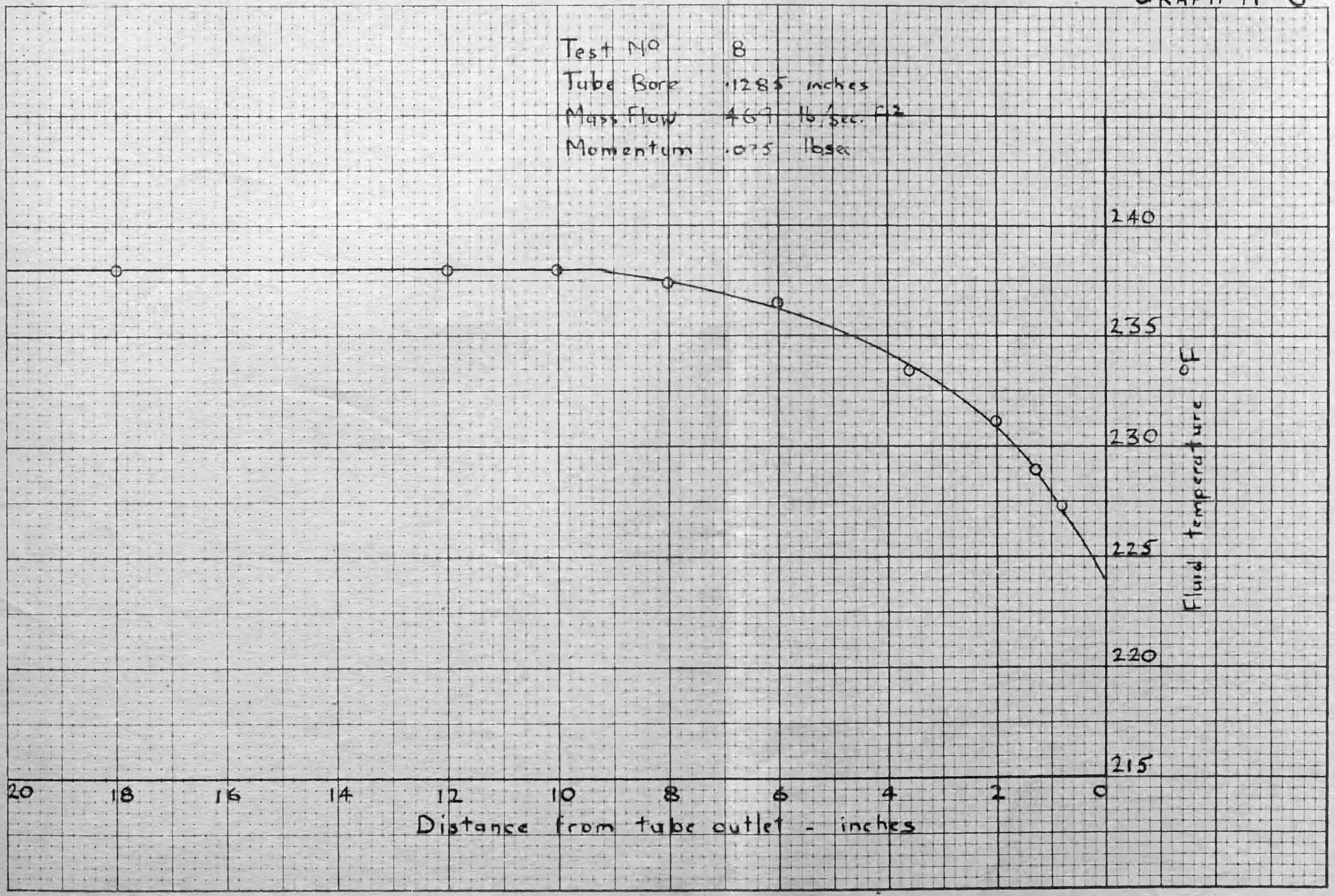

GRAPH N° 9

GRAPH N° 9

Test N° 9
Tube Bore .1285 inches
Mass Flow 384 lb/sec. ft²
Momentum .0914 lbsec

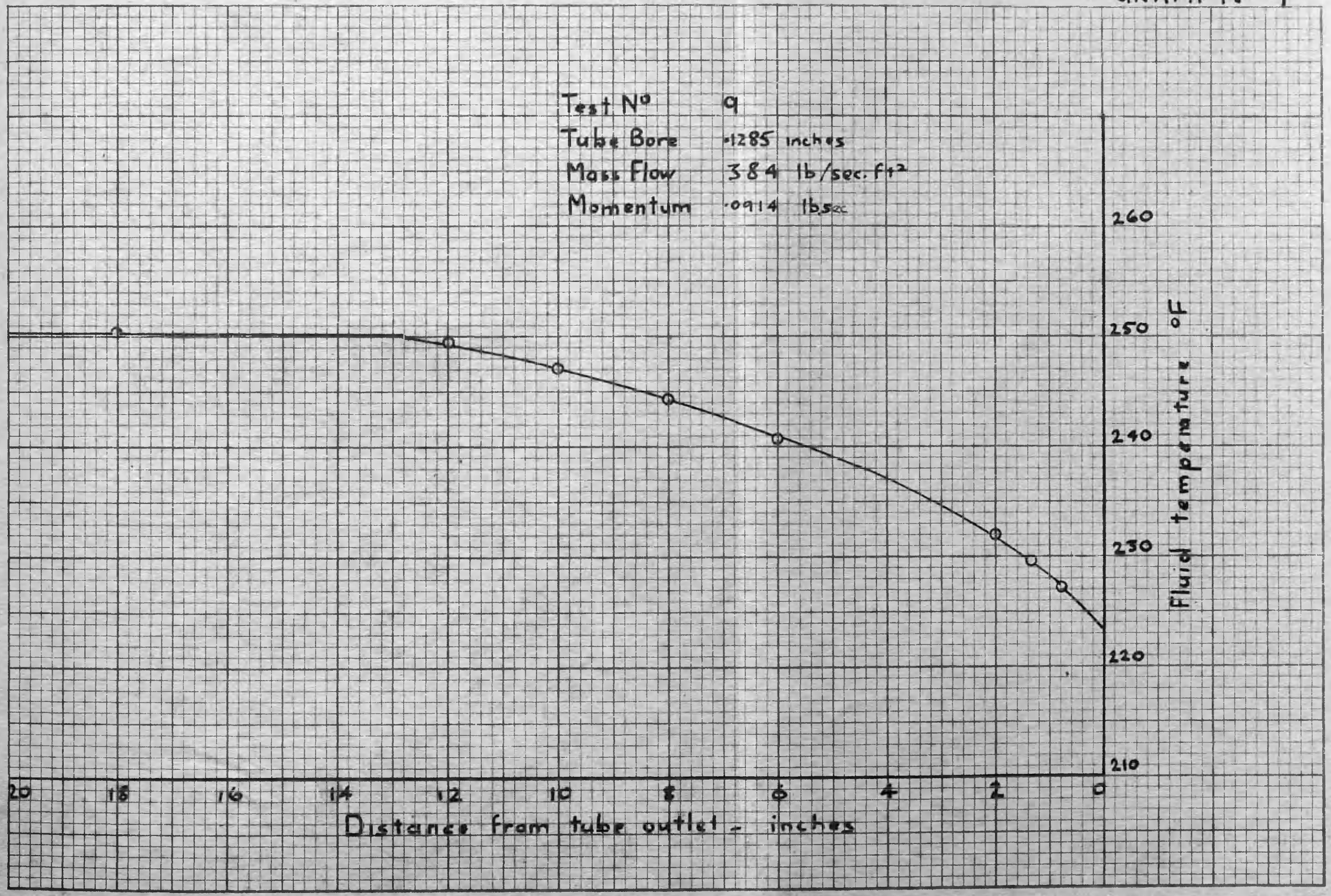

GRAPH N 1

GRAPH Nº 10

Test Nº 10
Tube Bore .1285 inches
Mass Flow 397 lb/sec.ft²
Momentum .0617 lbsec

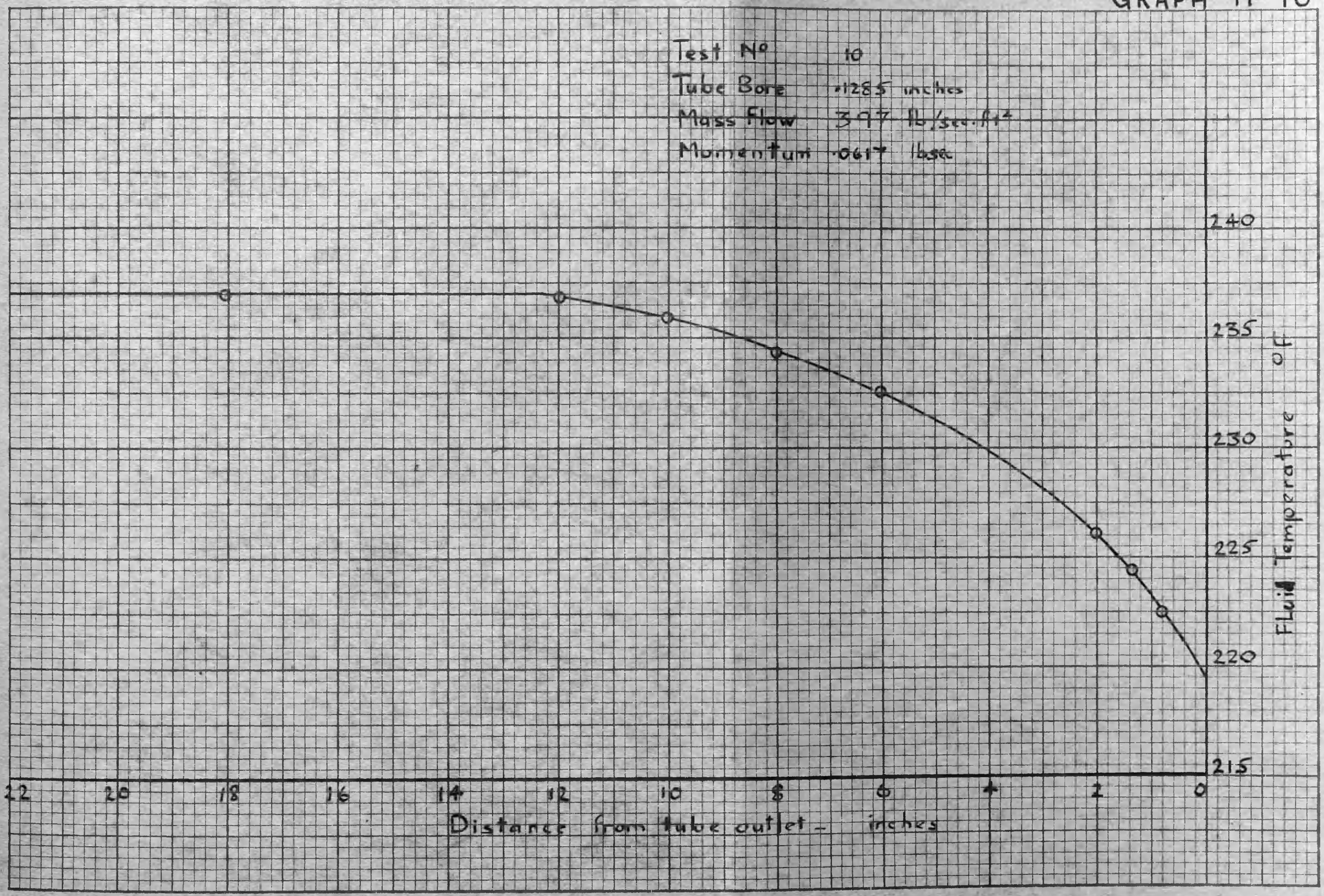

GRAPH N°11

GRAPH Nº 11

Test Nº 11
Tube Bore .1285 inches
Mass flow 410 lb/sec. ft²
Momentum .0472 lbsec

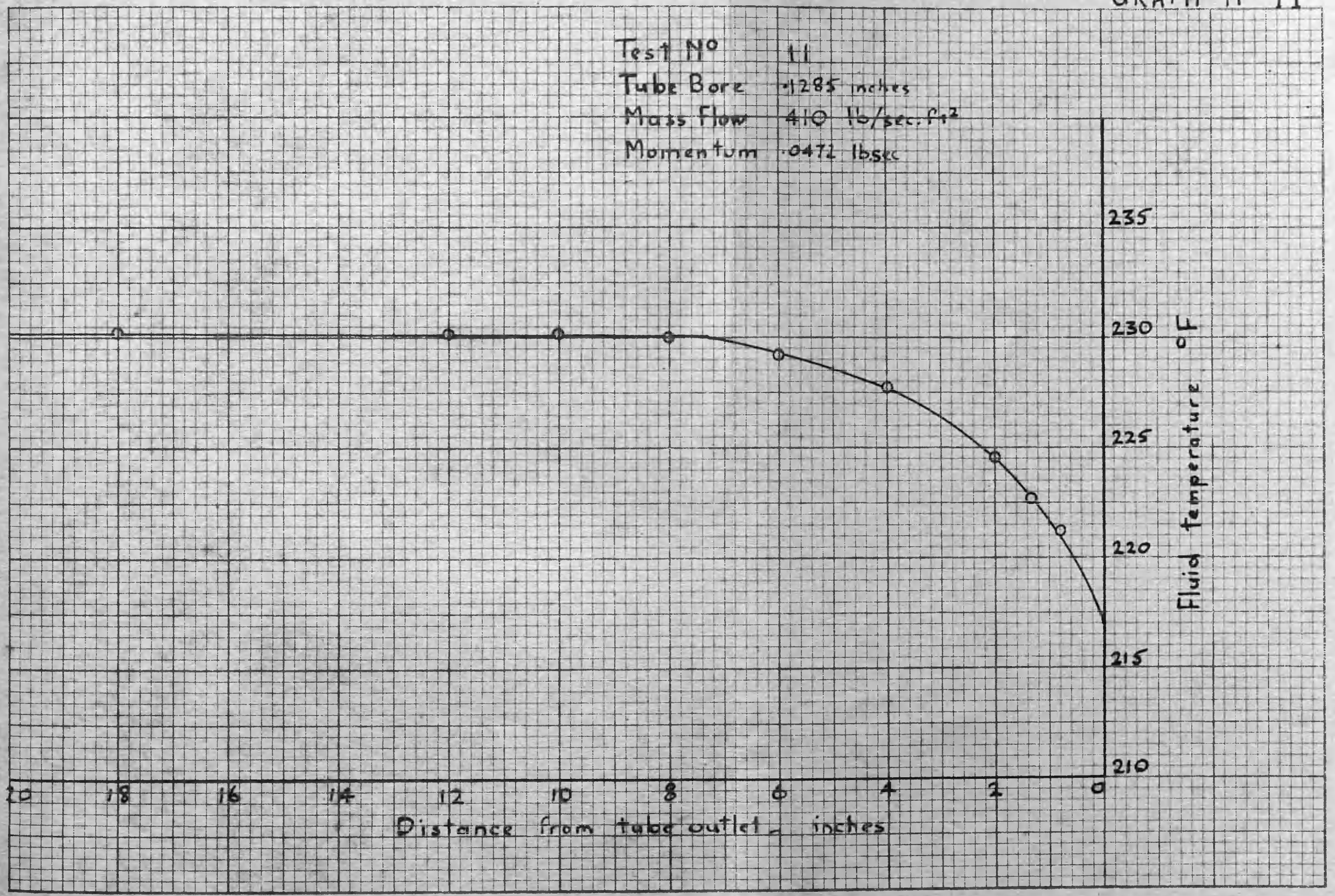

GRAPH N° 12

GRAPH Nº 12

Test Nº 12
Tube Bore .1285 inches
Mass Flow 429 lb/sec ft²
Momentum .0816 lbsec

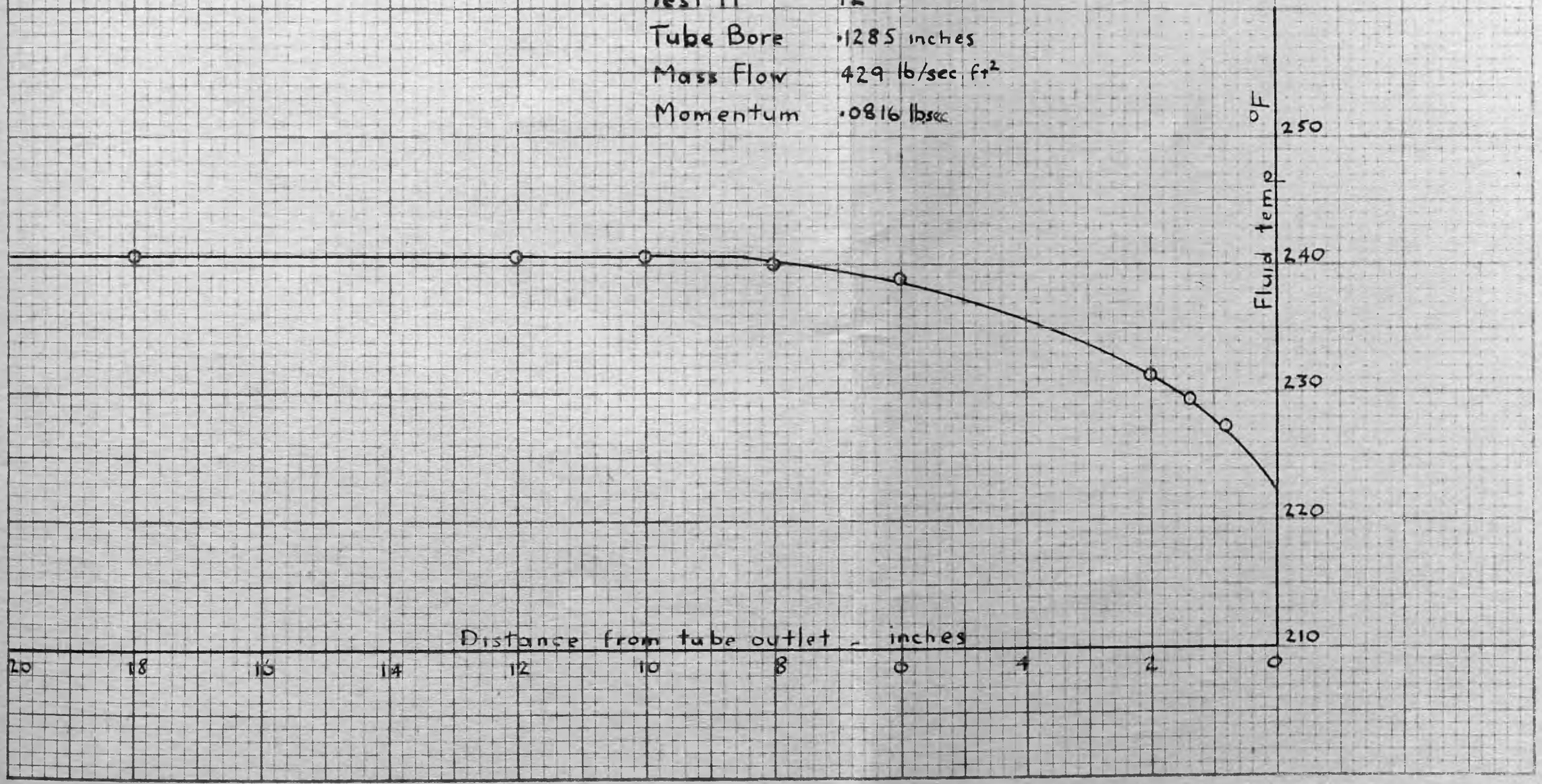

GRAPH N° 15

GRAPH N° 13

Test N° 1

Liquid Velocity ft/sec

30
25
20
15
10
5
0

Relative Velocity Factor

10
8
6
4
2
0

Liquid Velocity

Relative Velocity Factor

240 235 230 225 220 215 210

Fluid temperature °F

GRAPH Nº 14

GRAPH Nº 14

Test Nº 2

Liquid Velocity

Relative Velocity Factor

Liquid Velocity ft/sec

Relative Velocity Factor

30 25 20 15 10 5 0

10 8 6 4 2 0

238 236 234 232 230 228 226 224 222 220 218

fluid temperature °F

GRAPH N 15

GRAPH Nº 15

Test Nº 3

Liquid Velocity

Relative Velocity Factor

Liquid Velocity ft/sec

Relative Velocity Factor

Fluid temperature °F

35
30
25
20
15
10
5
0

10
8
6
4
2
0

245
240
235
230
225
220

GRAPH N°16

GRAPH N°16

Test N° 4

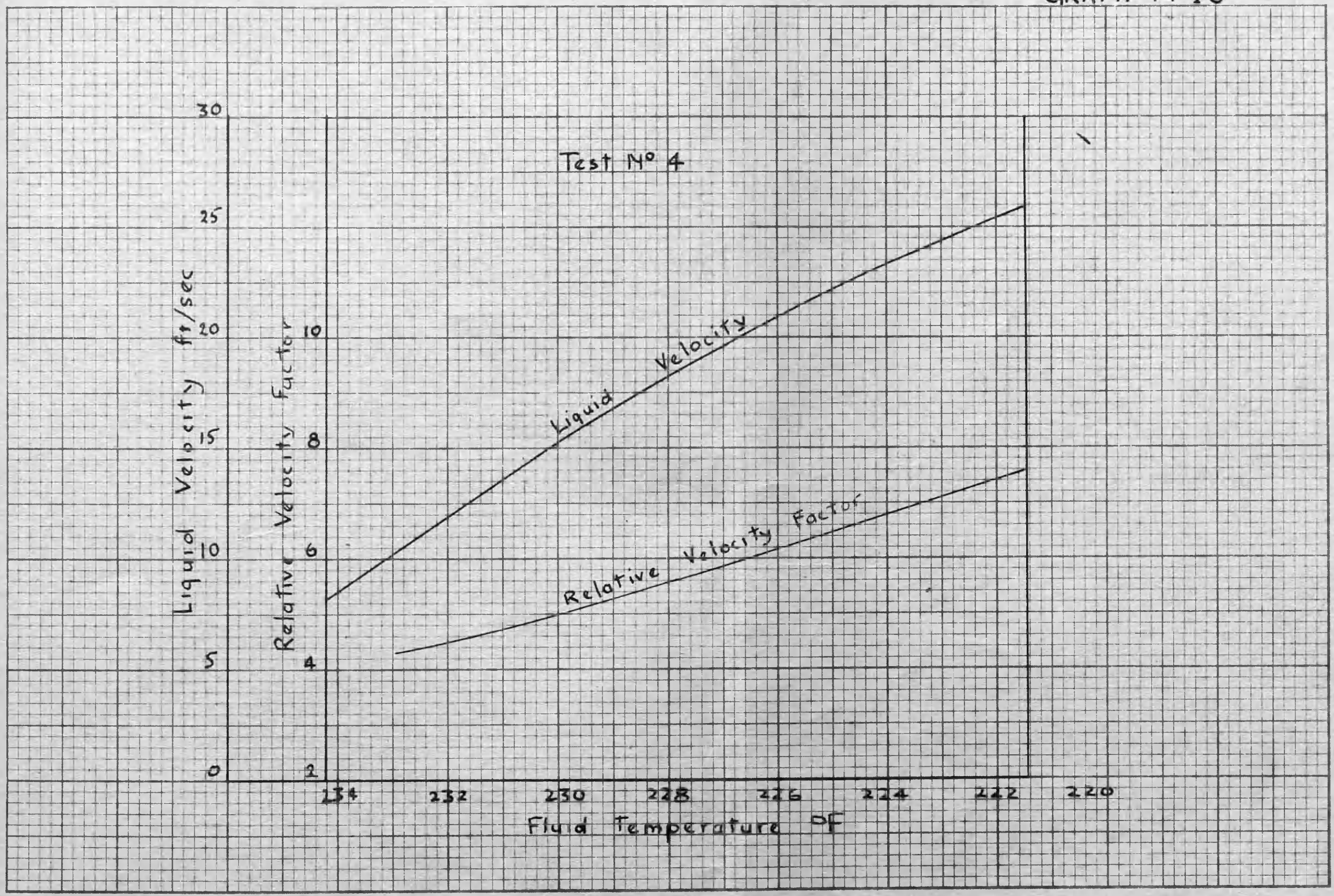

GRAPH N° 17

Test Nos 1 to 4.

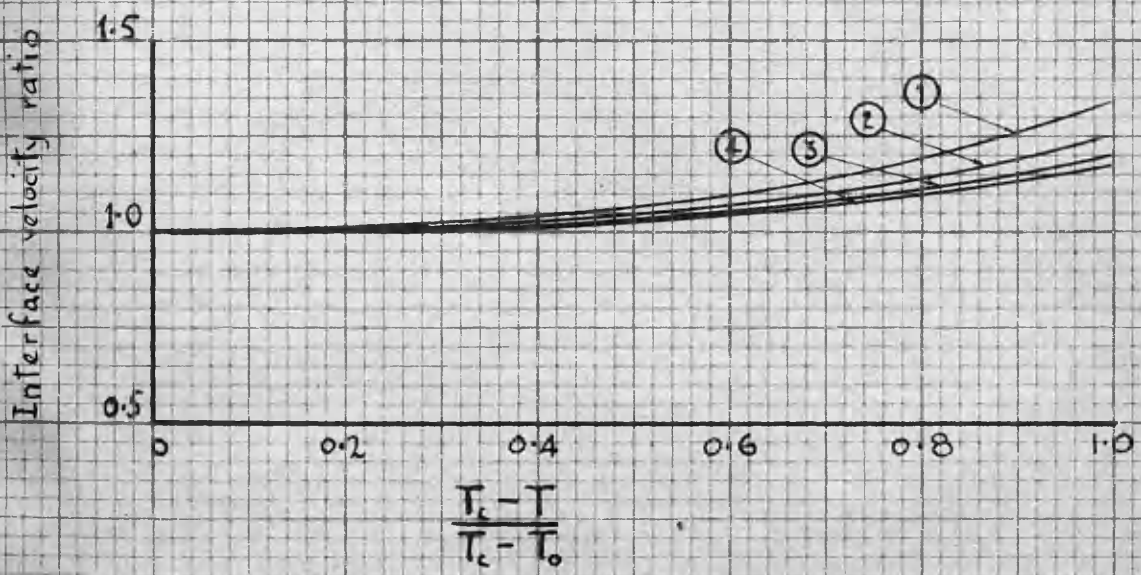

GRAPH 17 Interface velocity ratio as an empirical function of temperature for tests 1 to 4.

GRAPH N° 1

GRAPH Nº 18

Test Nº 5

Liquid Velocity ft/sec

Relative Velocity Factor

35
30
25
20
15
10
5
0

10
8
6
4
2

Liquid Velocity

Relative Velocity Factor

234 232 230 228 226 224 222 220 218 216 214 212

Fluid temperature °F

GRAPH N 19

GRAPH Nº 19

Test Nº 6

Liquid Velocity

Relative Velocity Factor

Liquid Velocity ft/sec

Relative Velocity Factor

35
30
25
20
15
10
5
0

234 232 230 228 226 224 222 220 218 216 214 212

Fluid temperature °F

GRAPH Nº 2

GRAPH Nº 20

Test A107

Liquid Velocity ft/sec.

Relative velocity Factor

$V_R = 10 \sqrt{T_f}$

Liquid

Relative Velocity Factor

30
25
20
15
10
5
0

8
6
4
2

232 230 228 226 224 222 220 218 216 214

Fluid temperature °F

GRAPH N°21

GRAPH NO 21

Test NO 8

Liquid Velocity ft/sec

Relative Velocity Factor

30
25
20
15
10
5
0

10
8
6
4
2

Liquid Velocity

Relative Velocity Factor

238 236 234 232 230 228 226 224

Fluid temperature °F

GRAPH N° 22

GRAPH N° 22

Test N° 5

Predicted temperature curve compared with experimental points on a base of tube distance.

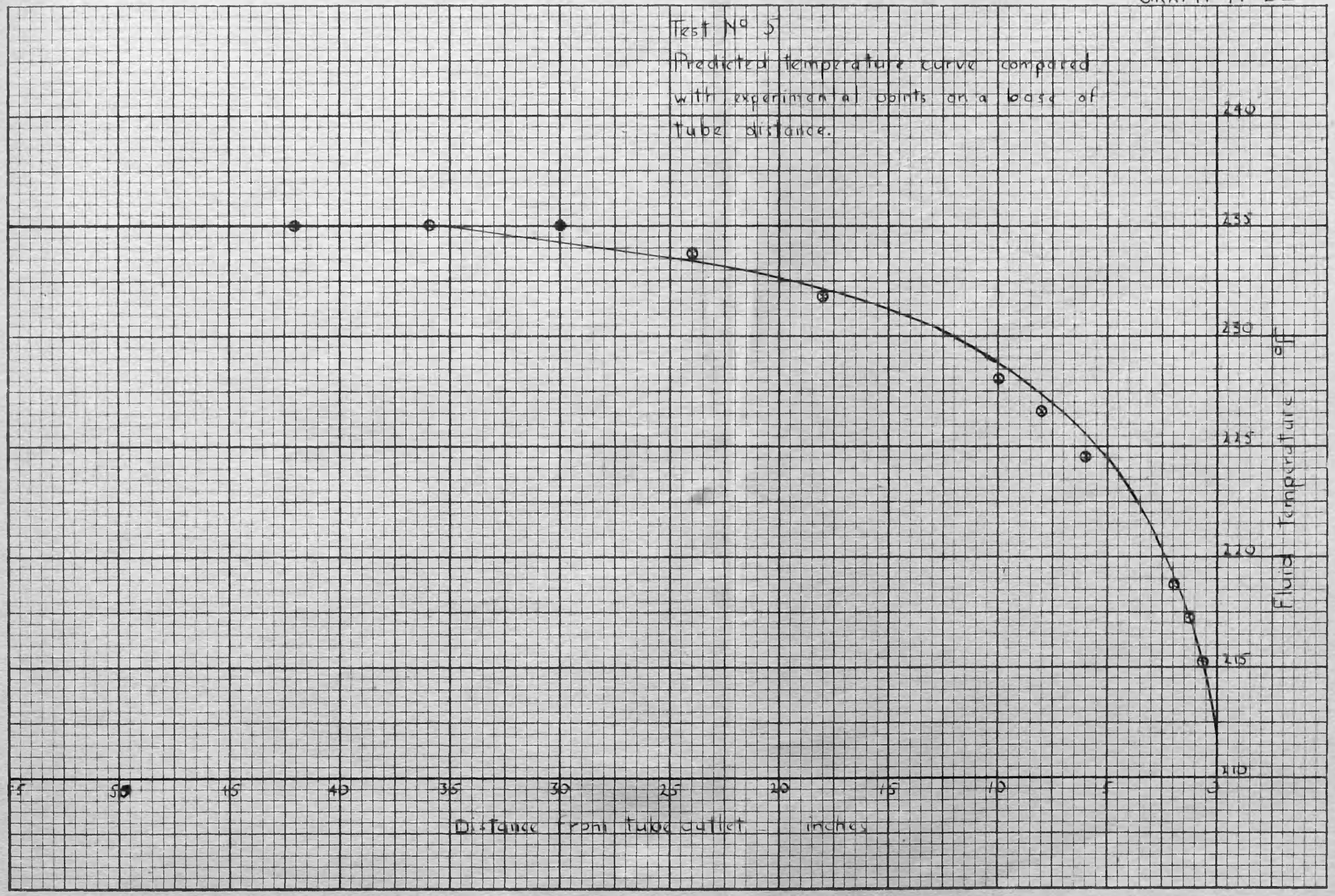

GRAPH N° 23.

GRAPH N°23

Test N°6

Predicted temperature curve compared with experimental points on a base of tube distance

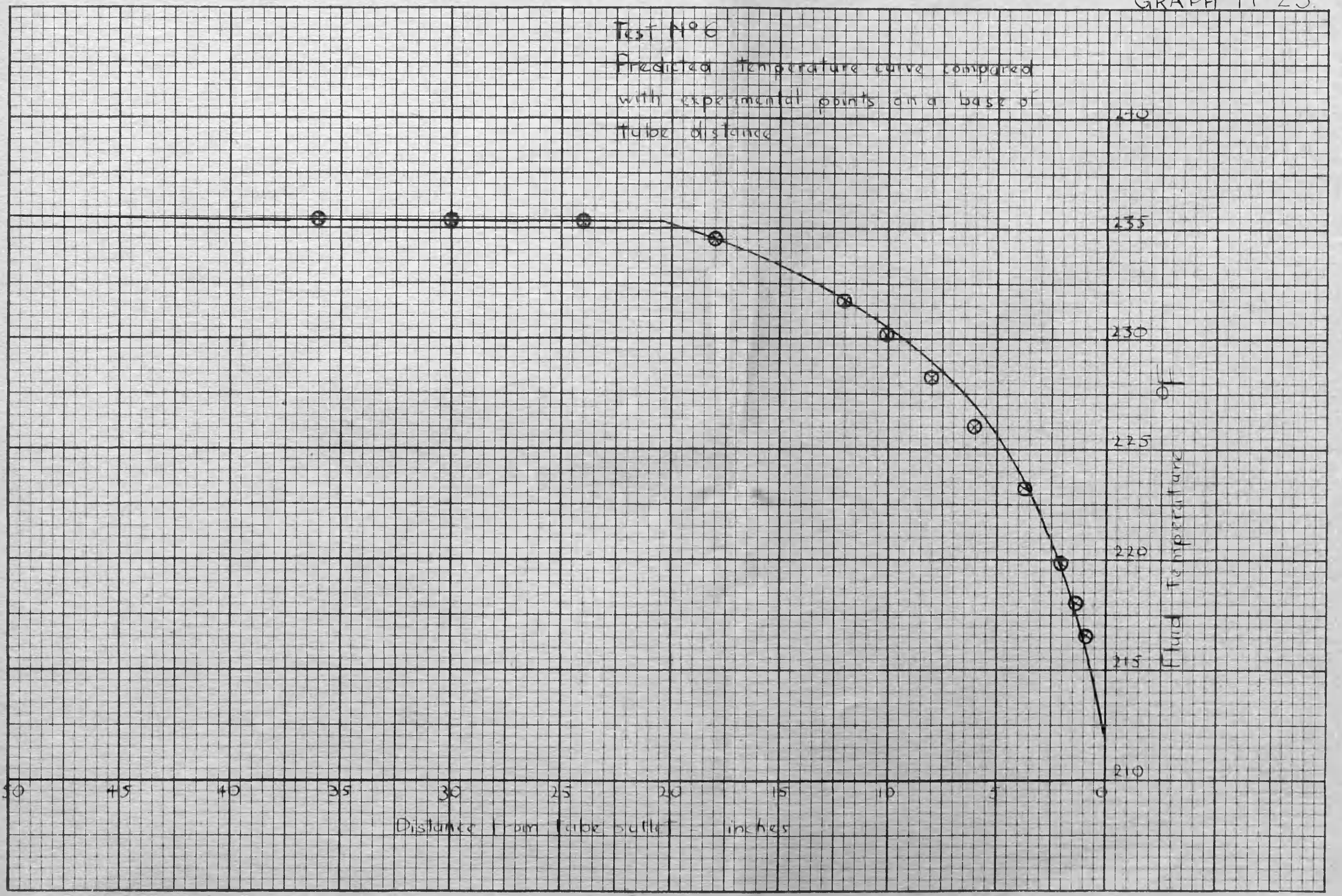

GRAPH N° 24.

GRAPH N° 24.

Test N° 7

Predicted temperature curve compared with experimental points on a base of tube distance.

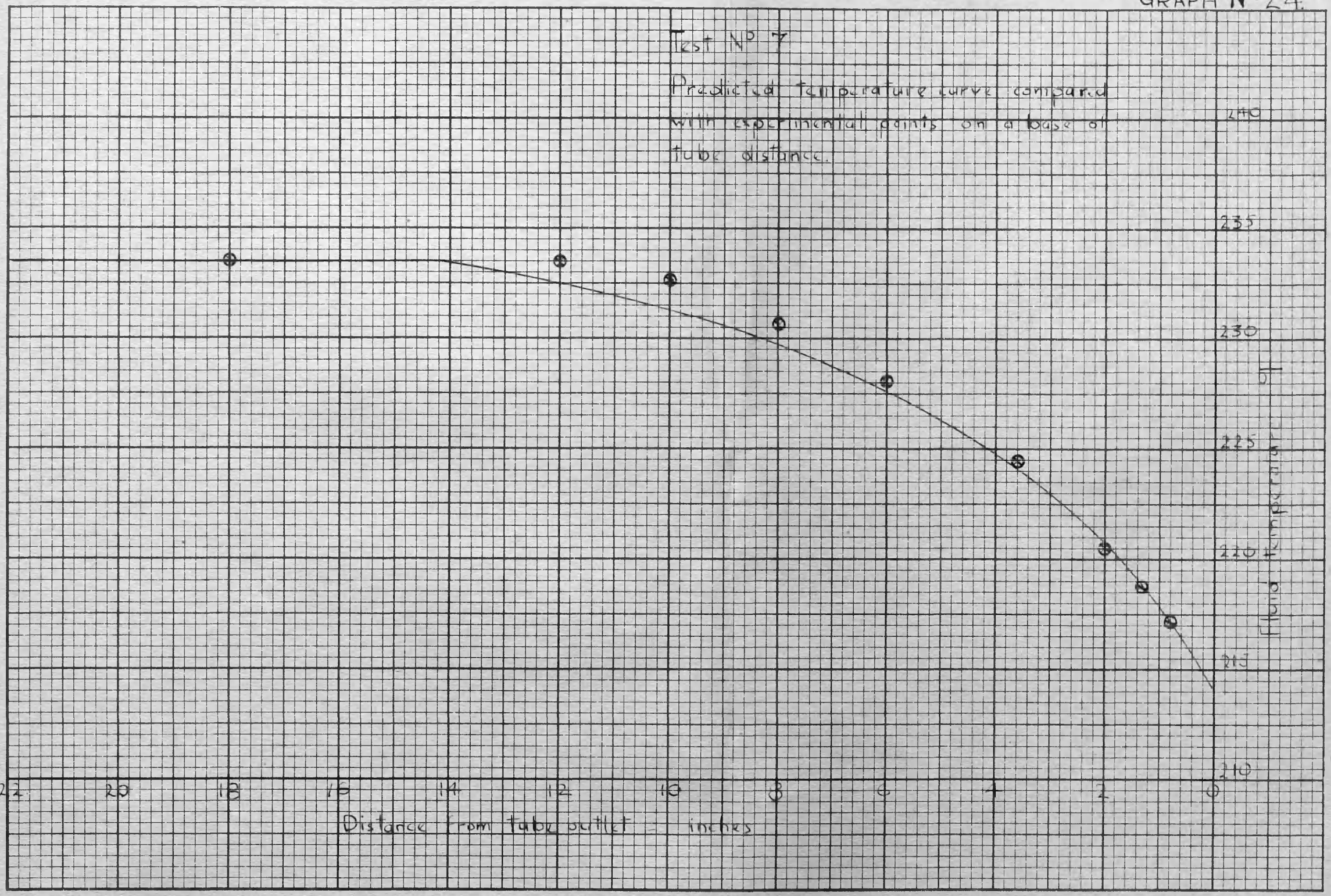

GRAPH N°25

GRAPH N°. 25

Test N° 8

Predicted temperature curve compared with experimental points on a base of tube distance.

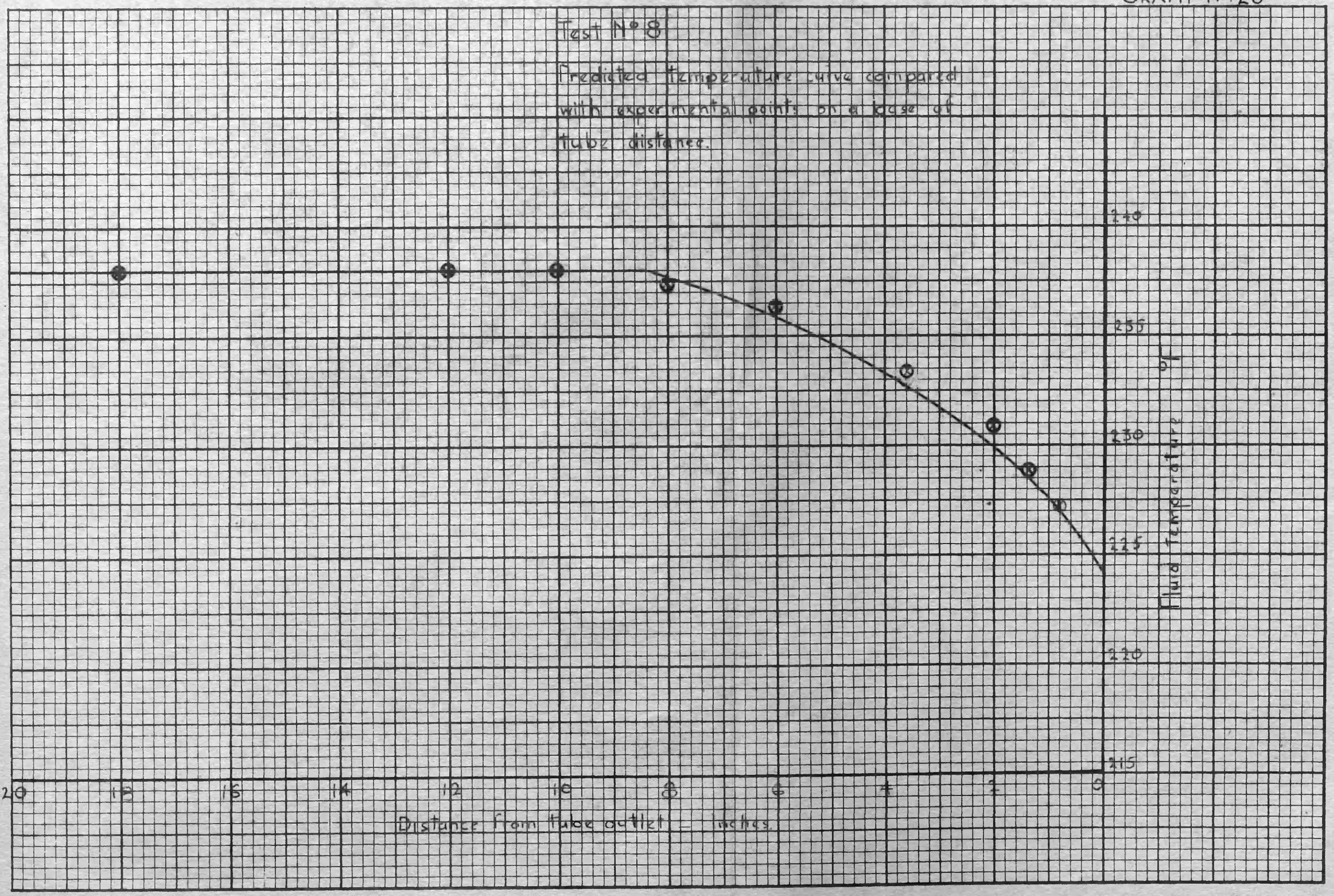

PART IV.

FREON 12 EXPERIMENTS AND ANALYSIS.

AIM AND SCOPE OF THE EXPERIMENTS.

As indicated by the review prefacing this report, a considerable amount of reliable expirical data has been acquired on the flow of evaporating freon 12 in connection with the capillary tube restrictor. None of these investigations concerned itself with the flow form adopted, but implicitly assumed the fluid to behave as though it were a homogeneous mixture. It is necessary to resolve this issue before making further studies of the problem and accordingly it is the primary object of the present investigation to obtain the data required for the purpose.

The thermodynamic properties of freon 12 are markedly different from those of water. A calculation of relative velocity factor based on the assumption of annular flow gives a value which is almost constant at 1.25 throughout expansion in the normal range of temperature. On the assumption of separated flow the value is slightly smaller.

The properties of the fluid do not therefore demand a high relative velocity between the phases and it would appear that the frothing form of flow is a possibility.

The difference between fluid momenta and temperature distributions for the various flow forms are too small to provide a positive determination. The corresponding critical outlet conditions are, however, widely divergent and it is this quantity which supplies the required criterion.

Capillary tubes of various internal diameters were tried in the apparatus. It was found that the compressor capacity was too small to produce critical outlet conditions on a 0.06" tube, while with a .03" tube steady conditions could only be attained running the compressor at an inconveniently low speed. The 0.042" tube provided the most satisfactory running conditions and it is on this tube that most of the experimental data were obtained.

Visual data were obtained by observing and photographing flow in a pyrex tube.

APPARATUS.

Figures 21 and 22 show a photograph and general layout of the apparatus respectively. The circulating freon 12 on leaving the compressor may flow through or bye-pass the oil separator according to the valve setting. Oil from the separator collects in the reservoir and is metered back to the sump via a reducing valve. After flowing through the water-supplied condenser and sub-cooler the refrigerant may pass to the drier and expansion valve or alternatively to the capillary tube, and thence through the evaporator to the compresser.

Thus the experimental apparatus consists of a standard refrigerator test unit having a capillary tube in parallel with the expansion valve.

When the unit is operating on the capillary tube the stable condition is very sensitive to the quantity of charge circulating and it is a useful feature of the apparatus that this may be conveniently fixed by using the liberally dimensioned drier as a reservoir for excess freon.

Since the refrigerator unit is standard apparatus whose function in the present experiments is limited to supplying sub-cooled freon 12 to the capillary tube and measuring the rate of mass circulation, a brief description of its component parts will suffice.

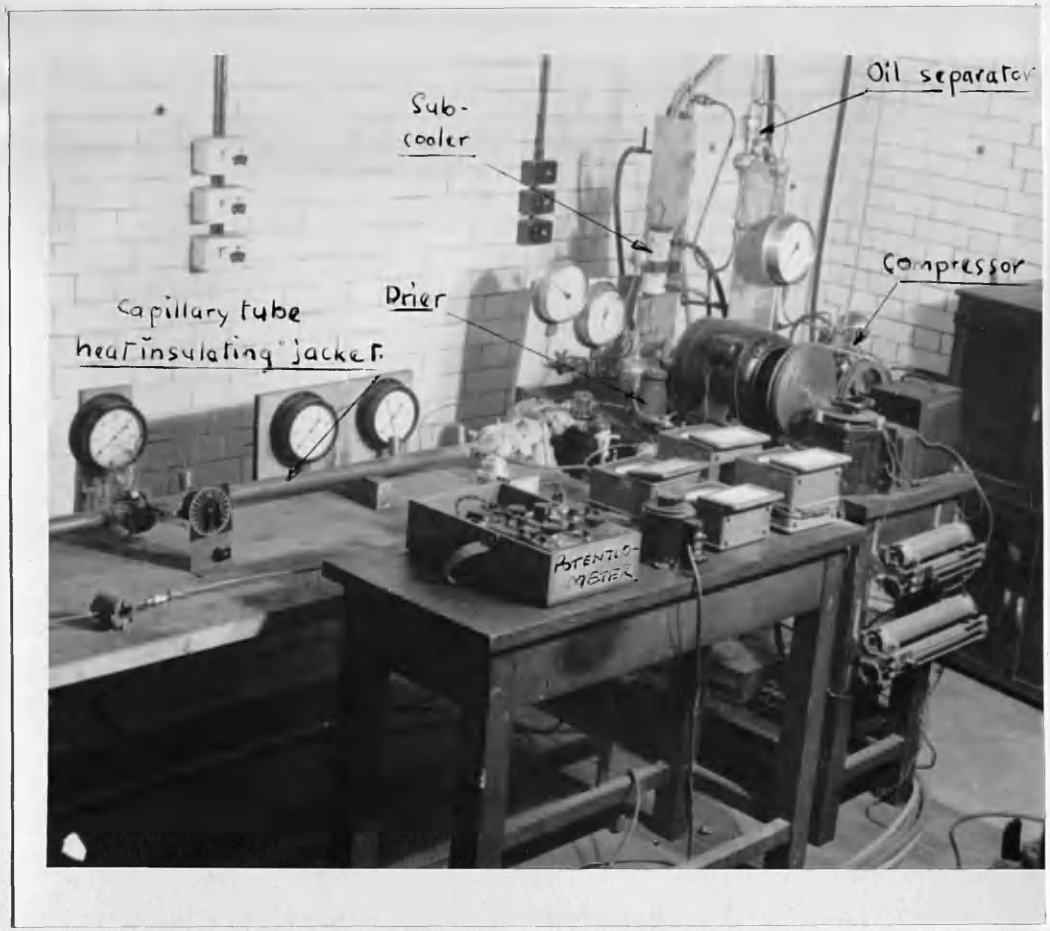

Figure 21. Freon apparatus.

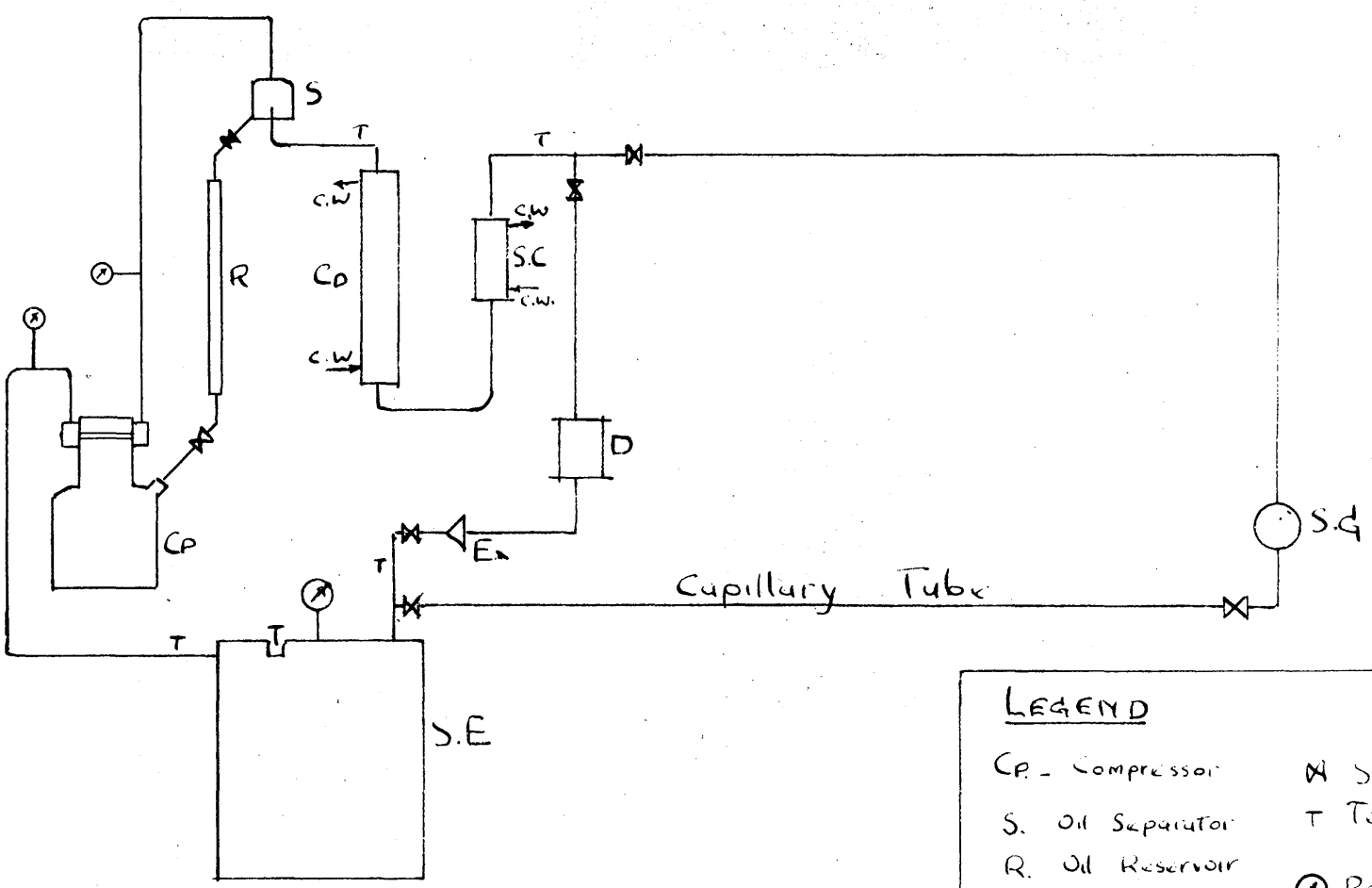

LEGEND

Cp. - Compressor
S. Oil Separator
R. Oil Reservoir
Co. Condenser
S.C. Sub-cooler
D. Drier
Ex. Expansion Valve
S.E. Secondary Evaporator
S.G. Sight Glass
M Stop Valve
T Temperature Measurement
Ⓟ Pressure Measurement

Figure 22 Diagrammatic Arrangement of Freon 12 Test Unit

Compressor Unit.

This unit consisted of a Sterne's 'A' type compressor, 1" stroke by 1½" bore, belt driven by a D.C. variable speed fractional horse-power motor. The standard rating for the compressor is 500 r.p.m. but it may quite safely be run at speeds up to 1500 r.p.m. for short periods.

The speed of the unit was controlled manually by rheostat, a stroboscope being used as the reference.

Oil Separator.

In small freon 12 refrigators the design is usually such as to encourage oil circulation throughout the unit. For the present tests it was desired to limit this effect to a minimum and to achieve this a "Supreme Vortex" oil separator was fitted in the vapour line immediately following the compressor.

This separator achieves its effect by means of a vane ring so proportioned that it induces a high whirl velocity in the fluid without serious loss of pressure. The relatively dense oil particles are thrown against the wall of the separator casing and drain into a reservoir, made from a boiler sight glass. Since there was a considerable quantity of freon dissolved in the separated oil it was necessary to meter the mixture back to the compressor sump at a steady rate. Figure 24, is a sketch of the separator and reservoir.

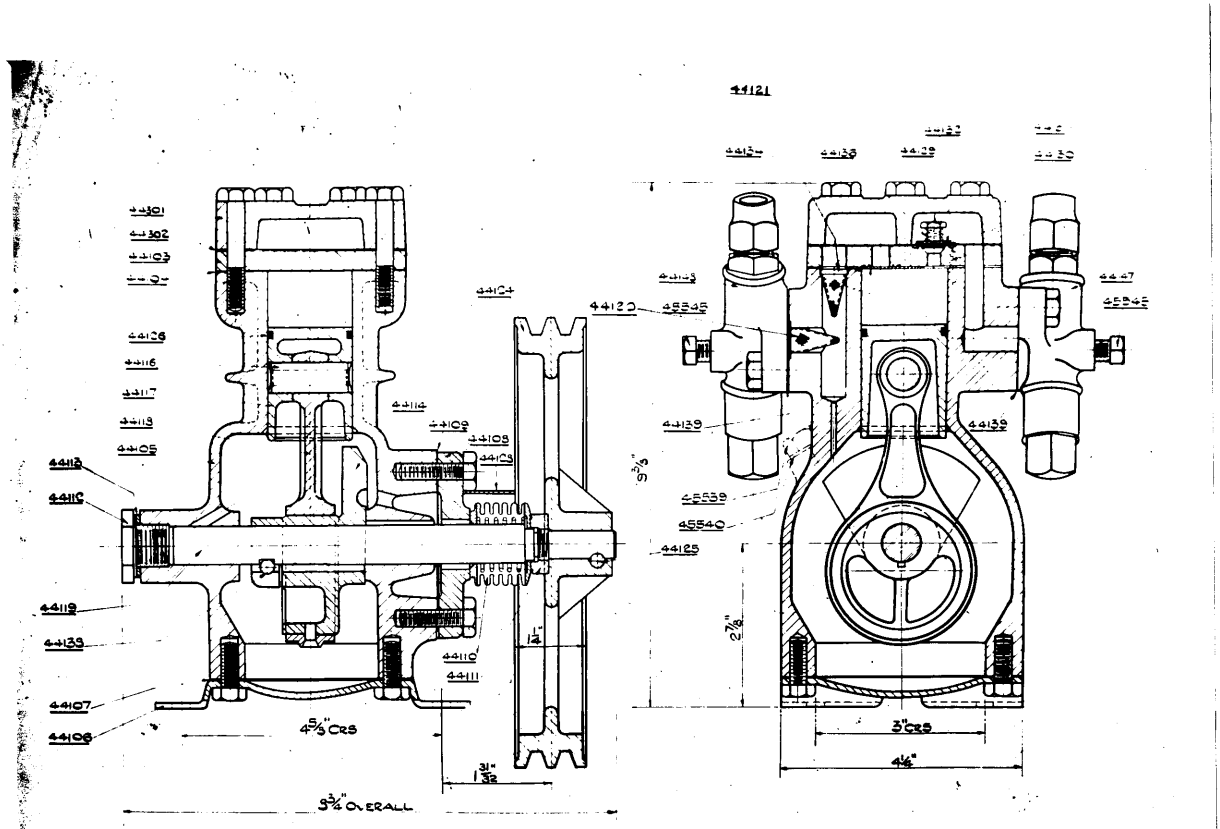

Figure 23. Compressor arrangement.

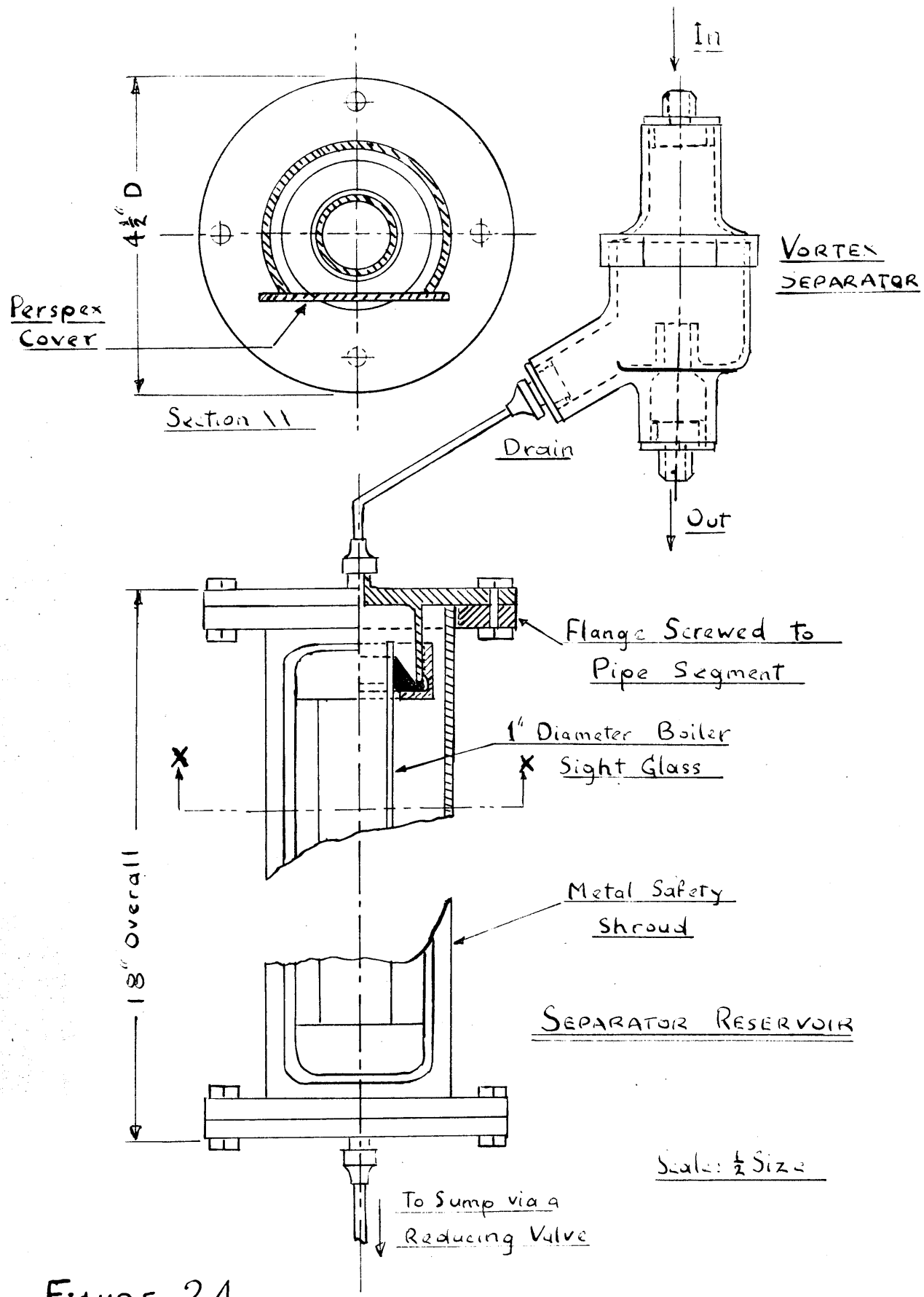
In
4½" D
Perspex Cover
Section XX
VORTEX SEPARATOR
Drain
Out
Flange Screwed to Pipe Segment
1" Diameter Boiler Sight Glass
X
X
18" Overall
Metal Safety Shroud
SEPARATOR RESERVOIR
Scale: ½ Size
To Sump via a Reducing Valve

FIGURE 24

Condenser and Sub-Cooler.

The condenser consisted of a cylindrical vessel $2\frac{1}{2}$" x 14", containing a coil of copper tubing through which the refrigerant passed. The condenser was supplied with water from a constant head tank.

The sub-cooler was of similar construction but smaller in size, and had an independent supply of water.

It was found convenient to separate the functions of condensing and sub-cooling because of the controlling influence exercised by the condenser on the high-side pressure.

Drier.

A minute quantity of moisture is sufficient to cause serious troubles in the operation of a refrigerator having freon 12 as refrigerant. Before charging, the present set-up was carefully dried by circulating it with nitrogen and subsequently connecting it to a vacuum pump for a period of 24 hours. As an extra safe-guard a drier containing silica-gel was placed in the liquid line.

Expansion Valve.

The expansion valve was of the constant pressure diaphragm operated type. The seat diameter was 0.04", and the maxium capacity at 20°F evaporating temperature and 100°F condensing temperature, was 5000 BTU/hr.

The Evaporator and Mass Flow Measurement.

The secondary evaporator is an example of a standard piece of apparatus which is almost unique in that all its characteristics are advantageous to its purpose.

It is simple in construction, quickly brings the unit to its stable condition and provides an accurate means of measuring mass flow.

Figure 25, is a sketch of the evaporator. It consists of a closed cylindrical tank having an electrical heater element immersed in the secondary fluid. The coiled tubing which carries the primary refrigerant occupies the vapour filled volume above the heater element.

When in operation the secondary fluid condenses on the primary coil and drips back to the bottom of the tank to repeat the cycle. The heat supply is adjusted to maintain the secondary fluid at atmospheric temperature, thereby entirely eliminating heat exchange with the environment. The small temperature difference is compensated for by the large heat transfer coefficients associated with condensation and evaporation. The low temperature of the heat source has the additional advantage that it enables easy control of the amount of superheat imparted to the primary vapour. Provided the available heat transfer area is ample for the capacity of the unit, the primary vapour always leaves the evaporator at a temperature just below that of the secondary fluid.

A sensitive pressure or temperature measurement of the secondary fluid is a necessary guide to the control of heat

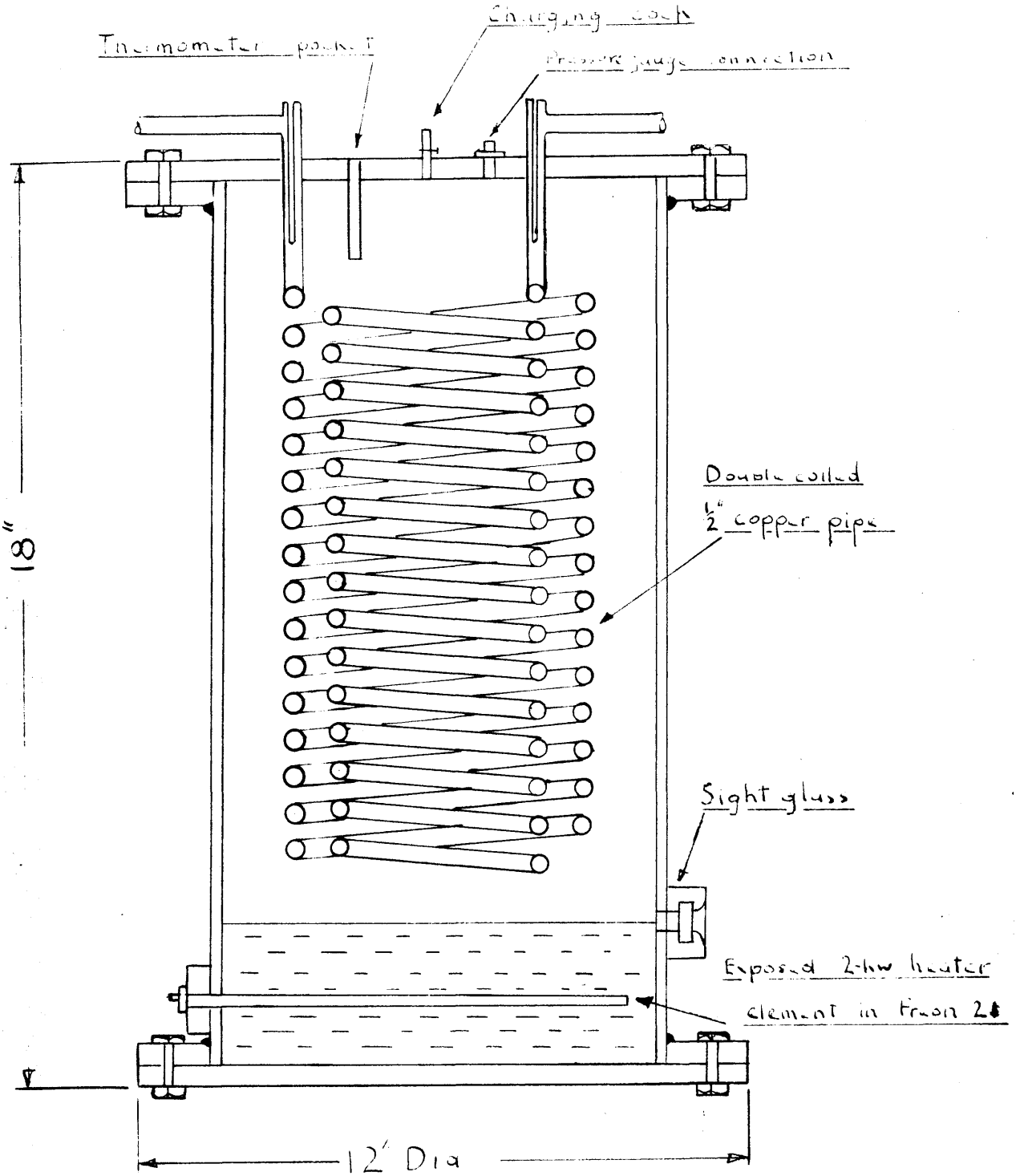

FIGURE 25. Secondary evaporator

input.

Finally, the response of the secondary evaporator to altered conditions is immediate and consistent.

Because of its high electrical resistance and low saturation pressure at atmospheric temperatures, freon 21 was used as the secondary fluid in the present instance.

The calculation of mass flow is based on a simple heat balance. The accuracy of the result depends on that of the electrical power measurement and also on the accuracy of the Thermodynamic data.

The electrical instruments used were substandard and were reckoned to have a combined accuracy of ± 1.2%, this being inclusive of parallax.

The Capillary Tube and Associated Apparatus.

Two different tubes of .060" bore and .042" bore respectively, were used in the tests. With the former, pressure and temperature measurements were made and with the latter, temperature only, it being observed from the first set of measurements that pressures and temperatures during expansion were in agreement.

The techniques and apparatus employed for these measurements were identical with those used for the water tests and are described in a previous section. Figure 26, shows the distribution of thermocouples and pressure taps for the tubes.

Before being fitted to the circuit each capillary tube was degreased and cleaned with alcohol and dried with nitrogen.

0·060" Tube. Scale: 1/20th

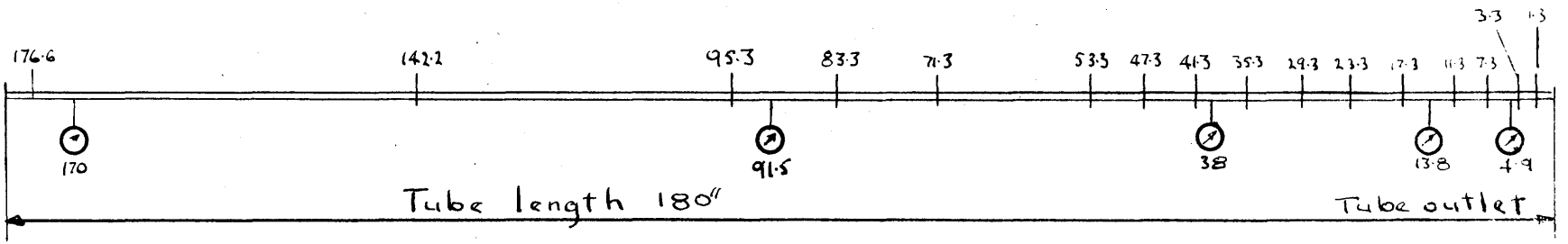

0·042" Tube. Scale: 1/4 and 1/20th

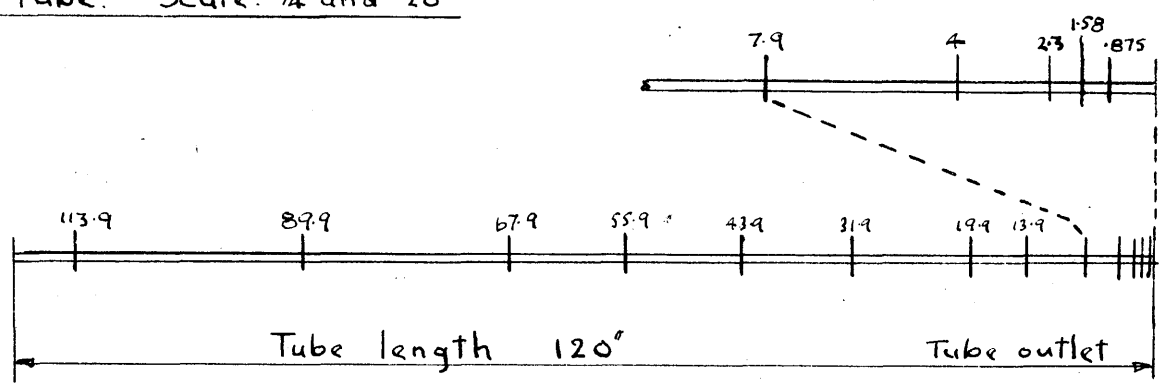

FIGURE 26 Thermocouple and pressure-tap distribution on Freon tubes

The ends were carefully finished by stoning and examined under a magnifying lens for small rags.

In order to assess the effective roughness and check for partial blockage by pressure tap rags the .06" bore tube was tested with dry nitrogen supplied from a pressure cylinder via an automatic reducing valve, mass flow and pressure drop being measured over a fair range of Reynold numbers. Figure 27, shows the friction factors thus obtained to a base of Reynold's number.

During normal test conditions the refrigerant fluid in a capillary tube falls below the freezing point of water and as a consequence the last two or three feet of tube becomes externally covered with dew or frost, the latter giving up unknown quantities of latent heat. To overcome this difficulty the last six feet of tube were enclosed in a gas-tight jacket made from $2\frac{1}{2}$" diameter copper tubing, the jacket being filled with nitrogen whose measured dew point was -40°F. Figure 28, is a sketch of the arrangement. The capillary tube was centralised in the jacket by means of a number of 3 - legged supports made of stiff rubber and the thermocouple leads were taken out between thick rubber gaskets covered with a layer of vacuum grease. In order to reduce heat gain at the pressure gauge leads and tube exit, advantage was taken of the neoprene seals to make a break in the continuity of the copper.

With this arrangement the heat gain per foot length of tube for a temperature difference of 30 F° was estimated at about .001 BTU/sec.ft. The corresponding heat gain at the tube

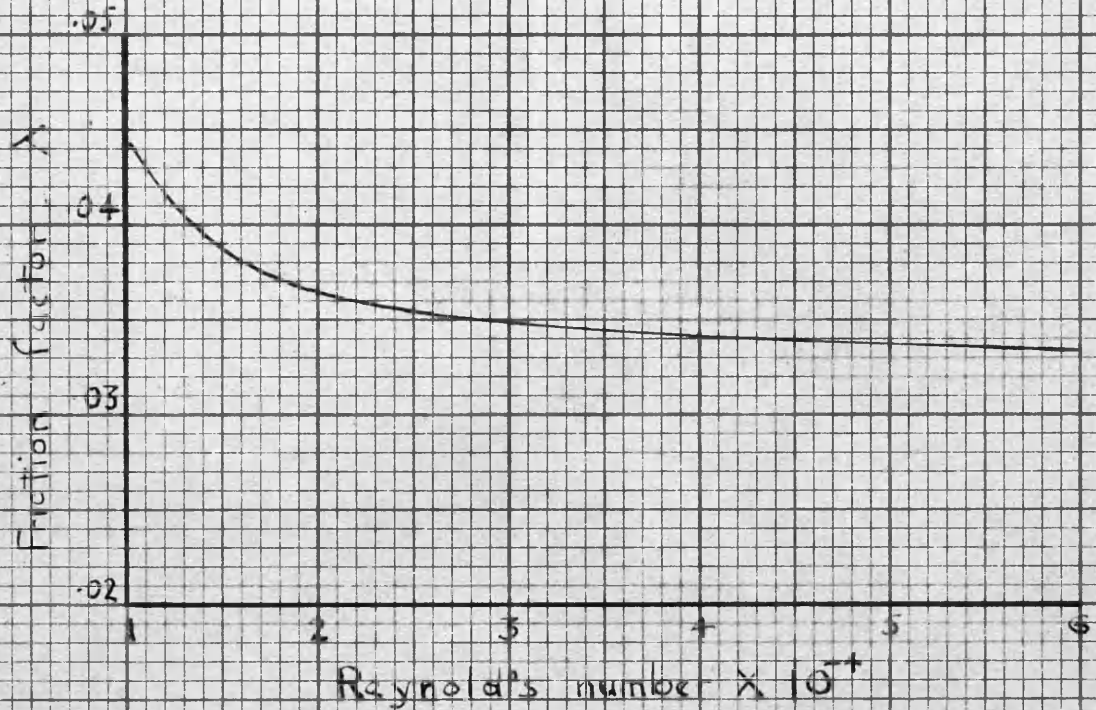

FIGURE 27. Friction factors for the .060" bore tube based on flow tests with nitrogen.

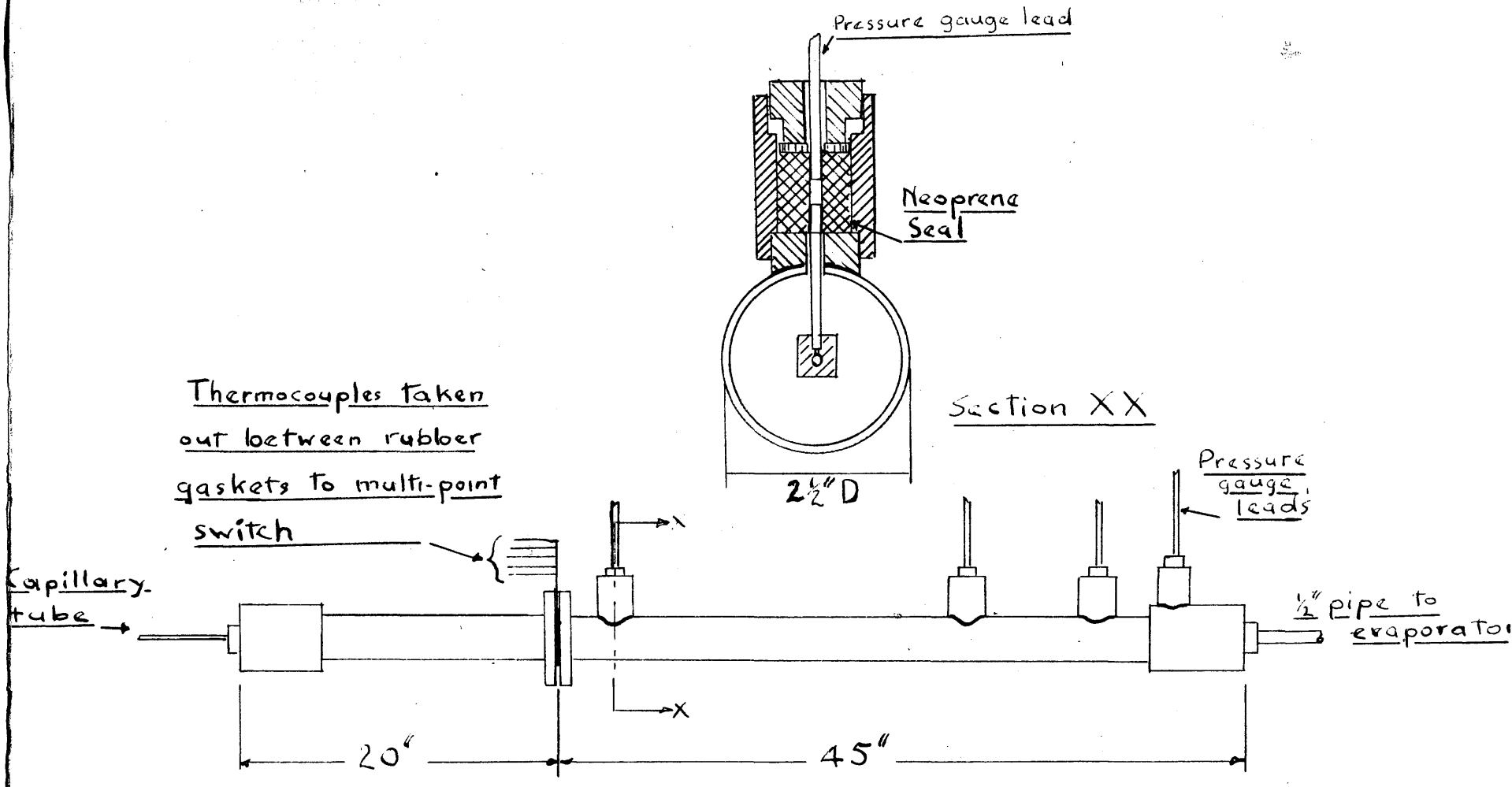

FIGURE 28 Capillary tube jacket.

exit and pressure gauge leads was .00004 BTU/sec. which is negligible.

PROCEDURE.

Tests were carried out over a range of delivery pressures between 110 and 160 lbs/in.^{2} absolute providing a mass flow range of 450 to 950 lbs/ft.^{2}sec.

It is impossible to pre-set the conditions for a refrigerator test because of the complex inter-relation between the quantities controlled by the operator. Increase in compressor speed tends to increase mass flow and delivery pressure, and the same effect is achieved by increase of charge quantity. Increase of the rate of condensation decreases delivery pressure and mass flow but increase in the degree of sub-cooling causes an increase in mass-flow rate.

The following procedure was adopted during testing. The compressor speed and cooling water supply to the condenser and sub-cooler were fixed and the circulating charge increased until the sight-glass before the capillary tube showed full bore flow. The electrical input to the evaporator was adjusted to maintain the secondary fluid at its saturation pressure corresponding to atmospheric temperature and the conditions thus obtained were accepted for testing. From this starting point, different test conditions were obtained by slightly varying one or other of the controllable quantities in the required direction. A particular set of test conditions were accepted as steady when the unit ran for $\frac{1}{2}$ an hour without variation.

The following quantities were recorded in repeating sequence during test:-

(1) Tube temperatures.

(2) Tube pressures.

(3) Electrical input to the evaporator.

(4) Evaporator primary pressure and temperature.

(5) Evaporator secondary pressure.

(6) Delivery pressure and temperature.

(7) Compressor speed.

PRESENTATION OF FREON 12 RESULTS.

Temperature distributions and corresponding mass flows are given for a series of tests on the .06" and .042" tubes in graphs 26 to 40. Tables 8 and 9 present critical outlet measurements and compare these with values predicted on the assumption of frothing flow, while Table 10 compares measured fluid pressures and saturation pressures corresponding to measured fluid temperatures.

Figure 29 is a photograph of evaporating freon 12 flowing in a 0.06" bore pyrex tube.

No independantly published data on critical outlet conditions for freon 12 were available, although Bolstad[1] and Jordan referred to the phenomenon and indicated its occurrence in their tests. A letter sent to these experimenters requesting quantitative information received no reply.

Visual Data.

The only fact which can be deduced from the photograph of Figure 29, is that the liquid and vapour do not separate and the appearance is that of full bore flow. In addition, observation by eye revealed no sign of slugging flow. The fluid entered the .06" bore glass tube as a clear colourless liquid becoming slightly milky in appearance at the point of evaporation. In a distance of a few inches this changed to an opaque whiteness, the appearance remaining unaltered for the r emainder of the expansion within the tube.

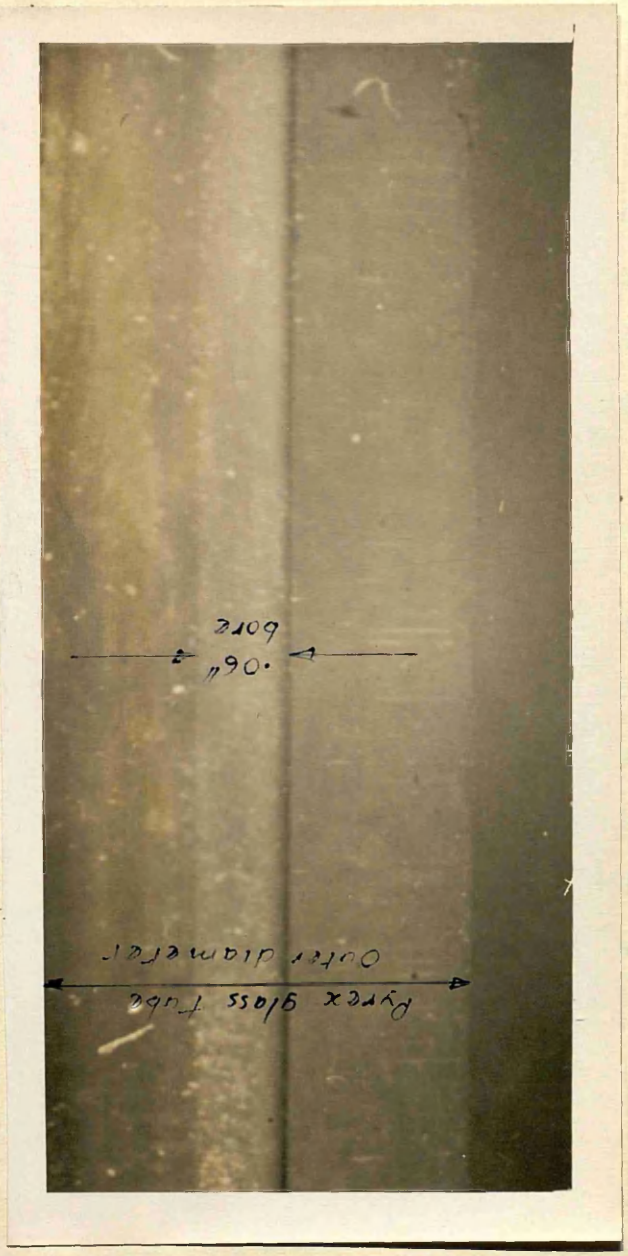

Figure 29. Evaporating flow of freon 12 in a pyrex tube of .06" bore.

ANALYSIS OF FREON 12 TESTS.

Critical Outlet Conditions.

The methods employed in constructing the critical outlet chart for freon 12 on the assumption of frothing flow are given in Appendix 8. Two charts are shown in Figures 30 and 31. It is noted here that of the two charts prepared relating critical mass flow and critical outlet temperture to, in the one case, outlet quality, and in the other, initial evaporation temperature, only the first is exact.

The second chart is derived from the first via the approximate equation

$$q = \frac{q_{\phi} + q_{H}}{2} \quad , \qquad (22)$$

this receiving general justification in Appendix 1. In order to assess the magnitude of this approximation calculations on a typical expansion, 70°F. to 20°F., were made, the result being shown graphically in Figure 32. The error involved is dependent on mass flow but in the range of experiments does not exceed $\pm$ 2%. In terms of temperature this is equivalent to $\pm$ 1°F. or in term of mass flow about $\pm$ 1.3%. These figures are of the same order as the experimental error and the approximation is considered satisfactory.

A critical outlet chart for annular or separated flow was not prepared since the experimental data correlated well with values predicted on the basis of frothing flow. However, in order to obtain an idea of the theoretical divergence between the

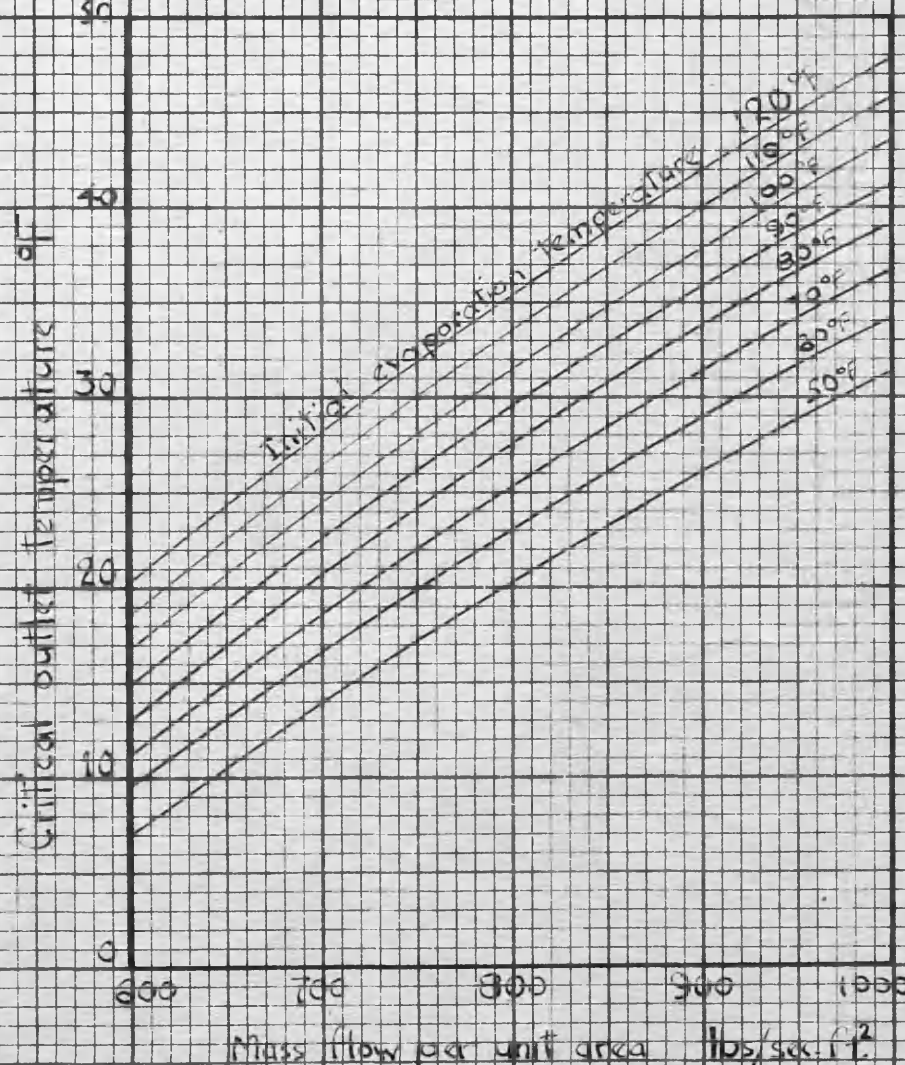

FIGURE 30. Critical outlet temperature charts for evaporating freon 12 flowing in horizontal pipes, under adiabatic conditions.

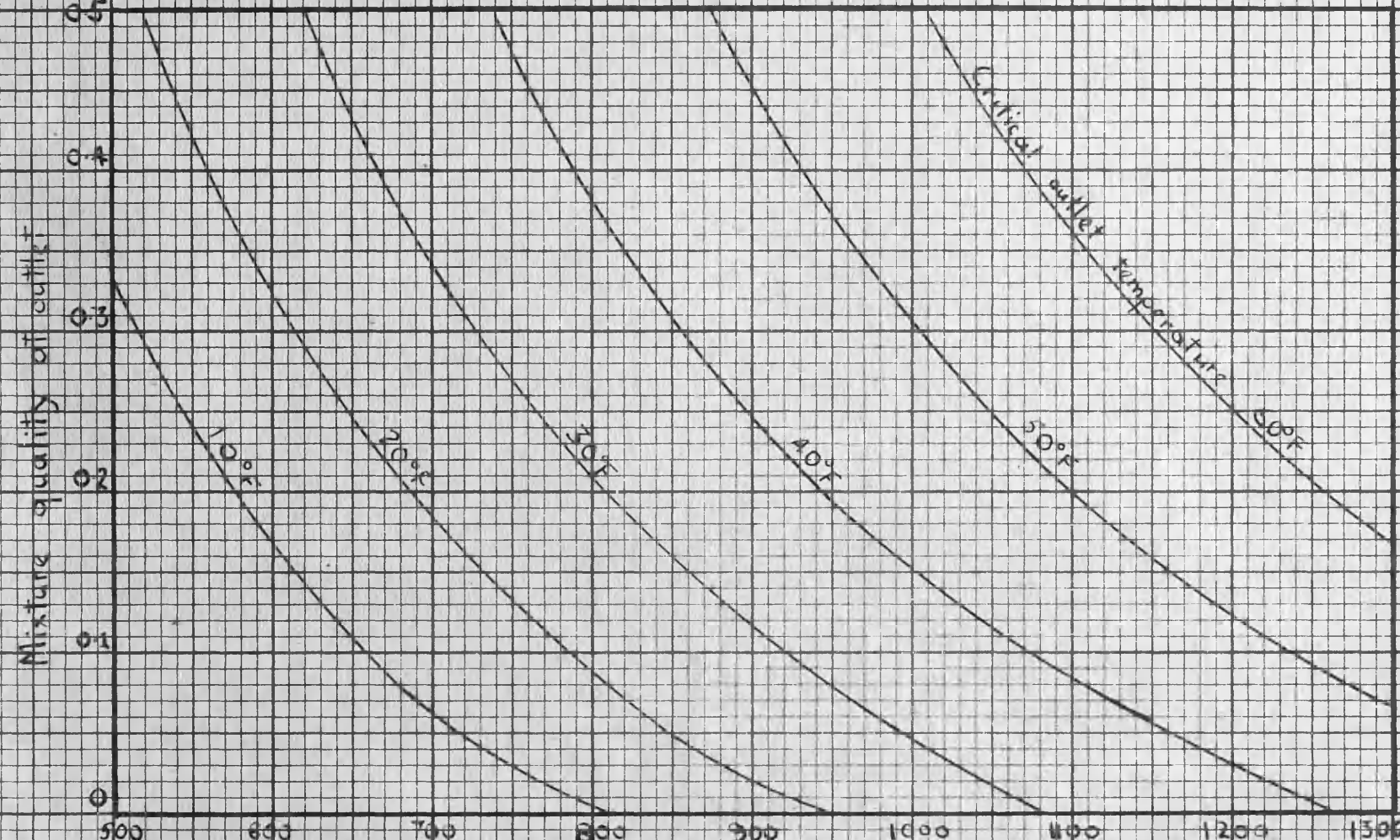

FIGURE 31. Critical outlet chart for evaporating freon 12 flowing in horizontal pipes under adiabatic conditions

two forms, A typical expansion was calculated and gave the following comparison.

Initial Evaporation Temperature.	Critical Outlet Temperature.	Critical Mass Flows.	
		Frothing.	Annular or Separated.
82°F.	20°F.	688 lbs/ ft²sec.	965 lbs/ ft²sec.

The theoretical critical mass flow for annular or separated flow under these conditions is 41% greater than that for frothing flow.

The above comparison between annular and frothing flow is expressed in terms of critical outlet temperatures below:

Initial Evaporation Temperature.	Critical Mass Flow.	Critical Outlet Temperatures.	
		Frothing.	Annular or Separated.
82°F.	965 lbs/ ft²sec.	38°F.	30°F.

It is not possible to make an exact estimate of what may be considered an acceptable correlation between measured and predicted critical mass flows. The following estimates, which are expressed as an equivalent percentage error in mass flow per unit area, are liberal.

Equivalent percentage error in term of mass flow:-

Power input to evaporation ± 1.2%.

Critical Outlet Temperature ± 1.0%.

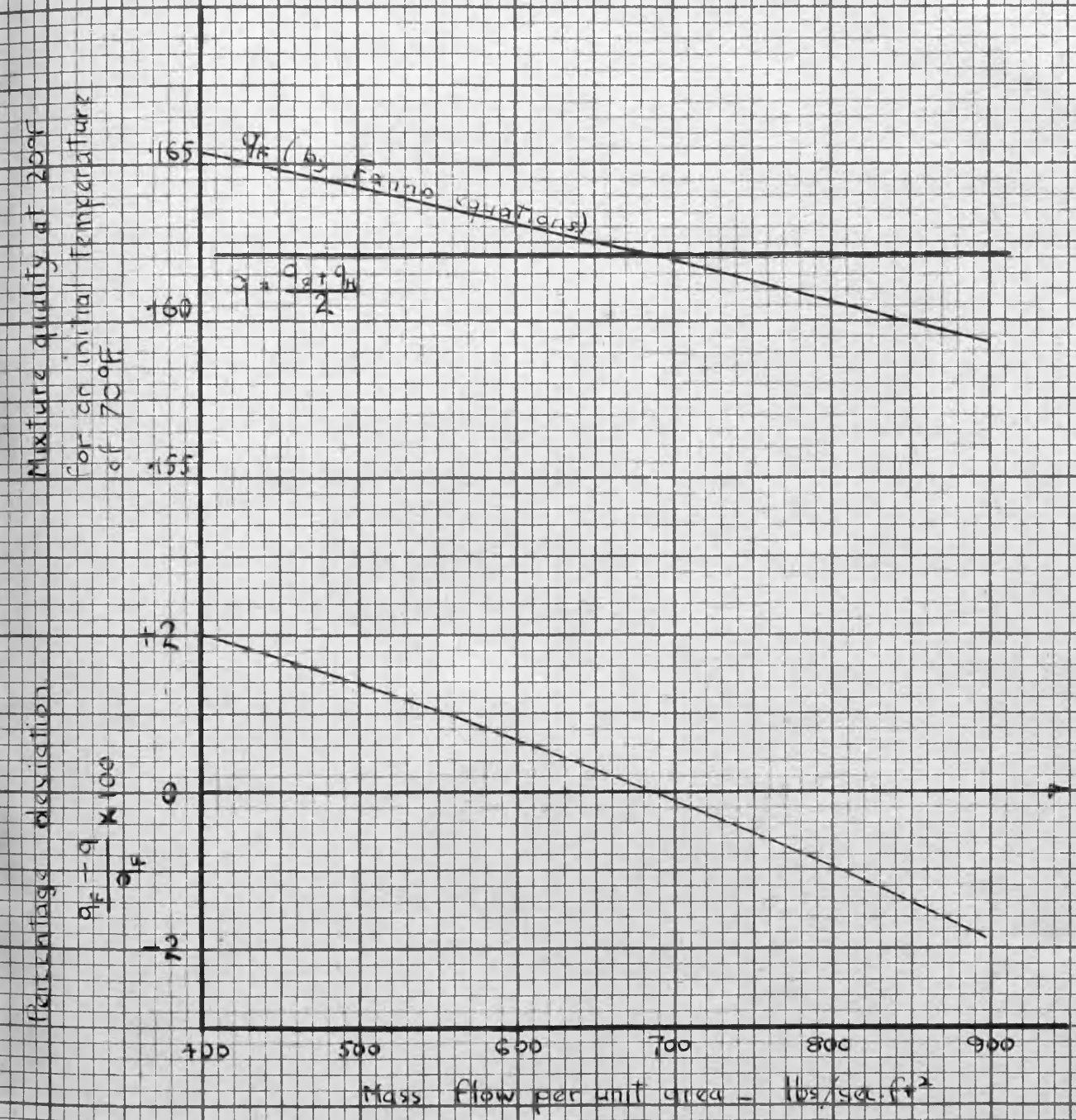

FIGURE 32. Illustrating the accuracy of the quality approximation in a typical case, and also its relation to mass flow per unit area

Initial evaporation temperature	± 0.4%.
Estimated increase in total heat pher lb. of fluid in evaporator	± 0.5%.
Accuracy of predicted mass flow	± 1.5%.

In addition to the accidental errors listed above, which total ± 4.6%, the following sources of error might produce a constant deviation.

Area of tube bore	0.3%.
Published thermodynamic data on F 12 -	Unknown.
Criculating oil not removed by separator -	Unknown - probably negligible.

It is reckoned that the overall correlation should be within ± 5% in terms of mass flow.

In the range of test conditions encountered this is equivalent to about ± 3°F. on critical outlet temperature.

Test No.	MEASURED VALUES			PREDICTED
	Mass Flow lb/sec.ft^2	Initial Temp. $^oF.$	Outlet Temp. T_o $^oF.$	Theoretical Outlet Temp. T_o $^oF.$
19	632	73	15	14.5
20	654	77.7	15	16.5
21	688	72.8	20	18.3
22	698	79	20	20
23	714	81	22	22
24	716	86	24	23
25	732	77.5	23	22.2
26	834	65.5	28.5	26.5
27	858	73	28	29.6
28	913	76.8	34.5	33.8
29	960	64.9	32	33.6
30	965	96.2	40.2	40.8

Table 8. Freon 12 tests on 0.042" tube.

Comparison of measured critical outlet temperatures with these predicted on the assumption of frothing flow.

Test No.	Measured Values				Theoretical Mass Flow lb/sec.ft^2	Percentage Difference.
	Initial Temp. °F.	Outlet Temp. °F.	Evaporator Temp. °F.	Mass Flow lbs/sec. ft^2		
19	73	15	-4	632	640	-1.25
20	77.7	15	8.5	654	630	3.8
21	72.8	20	7	688	715	- 3.8
22	7.9	20	0.5	698	695	0.4
23	81	22	3.0	714	716	- .3
24	86	24	4.8	716	736	-2.7
25	77.5	23	12	732	745	-1.8
26	65.5	28.5	17.5	834	870	-4.1
27	73	28	15	858	835	2.8
28	7.8	34.5	19	913	940	-2.8
29	64.9	32	26.5	960	940	2.1
30	96.2	40	28	965	956	1.2

Table 9. Freon 12 tests on 0.042" tube.

Percentage difference between measured mass flows and those calculated from the measured critical outlet temperatures.

Test No.	Gauge No.1. lb/in^2. abs.		Gauge No.2. lb/in^2. abs.		Gauge No.3. lb/in^2. abs.	
	Sat^n Press	Meas.Press	Sat^n Press	Meas.Press	Sat^n Press	Meas.Press
16	49.4	49.2	64.2	64.5	86.3	86.8
17	52.6	52.1	66.7	66.7	81.6	81.1
18	64.6	65.6	74.3	74.9	90.6	90.5

Pressure gauge distance from tube outlet:-

No.1. - 4.9" No.2. - 13.8" No.3. - 38"

Table 10. Freon 12 tests. Comparison of measured pressured with saturation pressures corresponding to measured temperatures.

Friction Factors.

Critical outlet data show the flow form to be frothing and consequently indicate the lines on which the problem of correlating friction factors should be approached.

It is reasonable to assume that the inertia forces and fluid heads associated with a fine froth are a function of the mean density. On the other hand the equivalent viscosity does not appear to have any clear meaning and in addition the existence of a large area of liquid-vapour interfaces makes surface tension a factor of possible importance.

From this it follows that the quantities which may influence the wall shear force, τ_o, are, tube diameter, D, fluid velocity V, mean density ρ, liquid viscosity μ_1, vapour viscosity μ_2, surface tension γ, mixture quality q.

Conforming to the usual grouping pattern this leads to :-

$$\lambda = \frac{8\tau_o}{\rho V^2} = f\left(\frac{\rho DV}{\mu_1}, \frac{\mu_1}{\mu_2}, \frac{\rho DV^2}{\gamma}, q\right)$$

It is possible that, on a basis of extensive experimental data, some of these groups might be eliminated or combined to the great simplification of the otherwise scarcely worthwhile task of correlation. The problem was considered to be, in any case, too formidable to be added to the present programme.

It was decided, however, that it would be of interest to determine friction factors on the basis of mean fluid density for the six tests, 16 to 21. The values obtained were found to

be of the same order of magnitude as those appropriate to single phase flow, and are plotted in graph 41, against a Reynold's number defined as,

$$R_D = \frac{\rho D V}{\mu_1 \left[\frac{(1-q)v_1}{v}\right]^{\frac{2}{3}}} \qquad (24)$$

It is explained that no claim is made for the use of the above number as a suitable or complete correlating parameter. It is included here chiefly to enable a plot of the calculated friction factors and also because it represents the first obvious step towards an elucidation of the meaning of viscosity in a froth mixture. The term $\mu_1 \left[v_1(1-q)/v\right]^{2/3}$ representing the effective viscous forces, is the liquid viscosity times the relative liquid area. For the purposes of comparison, the friction factors obtained by measuring the flow of nitrogen through the 0.06 tube are given in graph 41.

An example of the method adopted in calculating the friction factors is given in Appendix 9

In conbrast to the above method of analysis, a calculation of friction factor on the assumption of annular flow and using liquid density as a relevant variable yields results which bear no relation to normal values. Results for test 17, obtained on this basis, are summarised below:-

Test No. 17 $\frac{W}{A}$ = 507 lbs/ft^{2}sec. Tc = 80.5°F. To = 23°F.

T °F	59	49	39	29	23
λ	.0121	.0081	.0053	.0041	.0031.

GRAPH N°2 -

GRAPH N° 26

Test N° 16
Tube Bore .0600 inches
Mass Flow 450 lb/sec ft²

Fluid temperature °F

80
70
60
50
40
30
20
10

110 100 90 80 70 60 50 40 30 20 10 0

Distance from tube outlet - inches

GRAPH Nº 27.

GRAPH N° 27

Test N° 17
Tube Bore .060 inches
Mass Flow 507 lb/sec.ft²

Fluid Temperature °F

80
70
60
50
40
30
20
10

110 100 90 80 70 60 50 40 30 20 10 0

Distance from tube outlet - inches

GRAPH N°28.

GRAPH N° 28

Test N° 18
Tube Bore .060 inches
Mass flow 553 lb/sec ft²

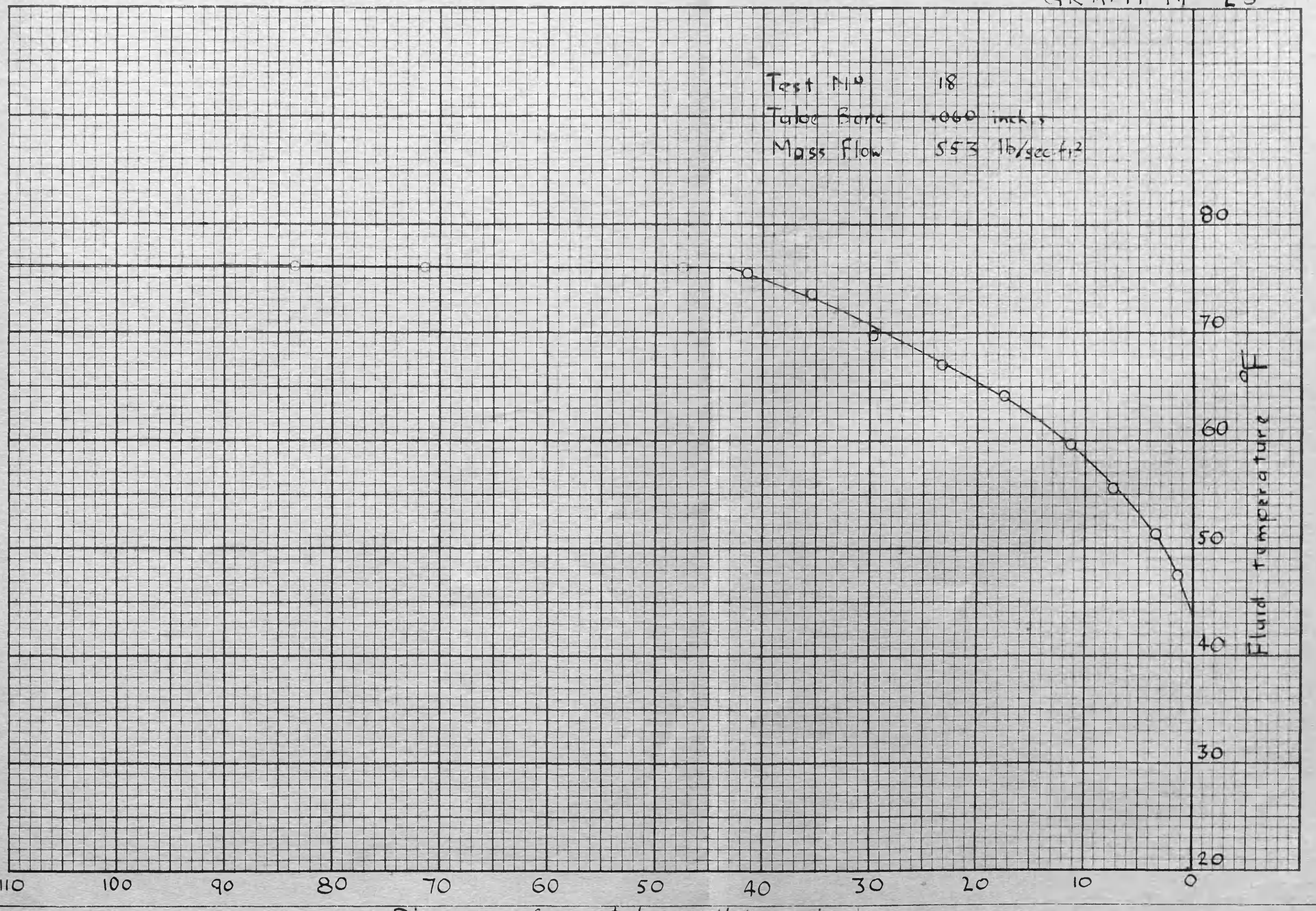

GRAPH N° 9.

GRAPH N° 29

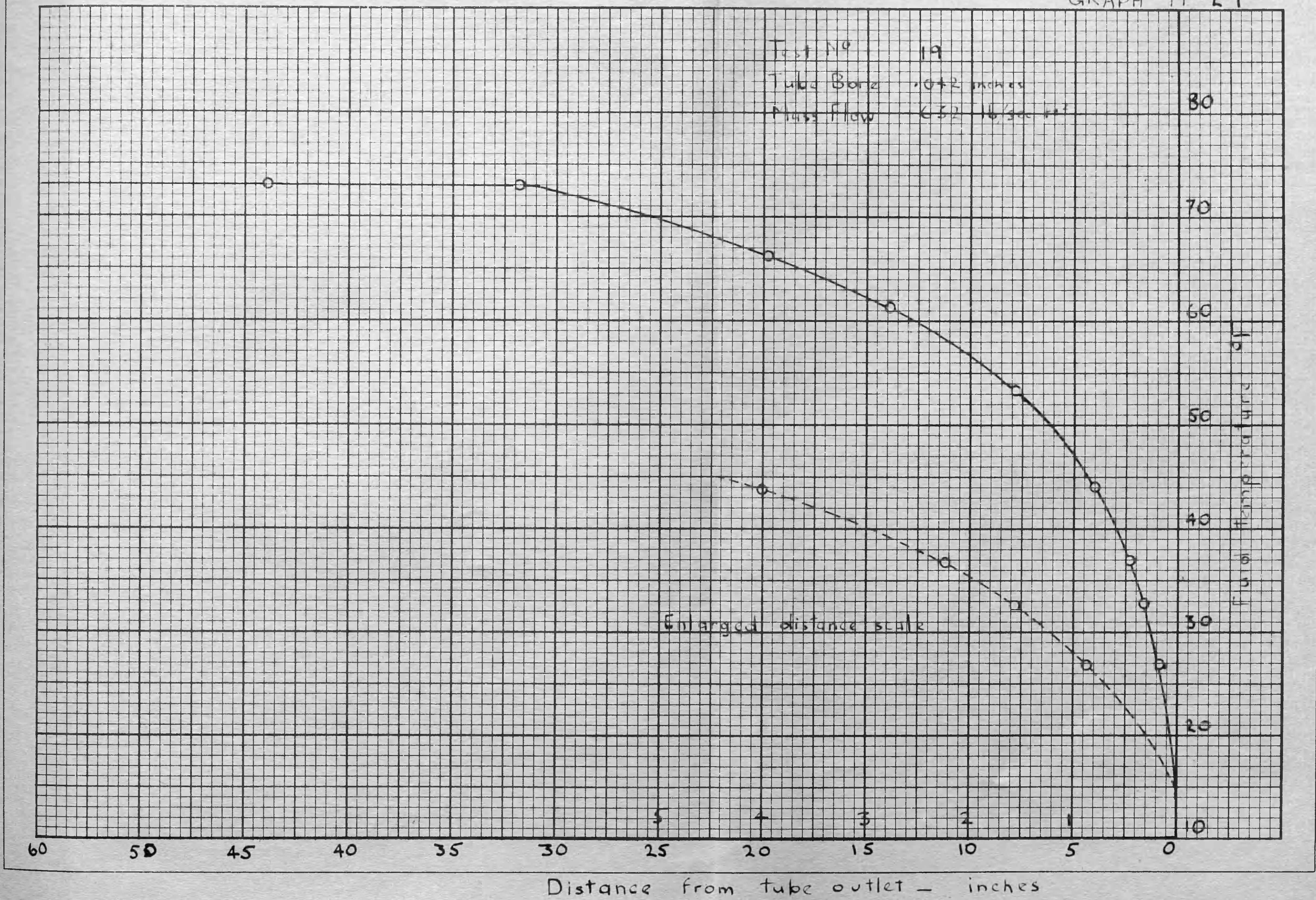

Test N° 19
Tube Bore .042 inches
Mass Flow 632 lb/sec ft²
Enlarged distance scale
Fluid temperature °F
80
70
60
50
40
30
20
10
5
4
3
2
1
60
50
45
40
35
30
25
20
15
10
5
0
Distance from tube outlet — inches

GRAPH N°30

GRAPH Nº 30

Test Nº 20
Tube Bore .042 inches
Mass Flow 6.54 lb/sec.ft²

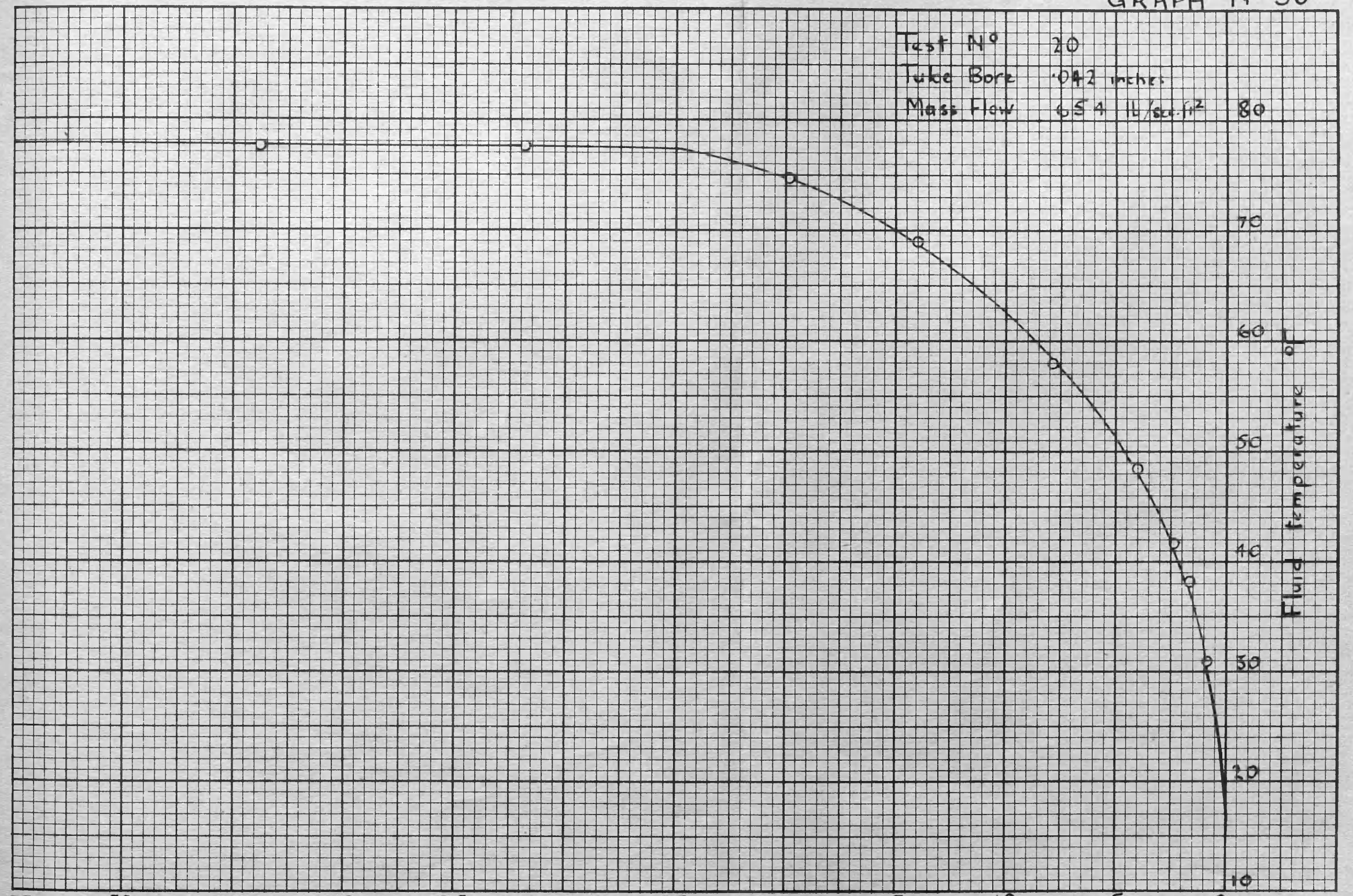

GRAPH N° 31

GRAPH N° 31

Test N° 21
Tube Bore .042 inches
Mass Flow 638 lb/sec.ft²

80
70
60
50
40
30
20
10

°F

Fluid temperature

55 50 45 40 35 30 25 20 15 10 5 0

Distance from tube outlet - inches

GRAPH N° 12.

GRAPH N°32

Test N° 22
Tube Bore .042 inches
Mass Flow 6.98 lb/sec-ft²

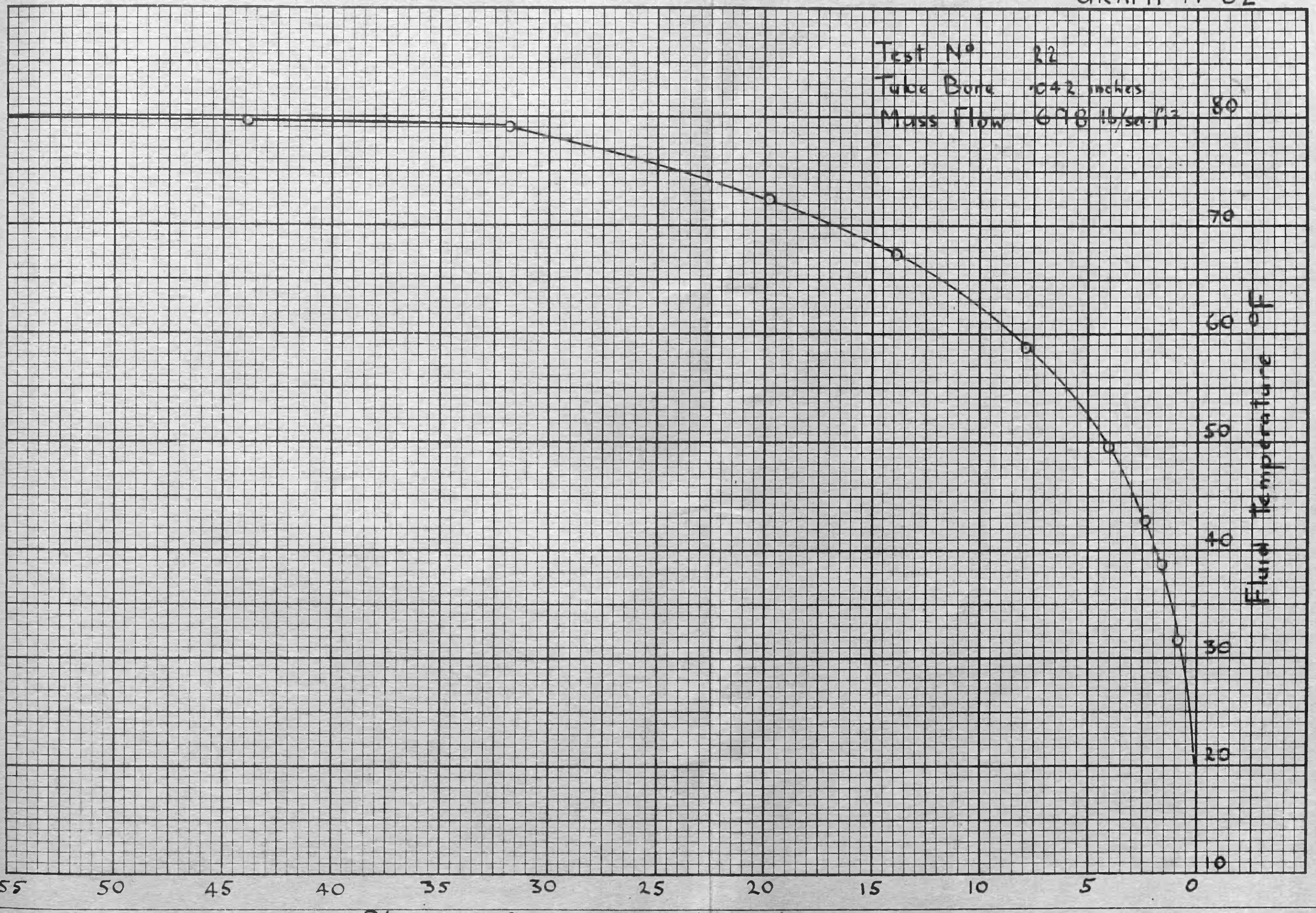

GRAPH N° 55.

GRAPH N° 33

Test N° 23
Tube Bore .042 inches
Mass Flow 714 lb/sec-ft²

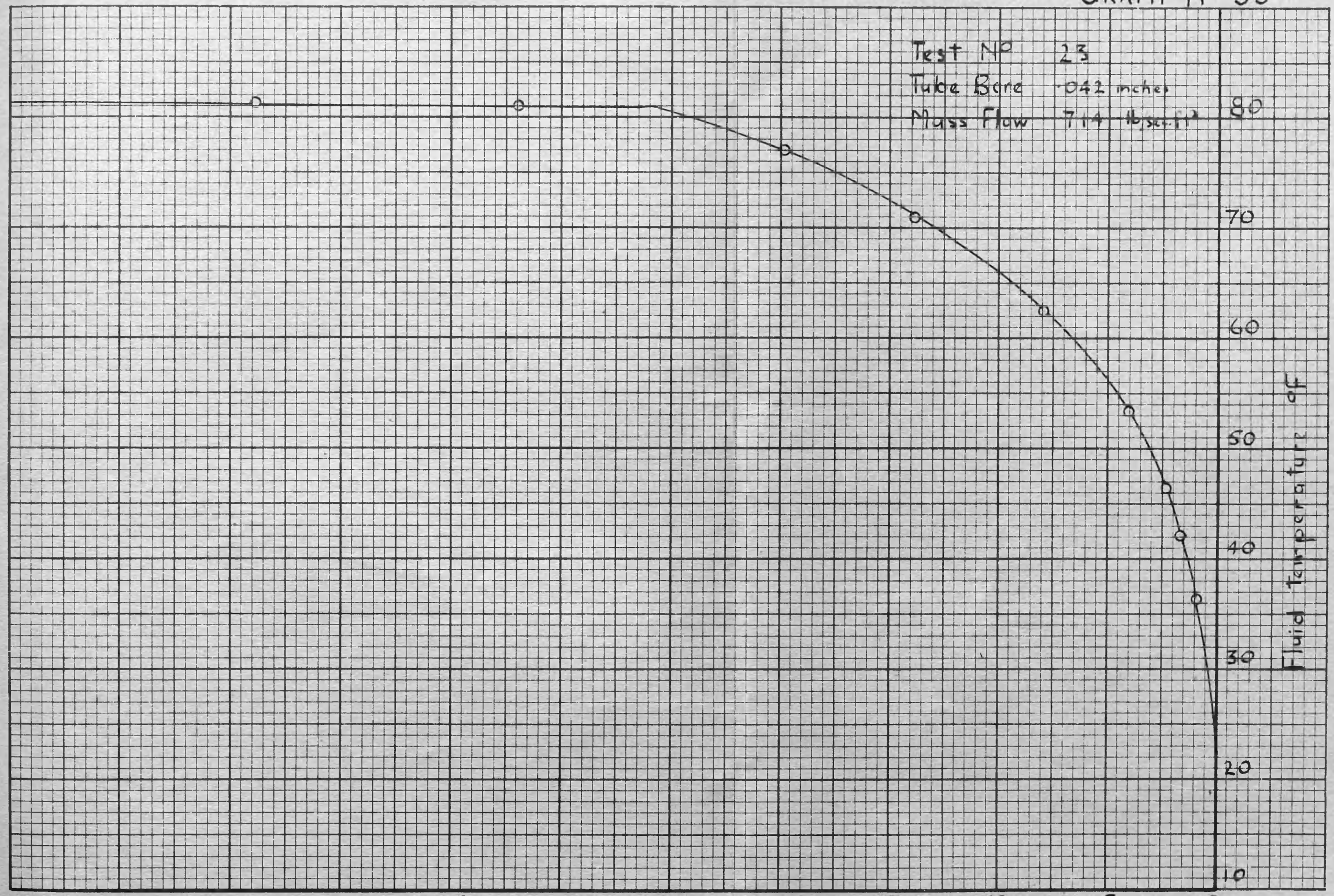

GRAPH N° 34.

GRAPH N° 3+

Test N° 24
Tube Bore 042 inches
Mass flow 716 lb/sec-ft²

GRAPH N° 35.

GRAPH Nº 35

Test Nº 25
Tube Bore .042 inches
Mass Flow 732 $\frac{lb}{sec.ft^2}$

70
60
50
40
30
20
10

$\frac{T}{D}$ Fluid temperature

55 50 45 40 35 30 25 20 15 10 5 0

Distance from tube outlet - inches

GRAPH N° 30

GRAPH N° 36

Test N° 26

Tube Bore .042 inches

Mass Flow 834 lb/sec. ft.²

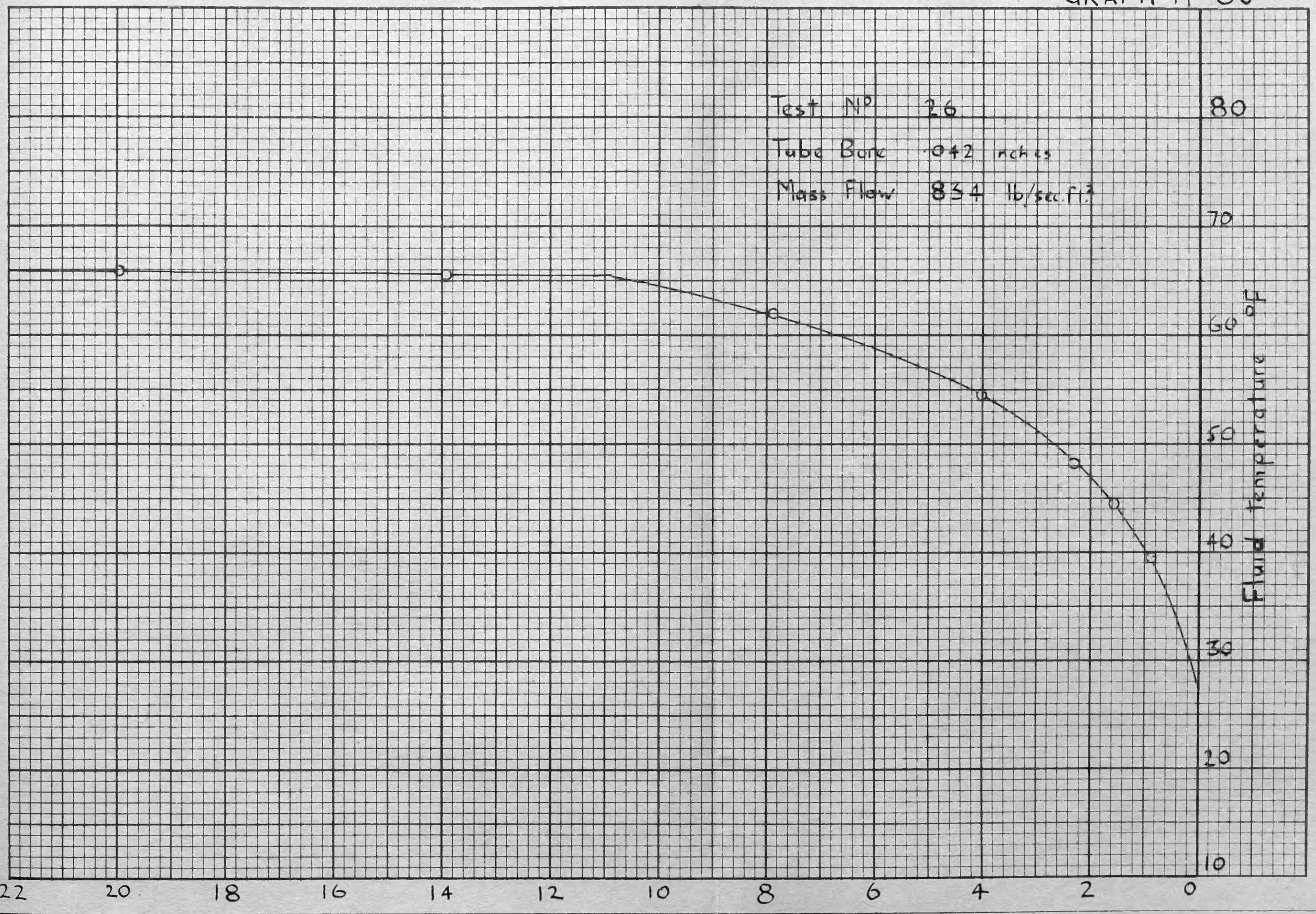

GRAPH Nº 37.

GRAPH Nº 37

Test Nº 17
Tube Bore .042 inches
Mass Flow 858 lb/ft²sec.

80
70
60
50
40
30
20
10

Fluid Temperature °F

22 20 18 16 14 12 10 8 6 4 2 0

Distance from tube outlet - inches

GRAPH N° 38.

GRAPH N° 33

Test N° 28

Tube Bore 0.42 inches

Mass Flow 9.13 lb/sec. ft.²

80

70

60

50

40

30

20

Fluid temperature °F

22 20 18 16 14 12 10 8 6 4 2 0

Distance from tube outlet - inches

GRAPH Nº 39.

GRAPH N° 39

Test N° 37
Tube Bore .042 inches
Mass Flow 960 lb/sec ft²

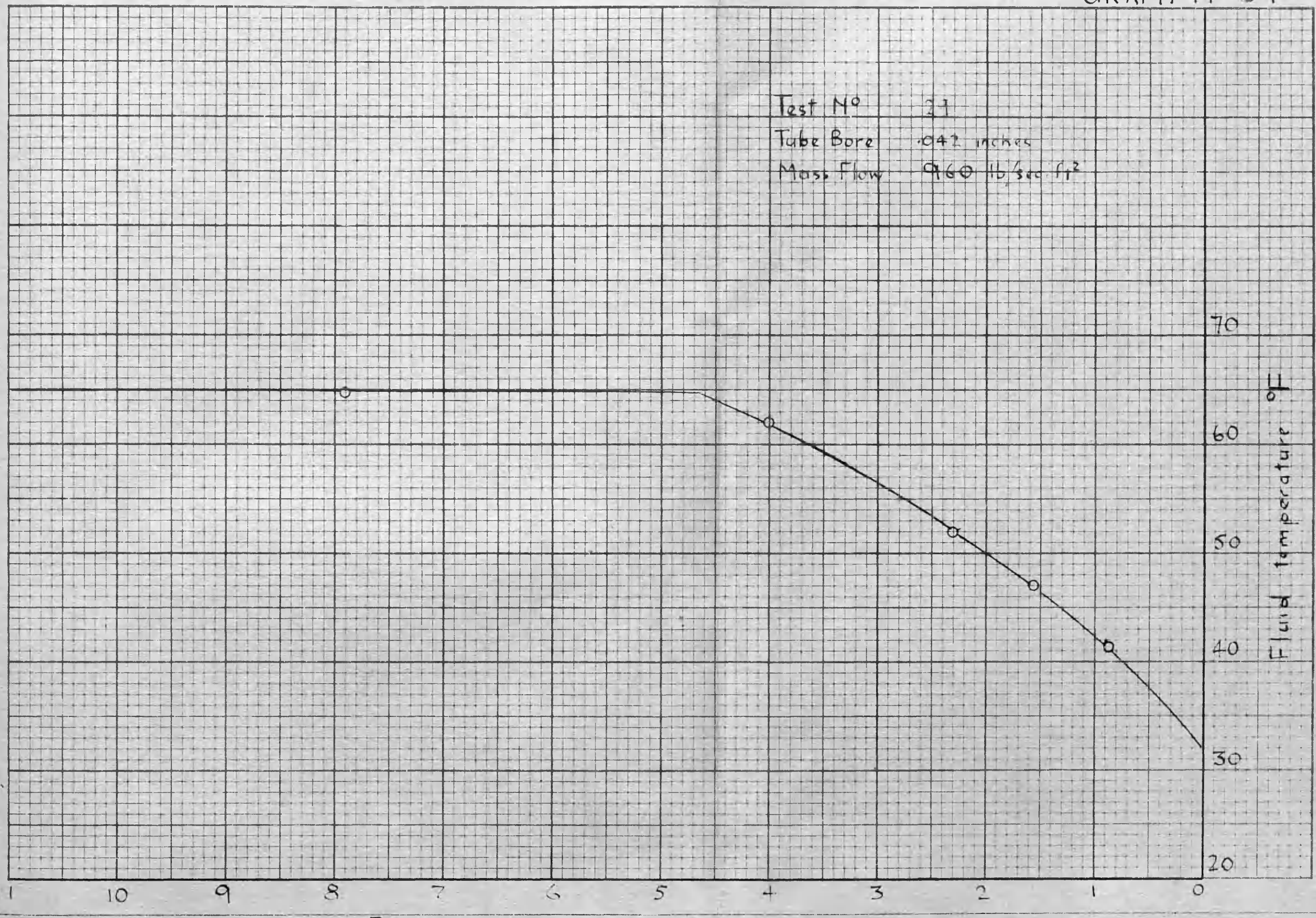

GRAPH N° 4C.

GRAPH N° 40

Test N° 30
Tube Bore .042 inches
Mass Flow 965 lb/hr ft²

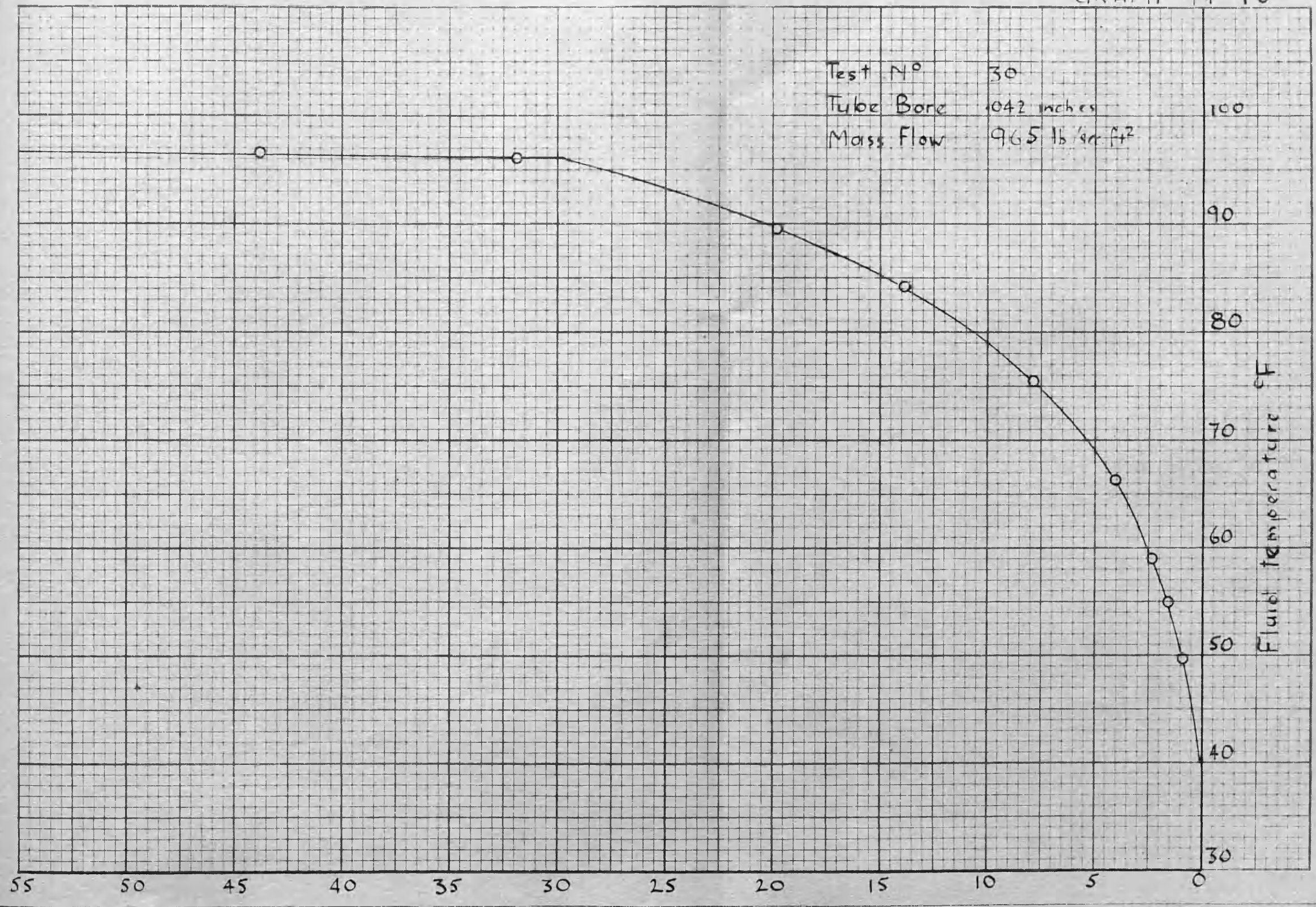

GRAPH No 41

Test Nos 16-14, 25-20.

o .042" bore tube.

x .060" bore tube.

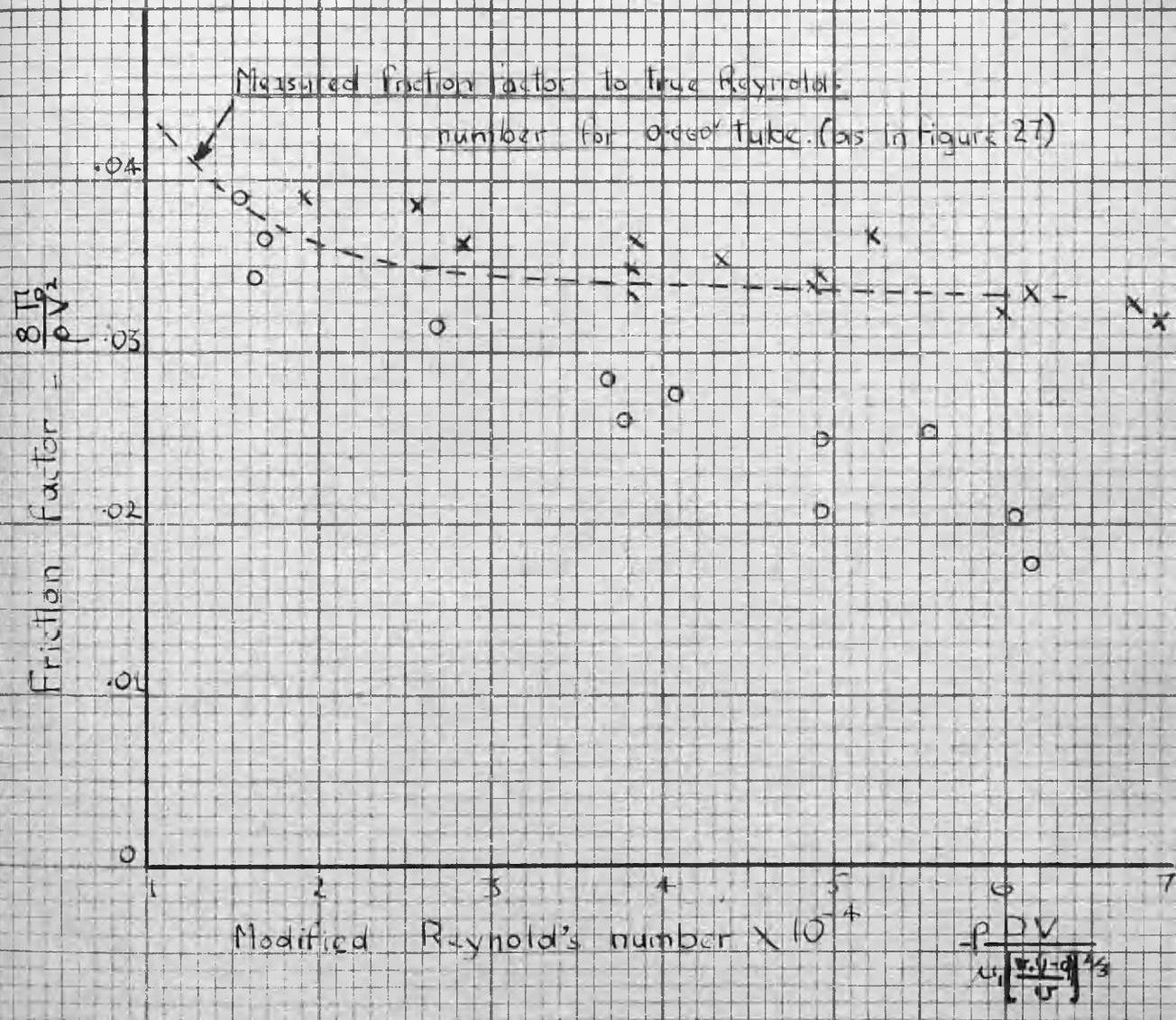

GRAPH 41. Friction factors for evaporating freon 12 against a modified Reynold's number

PART V.

DISCUSSION AND CONCLUSIONS.

DISCUSSION.

A. Annular Flow Theory and Water Experiments.

1. General.

Relative motion between the liquid and vapour components during the evaporating flow of water confers an extra freedom on the fluid resulting in a reduction in the momentum and kinetic energy associated with a particular mass flow. In consequence the mass flow associated with a given rate of pressure drop is greater than would be obtained were there no relative velocity.

Equation (7) expressing the relative velocity factor for annular flow is a bi-quadratic in k yielding, as is shown in Appendix 6, two positive and two negative roots. The latter have no physical significance. The theoretical deduction that there are two possible values of k may be compared with the parallel case of flow with a free surface in an open channel in which two different depths satisfy the conditions.

The appropriate value of relative velocity factor under various conditions is a matter for further investigation. The lower value was found to hold in all of the present experiments, although it seems possible that in vertically upwards evaporating flow, as in boiler tubes, the higher value might operate.

The critical outlet pressure is independent of the alternative k values, but the rate of pressure drop with pipe

length is not.

2. Critical Examination of Experimental Evidence.

Of the three assumptions on which the theory is based the one most requiring experimental support is that concerning thermodynamic equilibrium. The behaviour of fluids undergoing phase transition is notably unpredictable. Having justified the assumption for one set of conditions it is, however, possible to extend its application with considerable confidence to all similar conditions of the same fluid.

Since, in the annular flow equation there occurs the empirical factor ' n ', two independent sets of data are required for complete confirmation of the theory. These are provided by the critical outlet conditions and measured outlet relative velocity factors respectively. Of these two experimental checks the critical outlet condition is the more direct since the equation relating relative velocity factor to fluid momentum involves the basic assumptions.

An important direct check on the thermodynamic equilibrium of the fluid during expansion is the correspondence between measured pressures and saturation pressures corresponding to measured temperature.

The assumption regarding wall shear forces is confirmed over the test range within the limits of experimental accuracy by the outlet momentum measurements. That the assumption is true for all stages in the expansion is not directly confirmed. The value of interface velocity ratio calculated on this basis

is, however, repeated with great consistency and is entirely in accord with intuitive ideas regarding the flow. Further if the assumption holds near the tube outlet, there seems no reason why it should not hold at other sections where the proportion of liquid present in the mixture is greater.

It is considered that the foregoing evidence is sufficiencly strong to be accepted as conclusive.

3. Critical Outlet Conditions.

The measured and predicted critical outlet temperatures for the experiments on small bore tubes show excellent correspondence. Burnell's experimental results, obtained on pipes of larger bore ($\frac{1}{2}$" to $1\frac{1}{2}$" dia.) are slightly lower than those predicted by theory, the discrepancies being larger than can reasonably be attributed to experimental error.

As a preliminary to discussing possible explanations as to why this should be, the critical outlet phenomenon is considered from the view point that the fluid velocity at outlet should be not less than the local rate of propagation of a rarefaction wave.

In this respect it is tempting to treat the liquid and vapour components separately. However, such an approach would be untenable because of the inter-relating effects of the volume-pressure characteristics of the two components.

An element of liquid just below saturation pressure when subject to a pressure reduction, increases very slightly in volume until saturation pressure is reached at which stage evaporation begins. This results in a large effective

coefficient of volume expansion with pressure.

The converse occurs with an element of vapour just above saturation pressure when subject to a pressure increase.

When considering the effect of a free pressure drop at the tube outlet on the continuous annular liquid component of the fluid it is, in the light of the above, more correct to look upon it as a highly expansive medium than as an incompressible liquid.

Now any deviation from predicted critical outlet values must reflect upon the validity of one or more of the three basic assumptions. These are considered individually below.

(a) "The pressure and temperature across any section normal to the flow are constant".

A continuous layer of sub-cooled liquid, such as might occur in the laminar sub-layer, adjacent to a pipe wall losing heat to the environment would be capable of transmitting a pressure reduction of amount dependent on the degree of sub-cooling.

(b) "The fluid is in thermodynamic equilibrium at all stages in the expansion".

The occurrence of free pressure drop at the outlet presents the fluid with the possibility of a very rapid rate of pressure change. If under these conditions the liquid medium can exist temporarily in a meta-stable state the transmission of reduced pressures within the tube becomes possible.

(c) "The mean velocities on the bases of continuity, momentum, and energy are equal".

This assumption, although never strictly true, has proved to be a satisfactory basis for dealing with many problems in turbulent fluid flow. Its effect on the present phenomenon cannot be dismissed although it seems unlikely that a reduction in pipe bore would minimise its effect, as is indicated by the available experimental data.

Silver and Mitchell[9] have observed in experiments on the associated problem of the flow of boiling water through convergent-parallel nozzles that the critical outlet condition is not independent of the back pressure. In one test reported by them, reduction of the back pressure from 25 to 0 lbs/in^2 gauge resulted in the critical outlet pressure falling from 25.5 to 20.5 lbs/in^2 gauge, the mass flow increasing from 970 to 1240 lbs/hr. in the process.

Since the nozzle was exposed to the back pressure steam they attributed this to the effects of increasing in heat loss in suppressing steam formation.

In view of the high mass flows and small surface areas involed in these experiments it seems unlikely that the direct effects of heat loss on steam formation can be the sole cause of such a large variation.

B. Frothing Flow and Freon 12 Experiments.

From the thermodynamic point of view a frothing flow is simply one in which the liquid and vapour components have a

common velocity. The critical outlet data obtained on the .042" tube and listed in Table 8, provides ample evidence that the flow of evaporating freon 12 in small bore tubes is of this type. The calculated relative velocity factor as the assumption of annular flow is fairly constant at 1.25 over the test range, indicating suitable conditions for frothing flow. In this respect the observed flow form is consistent with the proposed thermodynamic theory of evaporating flow.

The data also indicate that the surface energy required for froth formation is sufficiently small to be neglected in connection with the energy relationships.

Thermodynamically, the problem of frothing flow is of a standard type and as such demands little comment. In its hydromechanic aspects, however, it presents a new field for experimental investigation.

As mentioned in the section on the analysis of the freon experiments, the extensive investigation of friction factors for frothing flow is outside the scope of this work. The data obtained from six tests and presented in graph 41, do not provide a sufficient range of variable to form a basis for authoritative statement and consequently the following comments are of a tentative nature.

Referring to graph 41, in which friction factors on the basis of mean fluid density are plotted against a modified Reynold's group, it will be observed that friction factors for the .042" and .06" tube coincide at the lower values of the group. Since, in this range, the fluid is mainly liquid and

the influence of surface tension and vapour accordingly slight, this result is one which might have been anticipated.

At the higher values of the modified Reynold's number the friction factors for the two tubes show a distinct divergence. This probably indicates surface tension effects since both velocity and diameter terms occur in the surface tension parameter. In making this deduction it is assumed that the modified Reynold's group, intended to represent the ratio of inertia to viscosity forces, is a suitable parameter. Nothing definite can be deduced from the experimental data as to whether or not this is the case.

In contrast to the friction factors calculated on the assumption of frothing flow, those obtained by the methods appropriate to annular flow bear no relation to normal values and show a disproportionate variation over a single expansion.

This further confirms the finding that the flow form is of the frothing type.

C. Factors Affecting the Flow Mechanism.

The only satisfactory method at present available for determining the flow mechanism appropriate to a particular fluid under a given set of conditions is direct experiment. However, a few general inferences may be drawn from the acquired knowledge on the subject.

The most important factors influencing the flow mechanism are; (1) thermodynamic properties; (2) mass flow per unit area; (3) frothing characteristics.

(1) The theoretical value of relative velocity factor as calculated from equation (7) may be regarded as a measure of the forces tending to produce relative motion.

The experiments on water and freon are consistent with this contention.

(2) Bergelin and Gazley[12] have investigated the effect of varying mass flow per unit area on the flow mechanism for air-water mixtures, the data obtained being shown in Figure 7. The annular form was found to hold in the higher mass flow range; that is, in the range which is likely to be of most interest to the engineer.

(3) An analysis of the frothing characteristics of a fluid constitutes a difficult problem in physical chemistry. It is generally found that; (a) a low value of surface tension coefficient is encouraging to froth formation; (b) solutions are more susceptible to frothing than pure liquids.

In connection with the latter statement it is noted that a small quantity of unseparated oil was present during the freon experiments and that this may have been to some extent responsible for the maintenance of the froth in these tests.

CONCLUSIONS.

A. On the Adiabatic Flow of Evaporating Water in Pipes.

The first two of the following statements receive experimental support from the work of Burnell[3] as well as that of the author, covering a pipe diameter range of 0.06" to 1.5".

The remaining statements refer to flow in small bore tube, being based on results obtained from the 0.1285" tube.

1. The liquid and vapour components flow with different mean velocities. These velocities can be calculated by theory derived from the usual assumptions made in connection with fluid flow.

2. Critical outlet conditions readily arise because of the large rates of volume expansion associated with evaporation. Critical outlet pressures, temperatures, and velocities may be calculated by means of equation (7).

For small bore tubes (.060" and 0.1285") experimental and predicted values correlate completely.

For pipes of larger bore (.529" to 1.5"), measured values are slightly lower than those predicted by theory.

3. The flow form is annular.

4. The interface velocity ratio increases from unity at the beginning of evaporation to about 1.2 at the critical outlet stage.

5. Equation (7) enables the calculation of relative velocity factor for any stage in an expansion.

6. The wall shearing force per unit area is a function of velocity and density. For smooth pipes the friction factor is that given by the standard Stanton curve, the length term in the Reynold's number being pipe diameter and the other terms being those appropriate to the liquid.

B. On the Adiabatic Flow of Freon 12 in Small Bore Tubes.

The following statements receive support from experiments carried out with tubes of 0.042" and 0.060" diameter fitted to a refrigerator test unit. Although a separator was employed in the vapour line there was undoubtedly a small quantity of oil in the circulating freon 12.

1. The flow form is of the frothing type.

2. Standard thermodynamic theory for compressible fluid flow may be employed to calculate velocities and critical outlet pressures and temperatures. The surface energy required for froth formation has a negligible effect on the flow.

BIBLIOGRAPHY.

1. M. M. Bolstad and R. C. Jordan.
"Theory and Use of the Capillary Tube Expansion Device". R. E. December, 1948 and June 1949.

2. W. T. Bottomley.
"The Flow of Boiling Water Through Orifices and Pipes". Trans. N.E.C. Institute of E. and S. Vol. LIII., 1936-7.

3. J. G. Burnell.
"Flow of Boiling Water Through Orifices, Nozzles and Pipes". Engineering, December, 1947.

4. H.F. Lathrop.
"Application and Characteristics of Capillary Tubes". R.E. August, 1948.

5. E. Giffen and T. F. Crang.
"Steam Flow in Nozzles: Velocity Coefficients at Low Steam Speeds". Proc. I. Mech. E. Vol.155. 1946.

6. W. T. Lewis and S. A. Robertson.
"The Circulation of Water and Steam in Water Tube Boilers and the Rational Simplification of Boiler Design". Proc. I. Mech. E. Vol. 143. 1940.

7. G. F. Marcy.
"Pressure Drop and Change of Phase in a Capillary Tube". R.E. January, 1949.

8. R. C. Martinelli, L. M. K. Boelter, T. H. M. Taylor, E. G. Thomsen, and E. H. Morrin.
"Isthermal Pressure Drop for Two-Phase Two-Component Flow in a Horizontal Pipe". Trans. A.S.M.E. Vol. LXVI. 1944.

9. R. S. Silver and J. A. Mitchell.
"The Discharge of Saturated Water Through Nozzles". Trans. N.E.C. Institute of E. and S. Vol.LXII. Dec. 1945.

10. L. A. Staebler.
"Theory and Use of a Capillary Tube for Liquid Refrigerant Control". R.E. January, 1948.

11. L. A. Staebler.
"Capillary Tubes: A Guide to Their Application on Freon 12 Hermetic Condensing Units". R.E. January, 1950.

12. Heat Transfer and Fluid Mechanics Institute; a collection of papers published by the A.S.M.E. for a meeting of the above Institute held at Berkeley, California,1949. Included were three papers on "Co-current Gas-Liquid Flow".

(i) "Flow in Horizontal Tubes". O. P. Bergelin and C. Gazley, Jr.

(ii) "Flow in Vertical Tubes". O. P. Bergelin,

P. K. Kegel, F. G. Carpenter, C. Gazley, Jr.

(iii) "Interfacial Shear and Stability".

C. Gazley, Jr.

Abbreviation: R.E. indicates Refrigerating Engineering, published by The American Society of Refrigerating Engineers.

APPENDICES.

APPENDIX 1.

The Determination of Mixture Quality.

Whilst the approximation implied in equation (8) may be justified for a particular fluid by a few sample calculations, some more general form of argument is desirable.

In an adiabatic expansion, the quality of the mixture must lie between values corresponding to constant entropy and constant total heat respectively. Making use of this fact it is possible to express, in general terms, a limit of error in the assumption of constant total heat expansion.

In Figure A1.1, the lines $\overline{12}$ and $\overline{13}$ represent expansions from the same initial condition at constant entropy and constant total heat respectively. Since the expansion is in the wet field, changes at constant pressure are also changes at constant temperature and,

$$H_3 - H_2 = T_0(\phi_3 - \phi_2) \qquad (A3.1)$$

Hence,

$$H_1 - H_2 = T_0(\phi_3 - \phi_1) \quad \text{or} \quad \int_2^1 v_\phi \, dp = T_0 \int_1^3 d\phi. \qquad (A1.2)$$

For a change taking place at constant total heat,

$$d\phi = \left(\frac{\partial \phi}{\partial p}\right)_H dp = -\left(\frac{\partial \phi}{\partial H}\right)_p \left(\frac{\partial H}{\partial p}\right)_\phi dp = -\frac{v}{T} dp$$

Thus, substituting in equation (A1.2),

$$\int_1^2 v_\phi \, dp = \int_1^3 \frac{T_0}{T} v_H \, dp$$

or

$$\int_c^0 \left[v_1 + q_\phi (v_2 - v_1)\right] dp = \int_c^0 \frac{T_0}{T} \left[v_1 + q_H (v_2 - v_1)\right] dp \qquad (A1.3)$$

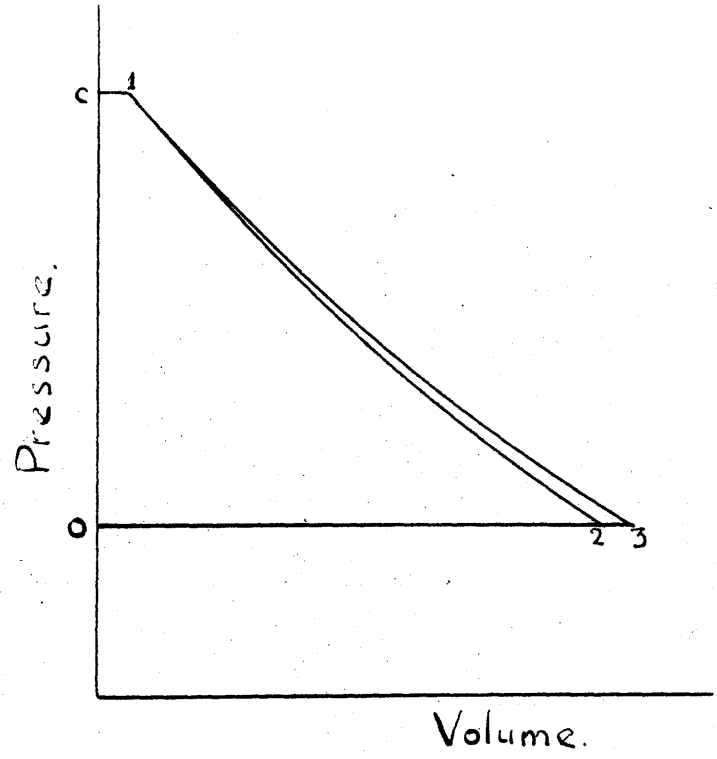

FIGURE A1·1

Pressure - volume diagram for expansions in the wet field from the saturated liquid condition at constant entropy and constant total heat.

In equation (A1.5), the quantity T_o/T increases from T_o/T_c to unity as p goes from C to C. The above equation cannot be integrated unless some equation relating p, v, and T be assumed, but it is possible to state by inspection that, since v_1, is negligible relative to v_2,

$$\left[\frac{q_\phi}{q_H}\right]_o > \frac{T_o}{T_c} \qquad \text{and since} \qquad \left[\frac{q}{q_H}\right]_o > \left[\frac{q_\phi}{q_H}\right]_o$$

then $\left[\frac{q}{q_H}\right]_o > \frac{T_o}{T_c}$ where Tc and To are the absolute temperatures of the fluid at the beginning and end of the expansion respectively. It is evident that the limit of error could be still further reduced by assuming q, the actual quality during expansion, to be the mean q_ϕ and q_H.

APPENDIX 2.

Sample Calculation of Relative Velocity Factor and Interface Velocity Ratio.

Given the measured temperature distribution, mass flow per unit area, and pipe diameter it is required to find relative velocity factors and interface velocity ratios throughout the expansion, on the assumption that friction factors are as defined in equations (14) and (15).

The equations necessary to this purpose are:-

$$-\frac{\lambda\pi D}{8gv_1}V_1^2\delta x - A\delta p - \frac{W}{g}\left[(1-q)\delta V_1 + (k-1)V_1\delta q + q\,\delta(kV_1)\right] = 0 \qquad (17)$$

$$V_1 = B(1+c/k) \qquad (1)$$

$$\delta V_1 = B/k^2\cdot(k\,\delta c - c\,\delta k) \qquad (18)$$

$$\delta(kV_1) = B(\delta c + \delta k) \qquad (7e)$$

$$k_B = k_A + (\delta k/\delta T)_{A-B}(T_B - T_A) \qquad (19)$$

The dependent variables in this set of equations are k , δk , V_1 , δV_1 . The remaining quantities are either experimental or else functions of the thermodynamic properties of the fluid.

These latter being determined, equation (17) was solved for each selected temperature in the expansion as follows.

A value of k was chosen and by trial and error the compatible value of δk found between (17) (18) and , (7e) Repeating this procedure for other values of k at the same temperature a curve relating k and δk was obtained.

A similar curve was calculated for an adjacent stage in the expansion, equation (19) being then used to find unique values of k and δk.

By repeating this procedure for several overlapping stages in the expansion the variation of k and V_1 was obtained over the complete temperature range.

As can be seen the calculations are extremely repetitive and are particularly suited to tubular methods. In the following pages an example of each type of table used is given, the data referring to test 1.

Thermodynamic data for steam and water were obtained from the tables compiled by Keenan & Keyes (1936 Edition).

Determination of Quality.

Equation (2) $$q = \frac{h_c - h + Q}{L}$$

is used for the purpose.

The heat loss to the atmosphere, $-Q$, was estimated from the temperature drop in the liquid stage over a number of experiments. The following empirical relation expressed the finding.

$$Q = -\frac{.01L}{W} \quad B.T.U/lb \qquad (A2.1).$$

where Q is the cumulative heat loss, L the length of pipe taken up by the expansion (feet), W the mass flow (lbs/sec.)

Graph (A2.1) is the experimental temperature distribution curve for test 1, the cumulative heat loss per lb. of fluid being related to the temperature by the straight line expressing equation (A2.1).

In the following Table 'q' is calculated for a number of selected temperatures, the result being shown in graph (A2.2).

Table A2.1.

Test No. 1. $T_c = 240.5^oF.$ $T_o = 212^oF.$

T °F.	h_c BTU/lb	h BTU/lb	Q BTU/lb	h_c-h+Q BTU/lb	Lt BTU/lb	q
240.5	208.34	208.34	0	0		0
236		204.29	-.45	3.60	954.8	.00377
232		200.25	-.50	7.59	957.4	.00793
228		196.20	-.63	11.51	960.1	.01198
224		192.17	-.72	15.45	962.6	.01606
220		188.13	-.79	19.42	965.2	.02012
216		184.10	-.84	23.40	967.8	.02430
212		180.07	-.86	27.41	970.3	.0282

In order to demonstrate quantitatively the degree of approximation involved in assuming that q may be calculated on the assumption that kinetic energy terms in equation (2 b) are negligible, Table A2.2 compares values of q_ϕ and q_H for an expansion in the wet field from saturated liquid at 240°F.

Table A2.2.

T°F	240	230	220	212
q_H	0	.0106	.0209	.0291
q_ϕ	0	.0104	.0205	.0285
%Diff	0	1	2	2

Determination of ($\delta x/\delta T$) as a function of T .

The standard methods of numerical differentiation are only worthwhile when a large number of experimental points, evenly speced in terms of the independent variable are available or when the mathematical form of the equation is known. Neither of these requirements can be satisfied in the present instance.

The method adopted was simply to tabulate distances for fixed increments of temperature and calculate the mean slope. This procedure has a distinct advantage over graphical methods in that errors in adjacent increments are compensatory.

Table A2.3, and graph A2.3, illustrate the procedure in relation to test 1.

Table A2.3. Calculation of $\delta x/\delta T$ Test 1.

T °F	x inches	Δx	$\delta x/\delta T$ in/°F	T_m °F
240	24.0			
238	18.9	5.1	2.55	239
236	15.5	3.4	1.7	237
234	12.7	2.8	1.4	235
232	10.3	2.4	1.2	233
230	8.3	2.0	1.0	231
228	6.6	1.7	.85	229
226	5.15	1.45	.73	227
224	4.0	1.15	.575	225
222	2.85	1.15	.575	223

T °F	x in	Δx	δx/δT in/°F	T_m °F
220	2.0	.85	.425	221
218	1.3	.70	.35	219
216	.75	.55	.275	217
214	.30	.35	.225	215
212	0	.30	.15	213

The Calculation of compatible values of k and δk at a selected temperature.

In the following calculations the basic incremental change is - 1 F^{o}. Quantities which increase as expansion proceeds are made to have a positive rate of change.

The following quantities are required in the solution and are given in order of their occurrence in equations (17) and (18). At the selected temperature of 223.5°F;

$\lambda = f\left(\frac{\rho D V}{\mu_1}\right)$ .....See figure (A2.1)

D = .0107 ft.

v_1 = .01679 ft^3/lb.

δx = .045 ft/°F

$A = 90 \times 10^{-6}$ ft^2

δp = - 50.6 $lb/ft^2{}^{o}F$.

$\frac{w}{g}$ = .000776 $lbs.sec^2ft$.

q = .01655

δq = .00102 /°F.

$B = \frac{W}{A}(1-q)v_1$ = 4.887 ft/sec.

C = 21.83

δC = 1.773 /°F.

In Table A2.7 the terms of equation (17) are calculated for two values of δk at each of three values of k. Since the expressions contained in (17) form a linear function of δk these calculations are sufficient to obtain compatible values of k and δk over the range selected for the chosen temperature. The result is given below.

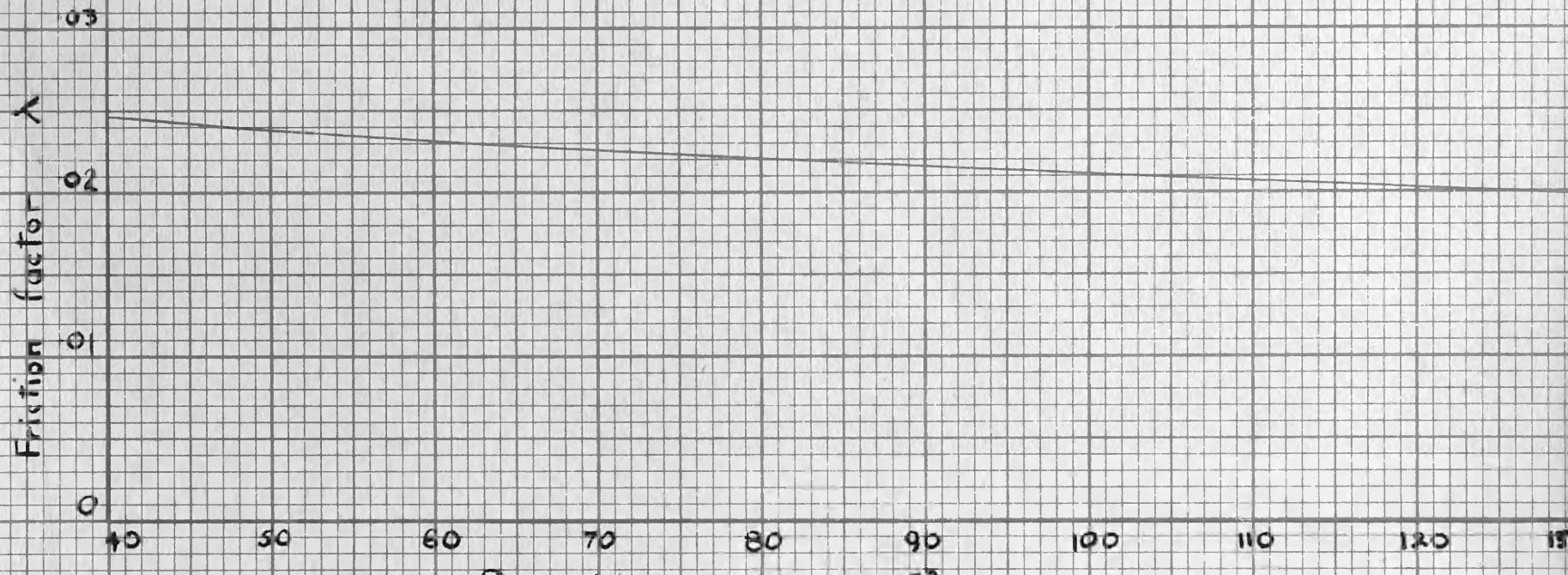

FIGURE A2·1 Friction factor to a base of Reynolds number for 0·1285" tube - based on flow tests with water

T	= 223.5°F.		
k	= 5	5.5	6
δk	= 0.48	0.30	0.15

In graph A2.4 curves of compatible values of k and δk are given for temperatures of 229.5°F. and 223.5°F.

Equation (19) is used in Table A2.8 to determine the actual values of k and δk at these temperatures.

Table A2.4.

Test No. 1. $T_c = 240.5^{\circ}F$ $T_o = 212^{\circ}F$ $\frac{W}{A} = 278$ lb/ft^{2}sec.

Equation: $V_1 = B(1 + c/k)$ (1).

T °F	223.5			
B ft/sec	4.587			
c	21.83			
k	5	5.5	6	
c/k	4.37	3.98	3.64	
V_1 ft/sec	24.6	22.8	21.7	

Table A2.5.

Equation: $\delta V_1 = B/k^2 (k\delta c - c\delta k)$

T °F	223.5					
δT °F	- 1					
B ft/sec	4.587					
c	21.83					
δc /°F	1.773					
k	5.0		5.5		6.0	
B/k^2 ft/sec	.183	.183	.152	.152	.127	.127
δk /°F	0	.4	0	.4	0	.4
kδc °F	8.87	8.87	9.75	9.75	10.62	10.62
cδk °F	0	8.75	0	8.75	0	8.75
kδc-cδk °F	8.87	.12	9.75	1.00	10.62	1.87
δV_1 ft/°F sec	1.62	.021	1.48	.152	1.35	.237

Table A2.6.

Equation: $\delta(kV_1) = B(\delta c + \delta k)$

B ft/sec	4.587		
δc /°F.	1.773	1.773	
δk /°F.	0	.400	
$\delta c + \delta k$ /°F.	1.773	2.173	
$\delta(kV_1)$ ft/sec °F.	8.12	9.96	

Table A2.7.

Equation: $-\frac{\lambda\pi D}{8gv_1} V_1^2 \delta x - A\delta p - \frac{W}{g}\left\{(1-q)\delta V_1 + (k-1)V_1\delta q + q\delta(kV_1)\right\} = 0$ (17)

or $X + Y + Z = 0$

T °f	223.5					
δT °F	-1					
k	5	5	5.5	5.5	6	6
V_1 ft/sec	24.6	24.6	22.8	22.8	21.7	21.7
R_D	87.8×10^3	87.8×10^3	81.2×10^3		77.5×10^3	
λ	.0217	.0217	0219		0221	
V_1^2	603	603	520	520	470	
δx ft/°F	.045	.045	.045		.045	
$\pi D/8gv_1$	.00778	.00778	00778		00778	
$-\lambda\pi D/8gv_1 V_1^2 \delta x$ lb/°F X	-.00458	-.00458	-.00398	-.00398	-.00364	-00364
$-\delta p$	+50.6					
$-A\delta p$ lb/°F Y	.00455		.00455		.00455	
X + Y	-.00003	-.00003	+00057	+00057	+.00091	+.00091

δk	0	0.4	0	0.4	0	0.4
δV_1	1.62	.0205	1.48	.152	1.35	.237
$\delta(kV_1)$	8.12	9.96	8.12	9.96	8.12	9.96
q	.01655					
$1-q$	.983					
$(1-q)\delta V_1$ (a)	1.590	.0201	1.452	.149	1.325	
$(k-1)V_1\,\delta q$ (b)	.101	.1010	.107	.111	.111	
$q\,\delta(kV_1)$ (c)	.136	.1620	.136	.162	.136	
$a+b+c$	1.827	.283	1.695	.422	1.572	
$-\frac{W}{g}[a+b+c]\frac{lb}{°F}$ Z	-.00142	-.00022	-.00131	-.00033	-.00122	-.00039
$X+Y+Z$ $\frac{lb}{°F}$	-.00145	-.00025	-.00074	+.00024	-.00031	+.00052

Table A3.8.

Equation: $k_B = k_A + \left(\delta k/\delta T\right)_{A-B}\left[T_B - T_A\right]$

$T_A = 229.5^{\circ}F$ $T_B = 223.5^{\circ}F$ (Refer to Figure A2.4.)

k_A	δk_A	Δk	k_B	δk_B
4	.3	1.8	5.8	.21
4.2	.2	1.2	5.4	.34
4.1	.26	1.56	5.66	.26

Hence:

At $229.5^{\circ}F$ $k = 4.1$

and at $223.5^{\circ}F$ $k = 5.7$

By repeating the whole of the above procedure for several overlapping stages of the expansion the variation of k and V_1 is obtained throughout. Graph 13 shows the variation of k and V_1 to a base of temperature for test 1.

The Calculation of interface velocity ratio.

The equations required for this are:

$$n = \frac{W}{V_1 \delta F_p}\left\{ - J_q \delta H_s - \frac{1}{2g}\left[2q_L k V_1 \delta(kV_1) + (k^2-1) V_1^2 \delta q_L \right] \right. \qquad (A2.2)$$

$$\delta F_p = \delta F_w + a_1 \delta p + \frac{W}{g}(1-q_L)\delta V_1 \qquad (4)$$

$$\delta F_w = \frac{\lambda \pi D}{8 g v_1} V_1^2 \delta x \qquad (16)$$

$$a_1 = \frac{A}{1 + c/k} \qquad (1c)$$

Equation (A2.2) is developed from equations (5) and (6).

In the following tables a sample calculation is carried through for test 1, T = 223.5°F.

Table A2.9.

Equation:

$$a_1 = \frac{A}{1 + c/k} \qquad (1c)$$

T °F	223.5	
A ft^2	90×10^{-6}	
k	5.6	
c/k	3.91	
a_1 ft^2	18.3×10^{-6}	

Table A2.10.

Equation: $$\delta F_w = \frac{\lambda \pi D V_1^2}{8 g \nu_1} \delta x \qquad (16)$$

T ^oF	223.5	
V_1 ft/sec	22.6	
$R_D \times 10^{-3}$	80.6	
λ	.0219	
$\pi D / 8 g \nu_1$	.00778	
V_1^2	510	
δx ft	.045	
δF_w lb/^oF	.0039	

Table A2.11.

Equation: $$\delta F_p = \delta F_w + a_1 \delta p + \frac{W}{g}(1-q)\delta V_1 \qquad (4)$$

T ^oF	223.5	
δF_w lb/^oF	.0039	
q_1 ft^2.	18.4×10^{-6}	
δp lb/ft^2 ^oF	-50.6	
$\frac{W}{g}$ lb, sec/ft	.000776	
$1-q$	.983	
δV_1 ft/sec ^oF	.69	
$\frac{W}{g}(1-q)\delta V_1$ lb/^oF	.00053	
δF_p lb/^oF	.0035	

Table A2.12.

Equation: $$n = \frac{W}{V_1 S F_p}\left\{-J_q \delta H_s - \frac{1}{2g}\left[2_q k V_1 \delta(kV_1) + (k^2-1) V_1^2 \delta_q\right\}\right. \quad (A2.2)$$

T ^oF	223.5	
q	.01655	
δH_s BTU/lb^oF	- .363	
$-J_q \delta H_s$ (1)	4.68	
k	5.6	
V_1 ft/sec	22.6	
kV_1 ft/sec	126.5	
$\delta(kV_1)$ ft/sec^oF	9.25	
$2qkV_1\delta(kV_1)$ ft^2/sec$^2{}^oF$ -(2)	38.7	
k^2-1	30.2	
V_1^2 ft^2/sec^2	510	
δq /^oF	.00102	
$(k^2-1)V_1^2\delta q$ ft^2/sec$^2{}^oF$-(3)	15.7	
(2) + (3)	54.4	
$-\frac{1}{2g}[2 + 3]$ (4)	- .845	
(1) + (4) ft/^oF (5)	3.83	
W lb/sec	.025	
V_1 ft/sec	22.6	
δF_p lb/^oF	.0035	
$W/V_1 S F_p$ ^oF/ft -(6)	.316	
$n = (5) \times (6)$	1.2	

The determination of the outlet relative velocity factor from the momentum measurement.

The momentum of the fluid at any section may be written

$$M = \frac{W}{g}(1-q)V_1 + \frac{W}{g}qV_2$$
$$= \frac{W}{g}V_1\left[1+q(k-1)\right]$$

Substituting $B\left(1+{}^{c}/_{k}\right)$ for V_1 and rearranging the terms,

$$\frac{W}{g}qBk^2 - \left[M - \frac{WB}{g}\left[1+q(c-1)\right]\right]k + \frac{W}{g}Bc(1-q) = 0$$

In the following table the calculation is given for test 1. In tests having a critical outlet condition the measured momentum must be corrected for free pressure drop.

Table A2.13.

Test No		1	
T_c	°F	240.5	
T_o	°F	212	
W/g	lb.sec/ft	.000776	
B	Ft/sec.	4.51	
WB/g	lb	.0035	
q		.029	
$W/g\ qB$	lb	1.015×10^{-4}	
M_o	lb	.0306	
C		47.8	

$q(c-1)$		1.585	
$\frac{WB}{g}[1+q(c-1)]$	lb	.00856	
$M-\frac{WB}{g}[1+q(c-1)]$	lb	222×10^{-4}	
$\frac{W}{g}Bc(1-q)$	lb	1622×10^{-4}	

The equation in k for the outlet condition is therefore

$$1.015k^2 - 222k + 1622 = 0$$

and $k = 7.6$ or 211 for the given momentum value. The relevant value is obviously 7.6.

GRAPH N° A2·1.

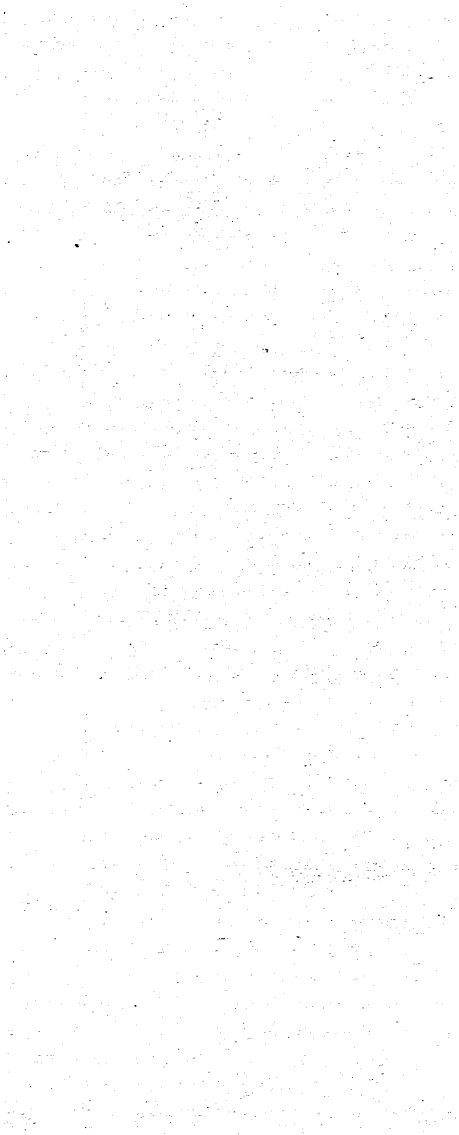

GRAPH N° A2·1

Test N°	1
Tube Bore	0·1285 inches
Mass Flow	278 lb/sec.ft^2
Momentum	0·0306 lb.sec.

240
235
230
225
220
215
210

°F Fluid Temperature

1
0 Cumulative heat loss B.T.U/lb

Heat loss to environment

50 45 40 35 30 25 20 15 10 5 0

Distance from tube outlet inches

GRAPH Nº A2·2

Test Nº 1

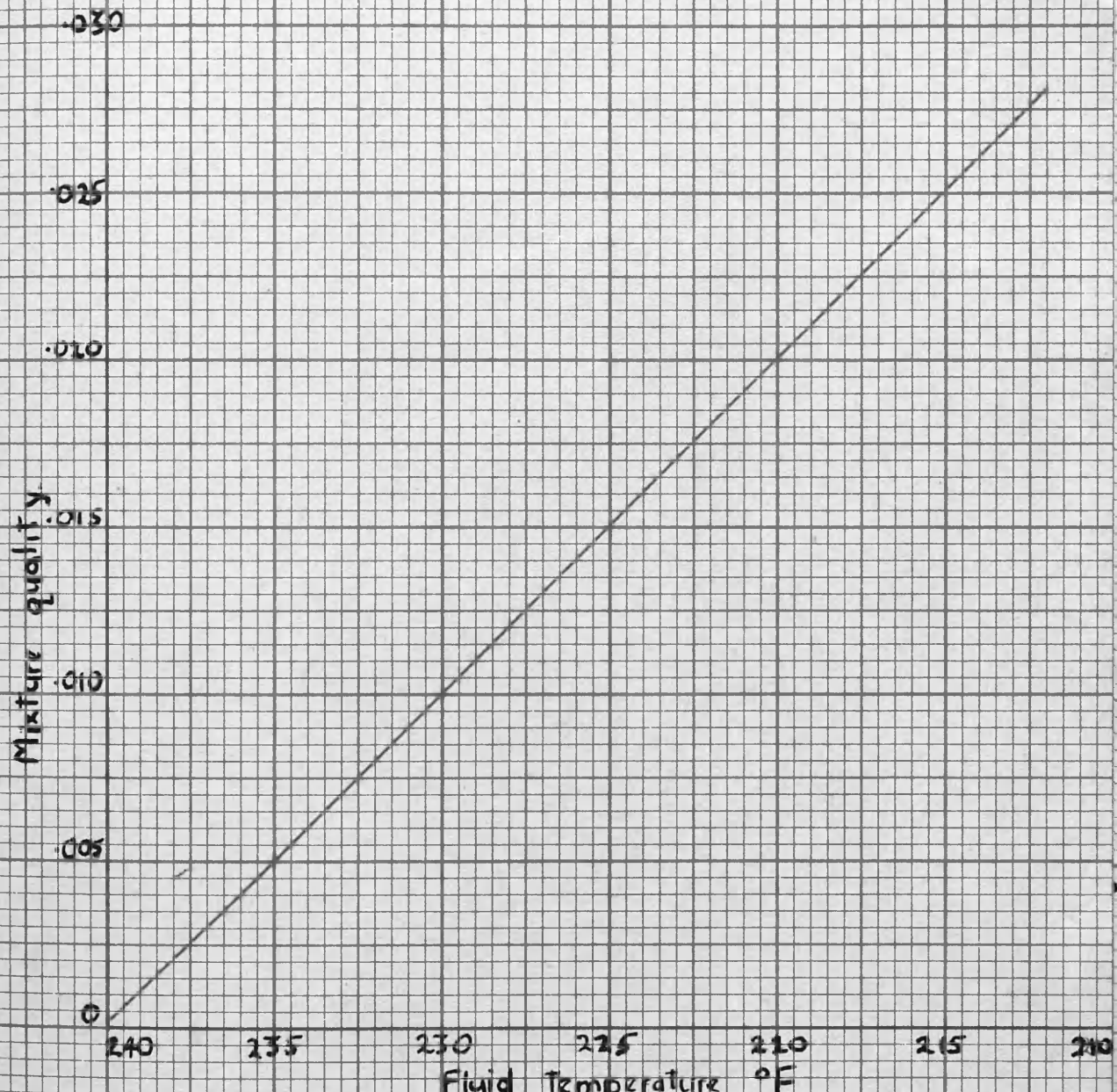

GRAPH A2·2 Mixture quality to a base of fluid temperature for test number 1

GRAPH N° A2-3

Test N°1

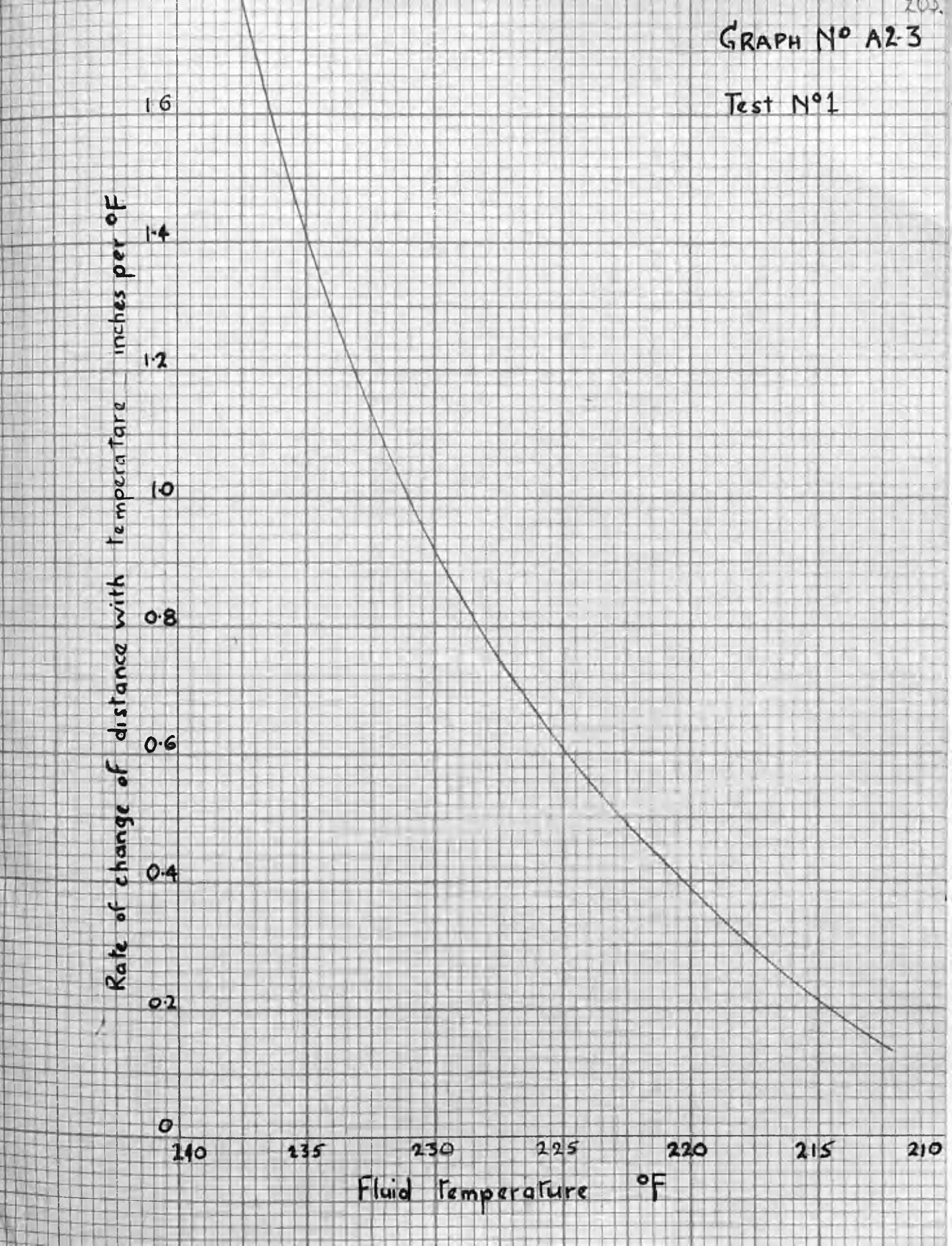

GRAPH Nº A2.4

Test Nº1.

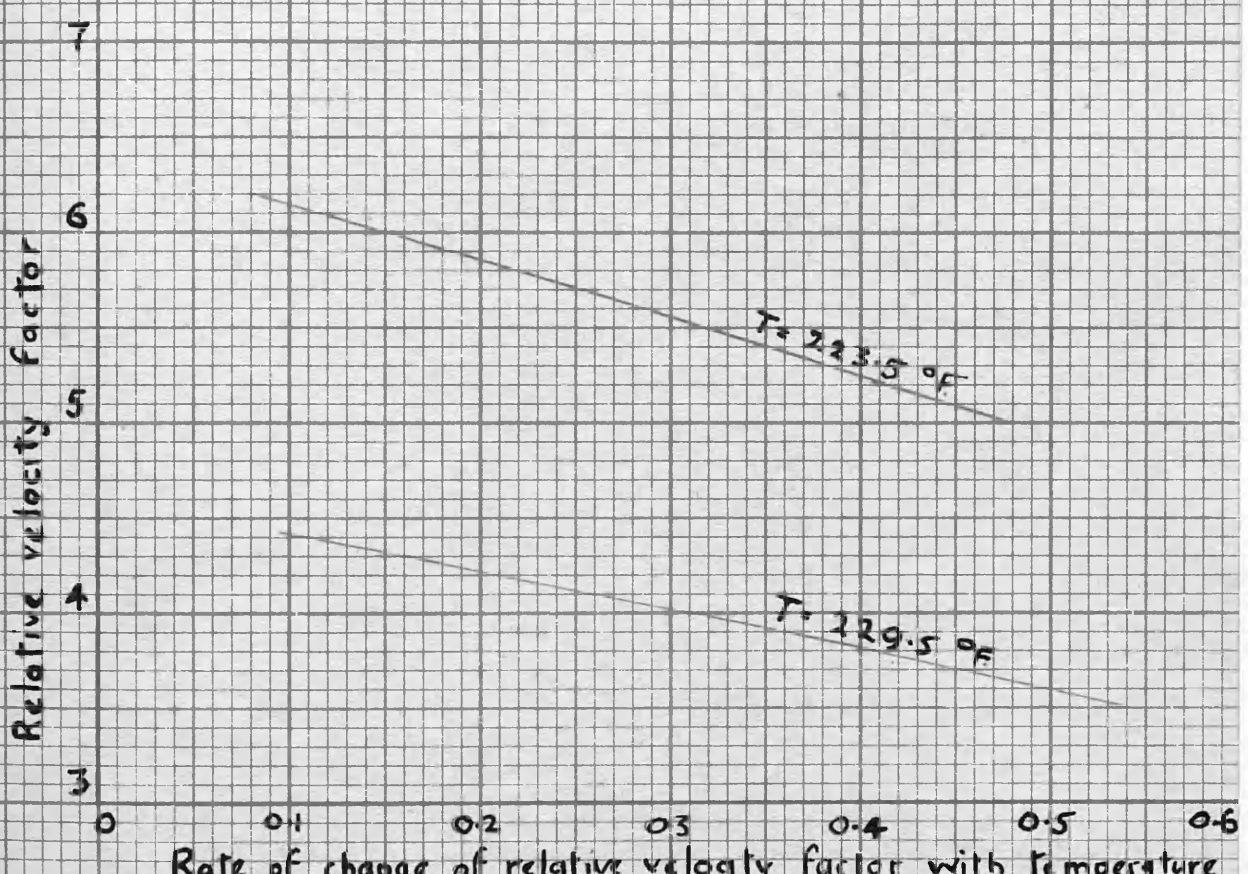

GRAPH A2.4 Compatible values of k and δk.

APPENDIX 3.

Prediction of temperature distribution in the evaporating flow of water, given; mass flow, pipe diameter and initial condition.

The required equations are:

$$\frac{kJ\delta H_s}{n v_2} - \delta p + \left(\frac{W}{A}\right)^2\left(1+\frac{k}{C}\right)\frac{v_1(1-q)}{2g}\left\{2q\left(\frac{k}{n}-1\right)(\delta c+\delta k) + \left(1+\frac{c}{k}\right)\left[\frac{1}{n}(k^2-1) - 2(k-1)\right]\delta q\right\} = 0 \qquad (7)$$

$$n = 1 + \alpha(T_c - T)^2 \qquad (20)$$

where $n = 1.2$ when $T = T_0$

$$\delta F_w = -A\delta p - \frac{W}{g}\left\{(1-q)\delta V_1 + (k-1)V_1\delta q + q\,\delta(kV_1)\right\} \qquad (4)$$

$$V_1 = B\,(1 + c/k) \qquad (1)$$

$$\delta V_1 = B/k^2\,(k\,\delta c - c\,\delta k) \qquad (18)$$

$$\delta(kV_1) = B\,(\delta c + \delta k) \qquad (7a)$$

$$\delta x = \frac{8g\,v_1\,V_1^2}{\lambda\,\pi\,D}\,\delta F_w \qquad (16)$$

$$x\Big]_{T_0}^{T} = \sum_{T=T_0}^{T=T}\left(\frac{\delta x}{\delta T}\right)\delta T \qquad (21)$$

A sample calculation is given in the following pages, the data referring to test 5.

Determination of mixture quality.

This was done as indicated inAppendix 2, the graph of q to T being shown in graph A3.1. A knowledge of the temperature distribution was presumed in assessing the external heat exchange.

Determination of k and δk.

For a given mass flow per unit area, and initial condition, equation (7) enables the calculation of k and δk as functions of temperature. The value of 'k' is relatively independent of δk, this being of convenience to the solution of the equation. By calculating k at adjacent stages for guessed values of δk, a sufficiently exact estimation of δk may be directly obtained.

Table A3.1 shows the calculation for test 5, at the selected temperatures of 219.5°F. The arithmetic is carried through for the guessed δk value of 0.2, and repeated for the corrected value of 0.11. As can be seen, the resulting alteration in k is negligible.

Graph A3.2 shows the solution obtained by plotting

$$-\frac{kJ\delta H_s}{n v_2} - \left(\frac{W}{A}\right)^2\left(1+\frac{k}{c}\right)\frac{v_1(1-q)}{2g}\left\{2q\left(\frac{k}{n}-1\right)(\delta c+\delta k)+\left(1+\frac{c}{k}\right)\left[\frac{1}{n}(k^2-1)-2(k-1)\right]\delta q\right\}$$

against $-\delta p$.

Repeating Table A3.1 for various temperatures the graph of k to a base of T, given in graph 18 was obtained.

From the equation,

$$V_1 = B(1+c/k) \qquad (1)$$

V_1 was calculated and plotted in the same graph.

Equation: $-\delta p = -\frac{k J \delta H_s}{n v_2} - \left(\frac{W}{A}\right)^2 \left(1+\frac{k}{c}\right) \frac{n(1-q)}{2g} \left\{ 2q\left(\frac{k}{n}-1\right)(\delta c+\delta k) + \left(1+\frac{c}{k}\right)\left[\frac{1}{n}(k^2-1)-2(k-1)\right]\delta q \right\}$

or $X = Y - Z$

Test No. 5. W/A = 266 lbs/ft^{2}in. T_c = 235°F. T_o = 212°F.

TABLE A3·1 D = 1285".

T °F.	219.5					
n	1.12					
q	.0153					
δq /°F	.00101					
c	21.65					
δc /°F	1.838					
v_2 ft^3/lb	25.37					
v_1 ft^3/lb	.01676					
$-\delta H_s$ B.T.U/lb°F	.366					
k	4.6	5	5.4	4.6	5	5.4
δk /°F	0.2	0.2	0.2	.11	.11	.11
$-\delta p$ lb/ft^2°F	47.6					
$-\frac{J\delta H_s}{n v_2}$ lb/ft^2°F	10.9					
$-k\frac{J\delta H_s}{n v_2}$ " Y	50.0	54.4	58.9			
$\delta k + \delta c$	2.038	2.038	2.038	1.948	1.948	1.948
$\frac{k}{n}-1$	3.14	3.40	3.82			
$2q(\delta k+\delta c)(\frac{k}{n}-1)$ (a)	.195	.211	.237	.186	.201	.226
$1+c/k$	5.7	5.53	5.01			
$\frac{1}{n}(k^2-1)-2(k-1)$	11	13.2	16.2			
$(1+\frac{c}{k})\left[\frac{1}{n}(k^2-1)-2(k-1)\right]\delta q$ (b)	.163	.072	.083			

(a) + (b)	.358	.358	.320	.249	.275	.309
$v_1(1-q)/2g$	2.5×10^{-4}	2.5×10^{-4}	2.57			
$1 + k/c$	1.212	1.231	1.249			
$(W/A)^2$	7.1×10^{4}	7.1×10^{4}	7.1			
$(W/A)^2(1+k/c)\frac{v_1(1-q)}{2g}$ (c)	22.1	22.3	22.8	22.1	22.3	22.8
$c[a + b]$ Z.	5.71	6.32	7.28	5.5	6.1	7.05
Y − Z $lb/ft^2\,^oF$	44.29	48.1	51.6	44.5	48.3	51.8

Determination of $(\delta F_w/\delta T)$ as a function of temperature.

The required equations are (4), (18), (7c), and are all incorporated in Table A3.2.

$(\delta F_w/\delta T)$ is shown to a base of temperature in graph A3.3.

Table A3.2.

Equations:

$$\delta F_w = -A\delta p - \frac{W}{g}\left\{(1+q)\delta V_1 + (k-1)V_1\delta q + q\,\delta(kV_1)\right. \quad (4)$$

$$\delta V_1 = B/k^2\,(k\,\delta c - c\,\delta k) \quad (18)$$

$$\delta(kV_1) = B\,(\delta c + \delta k). \quad (7e)$$

Test No. 5. $\frac{W}{g}$ = .000745 lbs sec/ft. T_c = 235°F.

T_o = 212°F.

T °F.	235	229.5	225.5	219.5	215.5
q	0	.0052	00924	.0153	.01935
1-q		.9948	.99076	.9847	.98065
δq /°F		.00101	.00101	.00101	.00101
c		6.1	11.63	21.65	29.59
δc /°F		1.183	1.489	1.838	2.107
B ft/sec		4.46	4.44	4.405	4.383
k		4	4.28	4.9	5.4
δk /°F		.10	.10	.11	.13
B/k^2		.279	.242	.183	.151
$k\,\delta c$		4.74	6.36	9.0	11.4
$c\,\delta k$		.61	1.16	2.38	3.35

$k\delta c - c\delta k$			4.15	5.80	6.62	7.55
δV_1	Ft/sec °F.		1.15	1.26	1.21	1.16
V_1			11.2	16.46	23.86	28.38
$\delta c + \delta k$			1.283	1.589	1.948	2.257
$\delta(kV_1)$			5.72	7.04	8.56	9.8
$q(\delta(kV_1)$	(a)	negligible	.0298	.0650	.131	.190
$(k-1)V_1\delta q$	(b)	negligible	.0340	.0546	.094	.126
$(1-q)\delta V_1$	(c)	1.3	1.140	1.219	1.190	1.138
$a+b+c$			1.2038	1.3686	1.415	1.454
$\frac{W}{g}(a+b+c)$	lb/°F	.00097	.000895	.001015	.001055	.001082
$-A\delta p$	lb/°F	00530	.00500	.00469	.00428	.00401
$(\delta F_w/\delta T)$	lb/°F	0043	0041	00367	00522	00293

The Determination of $(\delta x/\delta T)$ and the prediction of the temperature distribution curve.

The equations required for this purpose are:

$$\frac{\delta x}{\delta T} = \frac{\delta F_w}{\delta T} \cdot \frac{8 g v_1}{\lambda \pi D V_1^2} \qquad (16)$$

$$x\Big]_{T_0}^{T} = \sum_{T=T_0}^{T=T} \left(\frac{\delta x}{\delta T}\right) \delta T \qquad (21).$$

The calculation of $(\delta x/\delta T)$ is carried through for test 5 in Table A3.3 and the result plotted to a base of temperature in graph A3.4.

The numerical integration (21) is given in Table A3.4. Graph 22 compares the predicted curve with measured temperatures.

Table A3.3.

Equation: $\frac{\delta x}{\delta T} = \frac{\delta F_w}{\delta T} \cdot \frac{8 g v_1}{\lambda \pi D V_1^2}$ (16)

Test No. 5.

T °F	234	230	226	222	218	214
V_1 ft/sec	5.7	10.7	15.8	20.8	25.5	30
$R_D \times 10^{-3}$	21.4	39.4	56.6	73.5	88.5	102
λ	.028	.0245	.0231	0223	0217	0210
V_1^2	32.5	115	250	433	650	900
v_1 ft³/lb	01688	01684	01682	01679	01676	01673
$v_1/\lambda V_1^2$	.01855	.00598	.00291	.00174	.00119	.000884
$8g/\pi D$	7660					
$\delta F_w/\delta T$ lb/°F	.00425	.004	.00372	.00342	.00316	00288
$\delta x/\delta T$ ft/°F	.605	.184	.083	.0455	.0288	.0195
$\delta x/\delta T$ in/°F	7.26	2.20	.998	.544	.346	.234

Table A3.4

Equation $$x\Big]_{T_0}^{T} = \sum_{T=T_0}^{T=T} \left(\frac{\delta x}{\delta T}\right) \delta T$$

Test No.5. $T_c = 235\ ^{o}F.$ $T_o = 212\ ^{o}F.$

$T\ ^{o}F.$	212	214	216	218	220	222	224	226	228	230	232	233	234
$\Delta T\ F^{o}.$		2	2	2	2	2	2	2	2	2	2	1	1
$\left(\frac{\delta x}{\delta T}\right)_{mean}$ in/^{o}F		.21	.255	.315	.38	.48	.62	.84	1.2	1.75	2.85	4.25	6.0
Δx in.	0	.42	.51	.63	.76	.96	1.24	1.68	2.4	3.5	5.7	4.25	6.0
$\sum \Delta x$ in.	0	.42	.93	1.56	2.32	3.28	4.52	6.20	8.60	12.10	17.8	22.07	28.0

GRAPH Nº A3·1

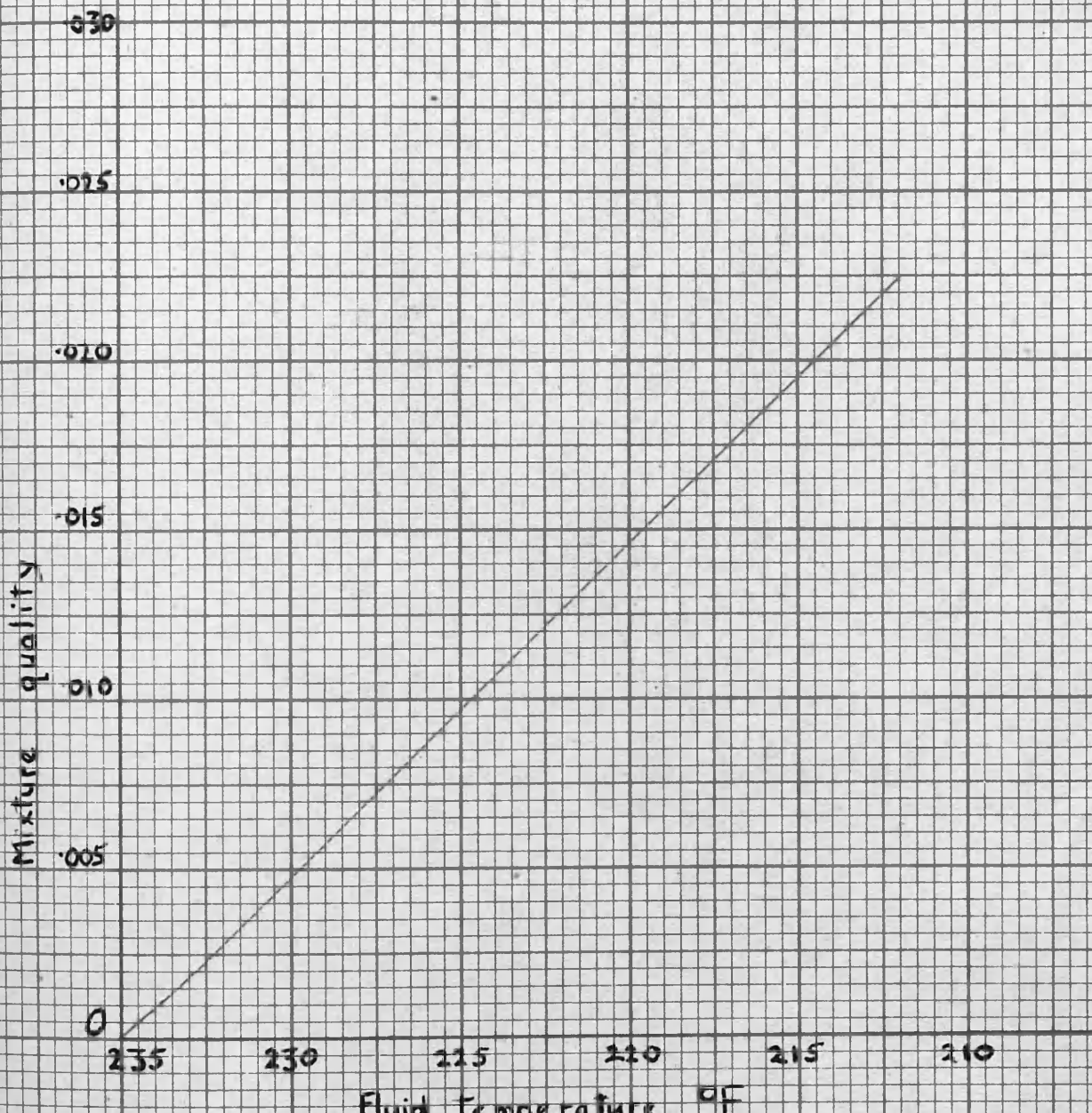

GRAPH A3·1 Mixture quality to a base of fluid temperature for test 5.

GRAPH Nº A3·2

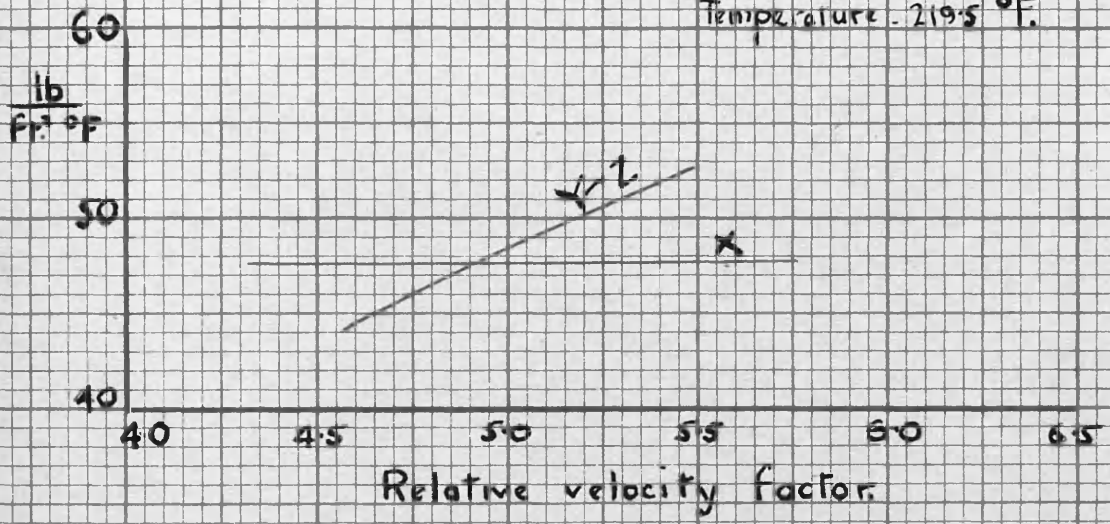

GRAPH A3·2 Graphical solution to equation (7) for test 5. (refer to table A3·1 for calculations)
T = 219·5 °F.

GRAPH N° A3·3

Test N° 5

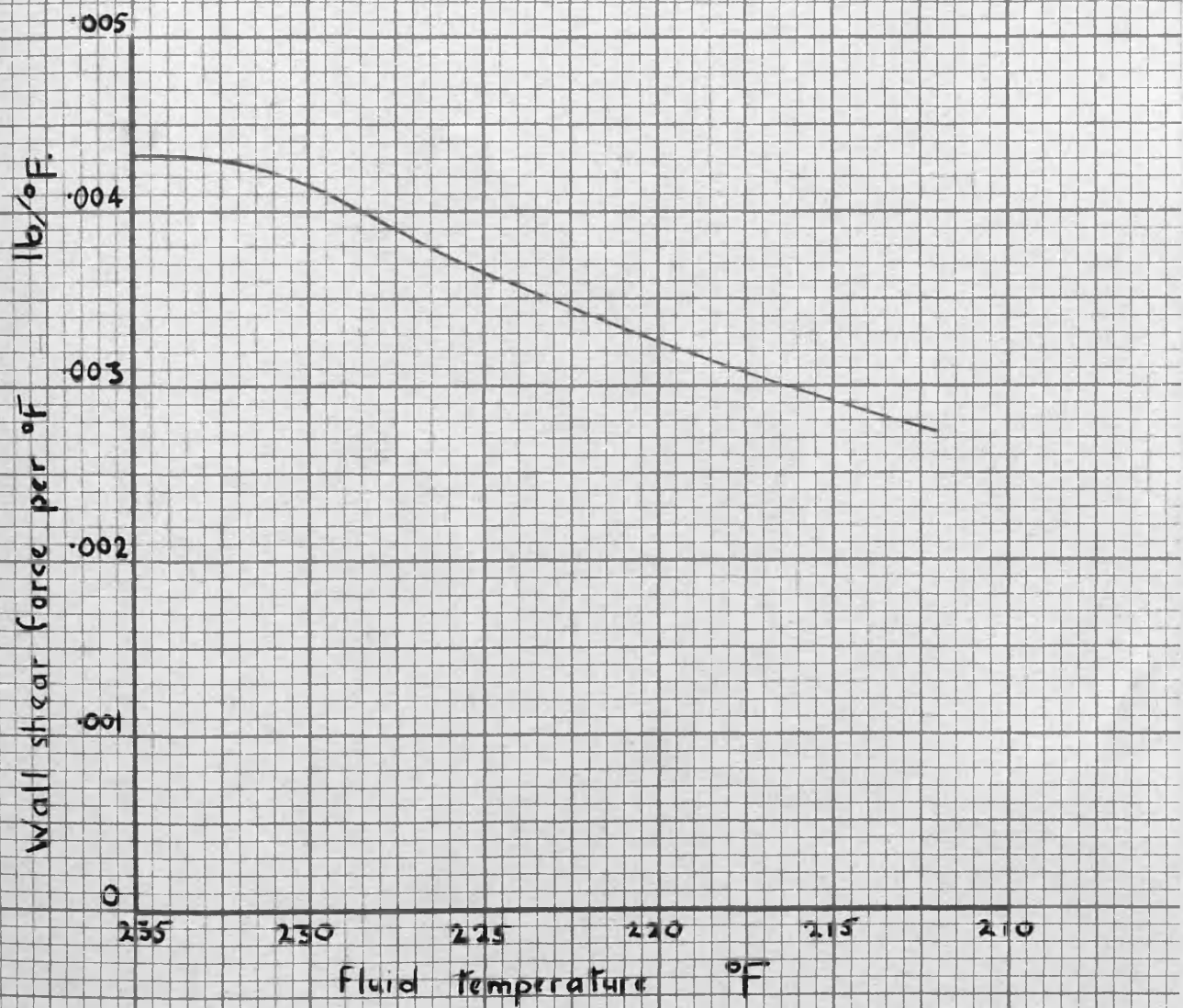

GRAPH A3·3 Wall shear force per °F temperature drop to a base of Temperature

GRAPH Nº A3·4

Test Nº 5.

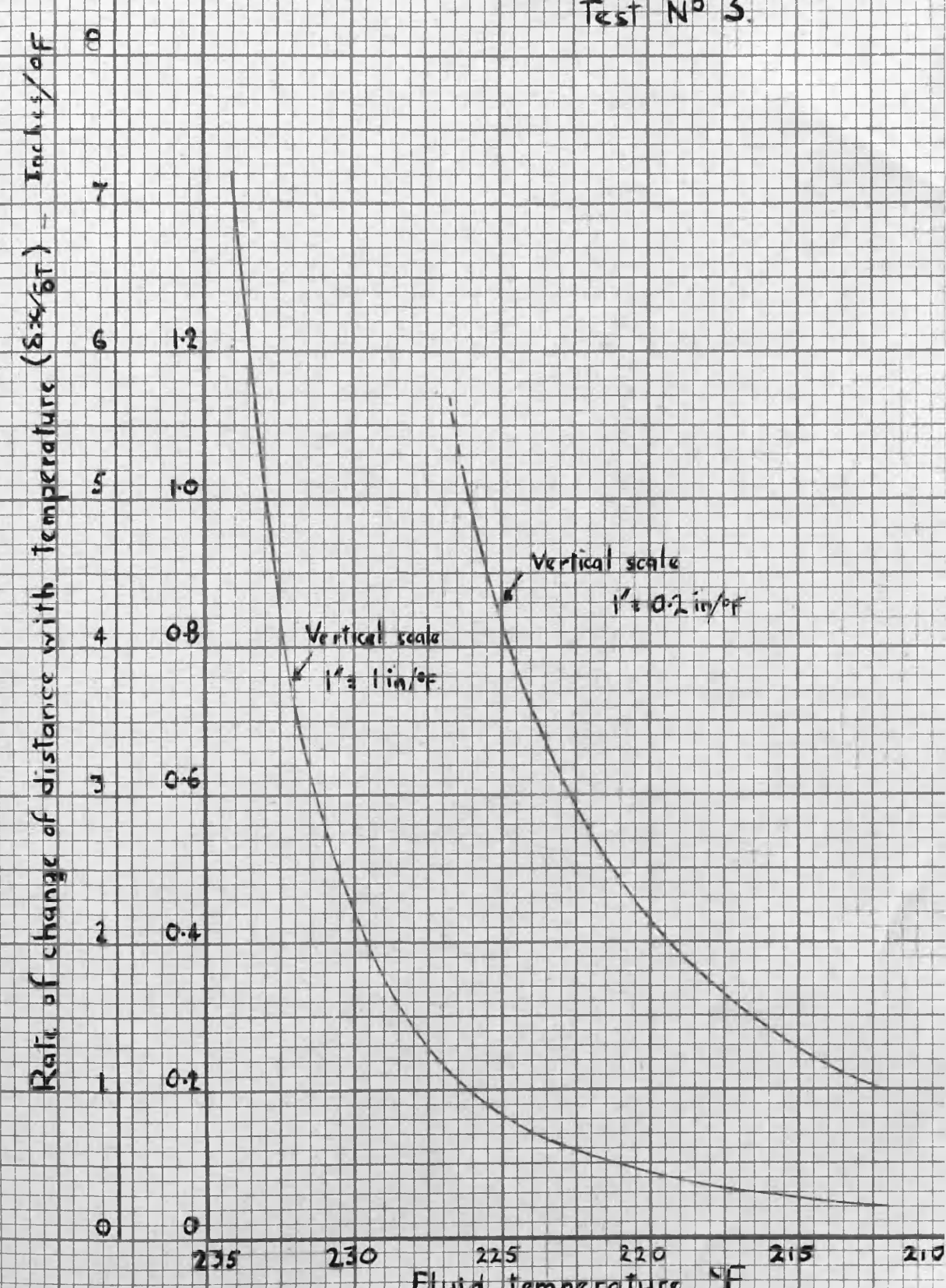

GRAPH A3·4 Rate of change of distance with temperature for a base of temperature

APPENDIX 4.

The relationship between fluid temperature and tube metal temperature.

Figure A4.1, shows an element of tube carrying an evaporating fluid. Heat is supplied by the fluid to the inside wall of the tube and is lost at the outer surface by convection and radiation. Further, since the tube metal temperature changes along its length there is an axial flow of heat where magnitude also varies with length.

Since the heat quantities involved are relatively small, as will be shown, and the conductivity of copper very high, it will be reasonable to assume that the tube metal temperature is constant across any normal section.

Using the nomenclature of Figure A4.1, the steady state heat equation applied to the metal element is:

$$k_m A_m \frac{d^2 T_m}{dx^2} \delta x + \delta Q_F - \delta Q_E = 0 \qquad (A4.1)$$

The effects of environmental heat loss and axial hear flow on the fluid-tube metal temperature relationship will be dealt with separately. This is possible owing to the linear relationship between heat flow and temperature difference.

1. Temperature effects resulting from heat loss to the environment.

The following equations are used:

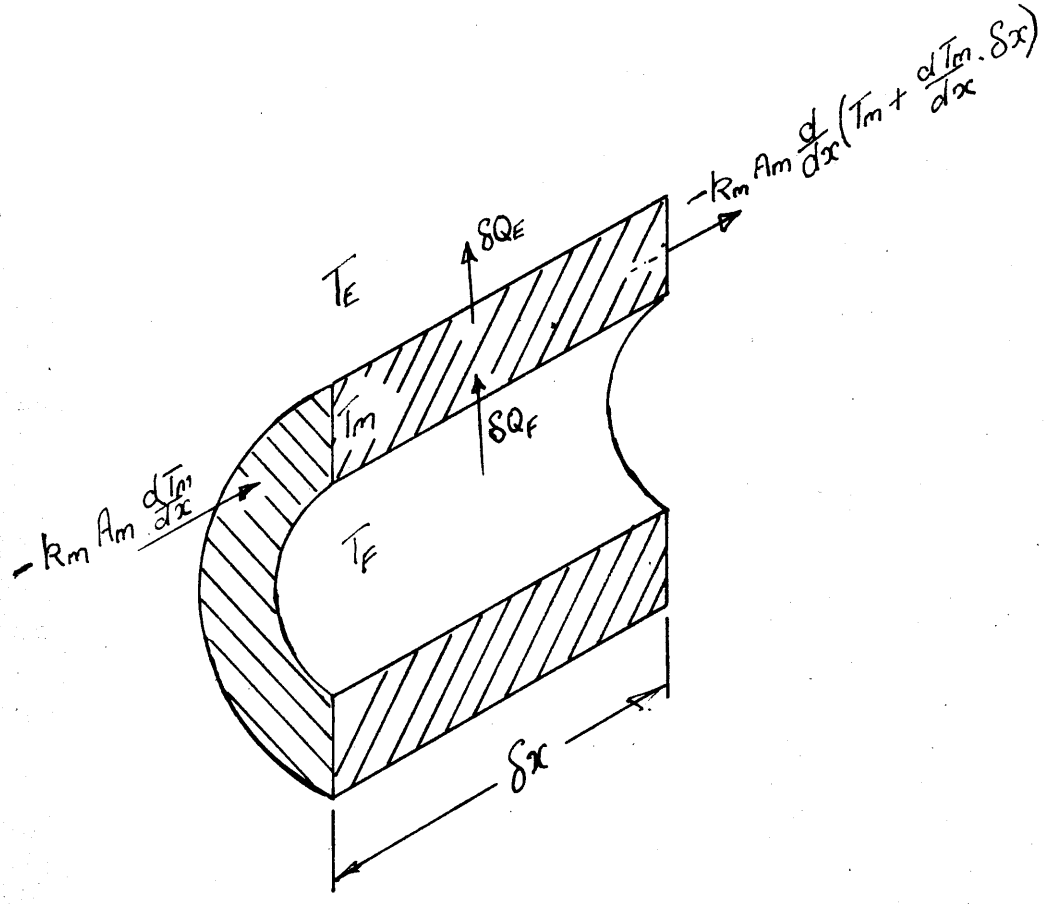
$-K_m A_m \frac{dT_m}{dx}$
T_E
δQ_E
T_m
δQ_F
T_F
$-K_m A_m \frac{d}{dx}\left(T_m + \frac{dT_m}{dx}.\delta x\right)$
δx

FIGURE A4·1

The film conductance between the fluid and the tube by Russelts' formula is

$$h_f = .0225 \frac{k_F}{D_I} (R_D)^{0.8} (P_R)^{0.4} \quad B.T.U./ft^2.sec.^oF \qquad (A4.2)$$

where k_F = fluid conductivity BTU/ft^{2}sec^{o}F.

D_I = internal tube diameter, ft.

The radial conductance of the tube metal referred to the outer surface area is,

$$h_m = \frac{2.41 \times 10^{-4} k_m}{D_o \log (D_o/D_I)} \quad B.T.U./ft^2.sec.^oF \qquad (A4.3)$$

where k_m = metal conductivity

D_o = external tube diameter. ft.

The conductance at the tube-environment interface is influenced by convection and radiation. The convective conductance is,

$$h_c = \frac{5.9 \times 10^{-6} (T_m - T_E)^{0.25}}{D_o^{.25}} \quad B.T.U./ft^2.sec.^oF \qquad (A4.4)$$

The radiant conductance is:

$$h_R = \frac{\sigma F_E F_A (T_m^4 - T_E^4)}{T_M - T_E} \quad B.T.U./ft^2.sec.^oF \qquad (A4.5)$$

where, σ = Stefan - Boltzmann constant = $.483 \times 10^{-12}$ BTU/ft^{2}sec

F_E = a factor dependent on the emmissivity of the tube surface.

F_A = the configuration factor.

A typical set of conditions relative to the water tests are as follows:

D_I = .1285"; D_o = .198"; V_1 = 7ft/sec; T_M = 230^{o}F; T_E = 60^{o}F.

(The velocity of the liquid phase in a typical expansion increases from about 7 ft/sec. to about 30 ft/sec.).

Substituting these values in the foregoing equations

and referring conductances to the outer surface area of the tube;

h_F = 0.65 BTU/ft^{2}sec$^\circ$F.

h_m = 15 BTU/ft^{2}sec$^\circ$F.

h_c = .0007 BTU/ft^{2}sec$^\circ$F.

h_R = .000044 BTU/ft^{2}sec$^\circ$F.

Thus the ratio of conductances fluid-to-tube and tube-to-environment is 880 under these conditions and for an average overall temperature drop of 170°F. the outer surface of the tube is approximately 0.2°F. below fluid temperature due to heat loss to the atmosphere. At the higher velocities this figure is even less.

2. Temperature effects resulting from the axial heat flow.

The heat supplied by the fluid to compensate for change in the magnitude of axial heat flow over an elementary length δx, is given by

$$\delta Q_A = - k_m A_m \frac{d^2 T_m}{dx^2} \delta x \qquad (A4\cdot6)$$

The temperature drop from the fluid to the tube associated with this heat flow is:

$$T_F - T_M = \frac{\delta Q_A}{h_F \pi D_I \delta x} = - \frac{k_m (D_o^2 - D_I^2) \frac{d^2 T_m}{dx^2}}{4 D_I h_F} \qquad (A4\cdot7)$$

If (d^2T_m/dx^2) is calculated in $^\circ$F/in^2 units, (A4·7) applied to the water tests is approximately given by:

$$T_F - T_M = - \frac{1}{20} d^2T_m/dx^2 \ ^\circ F \qquad (A4\cdot8)$$

Graph A4.1 shows d^2T_m/dx^2 to a base of tube distance for test 1, whilst the following table indicates the magnitude of the temperature effect due to axial heat flow, showing it to be negligibly small.

Test 1. $T_c = 240.5^\circ F$ $T_o = 212^\circ F$.

Distance from tube outlet - inches.	10	2	1	0.5
$T_F - T_m$ $^\circ F$.	.04	.03	.07	.10

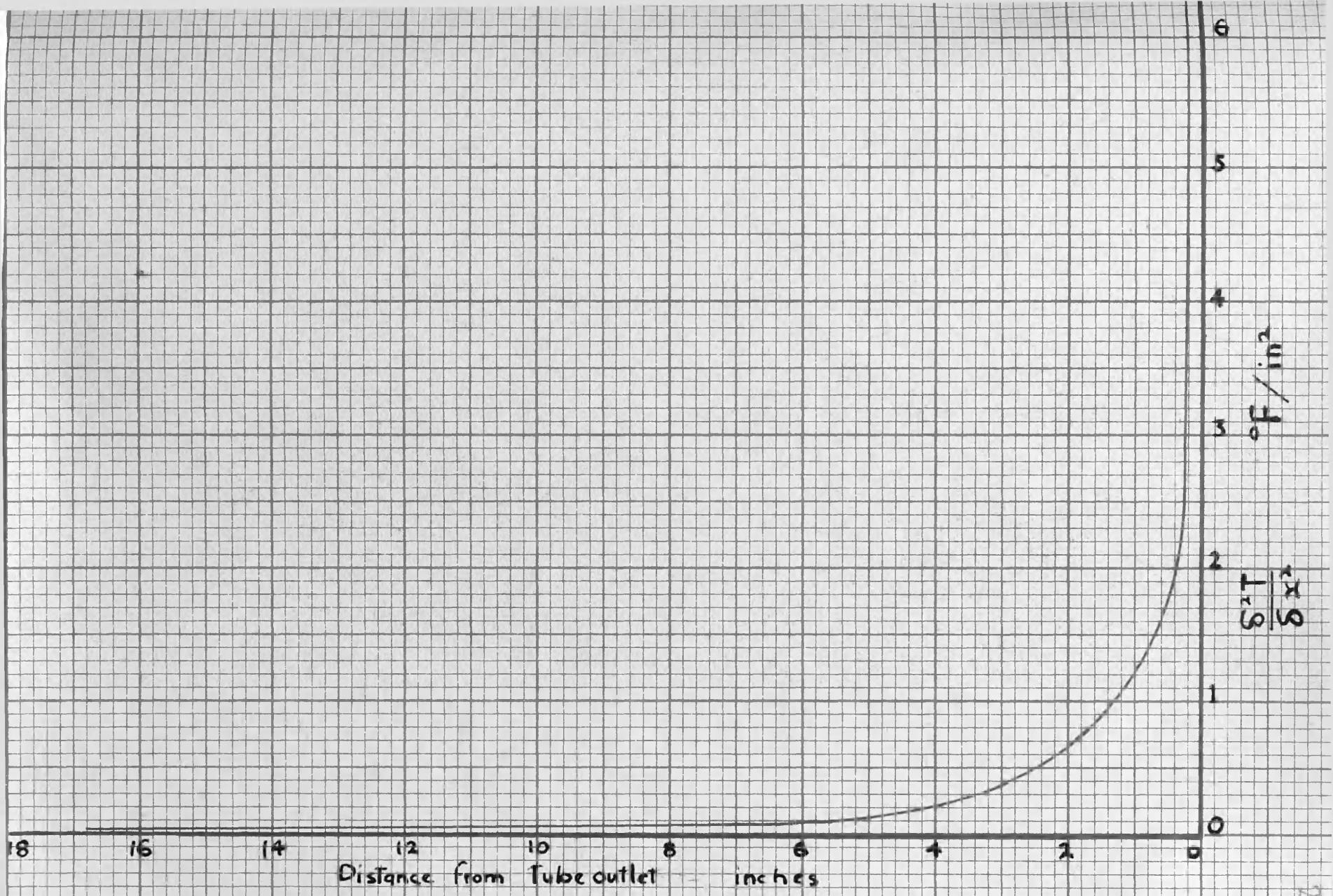

GRAPH A4-1 Second derivative of temperature variation with Tube distance, for Test 1.

APPENDIX 5.

Calculation of Critical Outlet Chart for Water.

In the text, the criterion for critical outlet condition is given as that stage in the expansion at which the roots of equation (7) just become imaginary; that is, at the stage where the two positive roots in k are co-incident.

It is more convenient, in constructing a chart, to find the critical outlet condition and quality, thereby specifying all the thermodynamic quantities, and to calculate the mass flow corresponding to the critical condition. For any arbitary value of k there are two possible values of $\left(\frac{W}{A}\right)$, the required value being that at which these are coincident. This is equivalent to the statement that the critical mass flow for a given outlet condition must satisfy the equation:

$$\left(\frac{\partial\left(\frac{W}{A}\right)}{\partial k}\right)_T = 0 \qquad (A5.1)$$

By fixing outlet temperature or pressure, and mixture quality, the unknown quantities in equation (7) reduce to $\frac{W}{A}$, k, $\frac{\delta k}{\delta T}$, and if the last can be determined the critical mass flow can be found by calculating $\frac{W}{A}$ for a few selected values of k.

Since the exact determination of δk makes the arithmetical work very unwieldy, the following approximation was adopted, $\delta k = \frac{k_o - 2}{T_o - T_c}$ this being based on a number of calculations for δk over the required range.

Now, δk occurs in equation (7) in the factor $(1 + \delta k/\delta c)$, and for water in the range considered $\delta k/\delta c$ has a

value which varies from about 0.1 to about 0.2. As a consequence, the rather inexact approximation quoted above for δk, is sufficiently accurate in terms of the factor $(1 + \delta k/\delta c$

The above procedure enables the construction of a chart in which the variable are W/A, T_o and q_o. This may be readily transformed to one in which the variable are $\frac{W}{A}$, T_c and T_o as given in Figure 19, or $\frac{W}{A}$, p_c and p_o as given in Figure 20.

Although the chart refers to adiabatic expansion, small amounts of heat exchange with the environment may be conveniently taken into account by calculating a fictitious initial condition giving the same outlet quality as the actual expansion. This procedure assumes that δq at outlet remains unaltered which must in most cases be nearly so, since the change of temperature with tube distance is at its greatest value at the pipe outlet. The applicability of the theory to expansions involving high rates of heat exchange has not yet received experimental investigation.

APPENDIX 6.

To show that there are two and only two values of relative velocity factor which satisfy the conditions of evaporating flow with relative velocity.

Expanding equation (7) and putting

$$\left(\frac{W}{A}\right)^2 \frac{v_1(1-q)}{2g} = \alpha \; ; \quad 2q(\delta c + \delta k) = \beta \; ; \quad n = 1.$$

(making n = 1 slightly simplified the working and in no way affects the validity of the conclusions.)

The following expression is obtained.

$$(\delta q/c)k^4 + \left[2\delta q(1-1/c) + \beta/c\right]k^3$$
$$+ \left[J\delta H_s/\alpha v_2 + \beta(1-1/c) + (c+1/c-4)\delta q\right]k^2$$
$$+ \left[2\delta q[1-c) - \beta - \delta p/\alpha\right]k + c\,\delta q = 0 \qquad (A6.1)$$

It may be found by inspection that the signs of coefficients are:

k^4 positive,

k^3 positive (provided $C < 1$),

k^2 Positive or negative,

k^1 positive or negative,

k^0 positive,

In the bi-quadratic equation (A6.1) there must be either two changes in sign or none. By Descartes' rule of signs it follows that there must be two positive real roots of the equation or none.

The number of variations in sign of $f(-k)$

is either two or four, indicating that there may be four, two or no real negative roots.

In physical terms this means that there are two and only two values of k or alternatively no values of k which satisfy the conditions of evaporating flow in pipes.

APPENDIX 7.

To show that there is an instantaneous change in the rate of pressure and temperature change with distance at the commencement of evaporation.

The liquid velocity at any stage in the flow may be written as,

$$V_1 = B(1 + c/k)$$
$$= \frac{W}{A}\left[(1-q)v_1 + \frac{1}{k} \cdot q v_2\right]$$

Assuming that k has a fixed value near to the section at which evaporation commences, and differentiating,

$$dV_1 = \frac{W}{A}\left[(1-q)dv_1 - v_1 dq + \frac{1}{k} \cdot q dv_2 + \frac{1}{k} v_2 dq\right]$$

At the commencement of evaporation $q = 0$, and noting that v_1 and dv_1, are negligibly small terms relative to v_2, and dq,

$$\left[dV_1\right]_c = \frac{W}{A} \cdot \frac{v_2 dq}{k}$$

Since there is a fluid acceleration at the instant of evaporation there must be an instantaneous change in the slope of the pressure distribution curve, and since temperature is a continuous function of pressure there must also be a change of slope of the temperature curve.

APPENDIX 8.

The Calculations of a Critical Outlet Chart for Freon 12.

In this Appendix a brief outline is given of the method adopted in constructing a chart, shown in Figure 30, which relates initial evaporation temperature, critical outlet temperature and critical mass flow per unit area for the adiabatic flow of evaporating freon 12 in horizontal tubes. The flow form is assumed to be of the frothing type.

The basic equation expressing the critical outlet relationships is:

$$\left(\frac{W}{A}\right)^2 = -g\left(\frac{dp}{dv}\right)_{\phi} \qquad (13).$$

It is convenient to express dv_{ϕ} in terms of q, v_1, and v_2 for a given temperature and accordingly, as a first step, a chart was made relating T_o, q_o, and $\frac{W}{A}$ at the critical condition.

$$v = (1-q)v_1 + q v_2$$

$$dv_{\phi} = (1-q)dv_1 - v_1 dq_{\phi} + q\, dv_2 + v_2 dq_{\phi}$$

With the exception of dq_{ϕ}, the above variables may be calculated directly from the tables.

Calculations of dq_{ϕ}

$$\phi = \phi_1 + q(\phi_2 - \phi_1)$$

$$d\phi = d\phi_1 + q\,d(\phi_2 - \phi_1) + (\phi_2 - \phi_1)dq = 0$$

for a constant entropy change.

Hence,

$$dq_{\phi} = -\frac{[d\phi_1 + q\,d(\phi_2 - \phi_1)]}{\phi_2 - \phi_1}$$

The above equations were used to calculate the critical mass flow for outlet qualities of 0.1, 0.2, 0.3 and 0.4, at outlet temperatures of 10, 20, 30, 40, 50°F., the resulting chart being shown in Figure 31.

This latter chart was converted to the more convenient form shown in Figure 30, by means of a third chart relating T_c, T_o, and q_o.

In calculating the conversion chart relating T_c, T_o, q_o, the approximate equation,

$$q = \frac{q_\phi + q_H}{2}$$

was used. The error involved in this approximation is dependent on the mass flow as shown in Figure 32, and a formula for a maximum limit of error is given in Appendix 1.

APPENDIX 9.

The calculation of friction factors for evaporating freon 12 flowing in small bore tubes.

The equations required are:-

$$\lambda = \frac{8 \delta F_w g v}{V^2 \pi D \delta x} \qquad (A9.1)$$

$$v = v_1 + q(v_2 - v_1) \qquad (A9.2)$$

$$V = \frac{W}{A}(v) \qquad (10)$$

$$q = \frac{q_\phi + q_H}{2} \qquad (22)$$

$$-\delta F_w - A \delta p - \frac{W}{g} \delta V = 0 \qquad (12).$$

A sample calculation is provided in the following pages, for test number 16. The experimental data for this test are given in graph 26. Thermodynamic data for freon 12 were obtained from the tables compiled by Buffington and Gilkey.

The calculation of mixture quality.

It is necessary to consider first the effects of heat exchange between the freon and the environment on mixture quality. The capillary tube, of 0.12" outside diameter, is housed in a copper pipe of $2\frac{1}{2}$" diameter, the pipe being filled with dehydrated nitrogen under a slight pressure. The heat loss from the fluid due to convection, radiation and conduction under these conditions is given for Test 1, by,

$$\delta Q = 7 \times 10^{-4} (T_F - T_E)^{1.25} + 7 \times 10^{-4} (T_F - T_E) + 8 \times 10^{-14} (T_F^4 - T_E^4) \quad \frac{B.T.U.}{lb.\ ft.\ sec.}$$

where,

δQ = Heat loss in BTU per ft. length pipe per lb. of fluid.

T_F = Fluid temperature ^oF.

T_E = Environmental temperature ^oF.

The influence of this heat exchange on mixture quality is small being, less than 1% over the greater range of expansion and reducing to about 0.1% at the outlet. The overall accuracy of the experiments is expected to be about $\pm 5\%$ and the accuracy of the freon tables, whilst not known definitely is probably not as good as $\pm 2\%$. It was accordingly considered that the effects of heat exchange on mixture quality might be neglected.

Graph A9.1 shows quality and percentage error due to neglect of heat exchange to a base of temperature.

The determination of rate of change of tube distance with fluid temperature.

The procedure adopted is described in Appendix 2. Quantities which increase as expansion procedes are made to have a positive rate of change. Graph A9.2 shows the curve of to a base of temperature.

The calculation of velocity and acceleration as functions of temperature.

Table A9.1 and graph A9.3 give calculations and curves for fluid velocity and acceleration with respect to temperature.

Table A9.1.

Equations: $$v = v_1 + q(v_2 - v_1) \qquad (A\ 9.2)$$

$$V = \left(\frac{W}{A}\right) v \qquad (10)$$

Test No. 16.

$$\left(\frac{W}{A}\right) = 450 \text{ lb/ft}^2\text{.sec.}$$

T °F	$v_2 - v_1$ ft³/lb	q	$q(v_2 - v_1)$ ft³/lb	v_1 ft³/lb	v ft³/lb	V ft/sec	ΔV ft/sec.2°F	$\frac{\delta V}{\delta T}$ ft/sec.°F	T_m °F
80	.412	.0177	.00778	.0123	.02008	9.04			
78	.486	.025	.01065	.0123	.02295	10.30	1.26	.63	79
70	.481	.055	.0264	.0121	.0385	17.32			
68	.496	.062	.0308	.0121	.0429	19.30	1.98	.99	69
60	.563	.090	.0507	.0119	.0626	28.20			
58	.581	.0965	.0561	.0119	.0680	30.60	2.40	1.20	59
50	.661	.123	.0814	.0117	.0931	41.9			
48	.683	.130	.0887	.0117	.1004	45.2	3.3	1.65	49
40	.780	.153	.1192	.0116	.1308	58.7			
38	.807	.159	.1285	.0116	.1401	63.1	4.4	2.2	39
30	.927	.183	.1698	.0115	.1813	81.6			
28	.961	.1885	.1815	.0115	.1930	87.0	5.4	2.7	29

The Calculation of Friction Factors.

In Table A9.2, the calculation of friction factors is carried through for test 16. The results are plotted along with those for other tests in graph 41.

Table A9.2.

Equations:

$$\frac{\delta F_w}{\delta T} = -A\frac{\delta p}{\delta T} - \frac{W}{g}\cdot\frac{\delta V}{\delta T} \qquad (12).$$

$$\lambda = \frac{8g\sigma}{\pi D V^2}\cdot\frac{\delta F_w}{\delta T}\,\frac{\delta T}{\delta x} \qquad (A9\cdot1).$$

Test No. 16.

$\frac{W}{A} = 450$ lb/ft² sec. $\qquad D = .060''$

T_{mn} °F	δT °F	δp lb/ft².2°F	$A\delta p$ lb/2°F.	δV ft/sec.2°F	$\frac{W}{g}\cdot\delta V$ lb/2°F.	δF_w. lb/2°F.	δx ft/2°F	V ft/sec.	λ
79	-2	416	.00814	1.25	.000342	.00780	.726	10.0	.0390
69		386	.00728	1.80	.000494	.00679	.379	18.3	.0365
59		333	.00651	2.45	.000672	.00584	.204	29.6	.0350
49		294	.00575	3.30	.000905	.00484	.118	43.5	.0340
39		259	.00507	4.30	.001180	.00389	.0716	61.2	.0322
29		226	.00442	5.40	.001480	.00294	.0417	84.2	.0302

GRAPH Nº A9·1

Test Nº 16

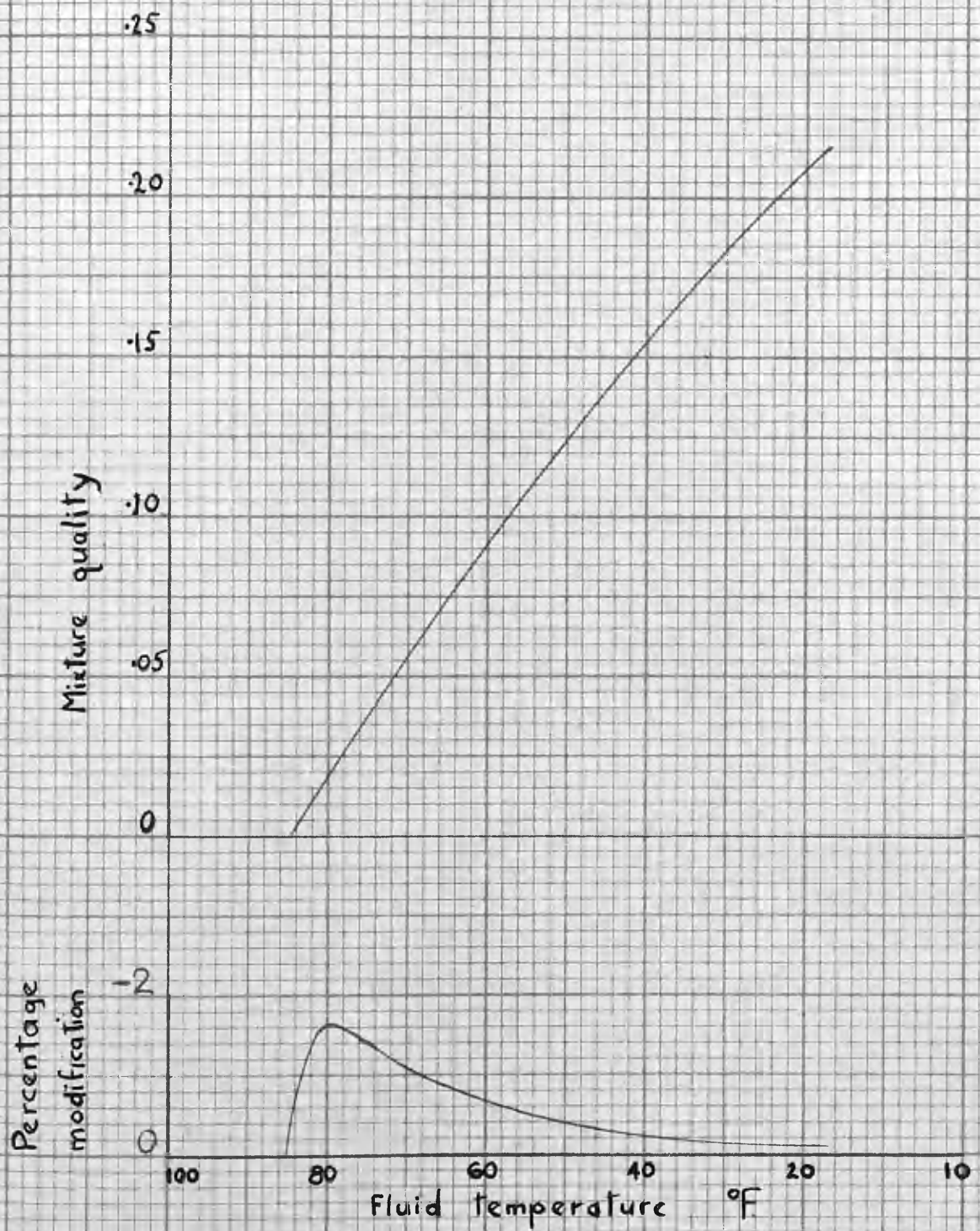

GRAPH A9·1 Mixture quality and percentage modification required to include effects of heat exchange to a base of fluid temperature.

GRAPH N° A9·2

Test N° 16.

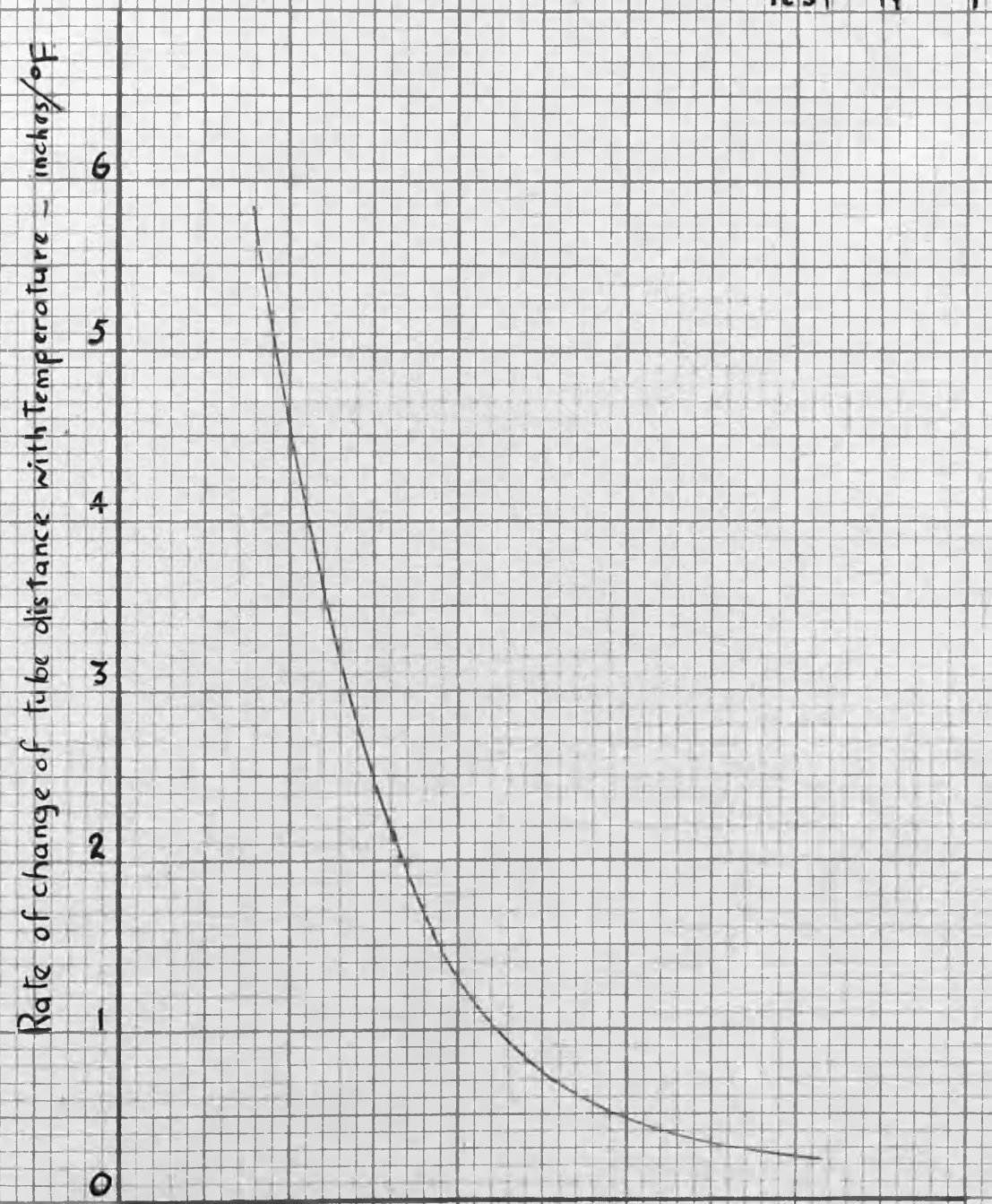

GRAPH A9·2 Rate of change of tube distance with temperature to a base of fluid temperature.

GRAPH Nº A9·3

Test Nº 16

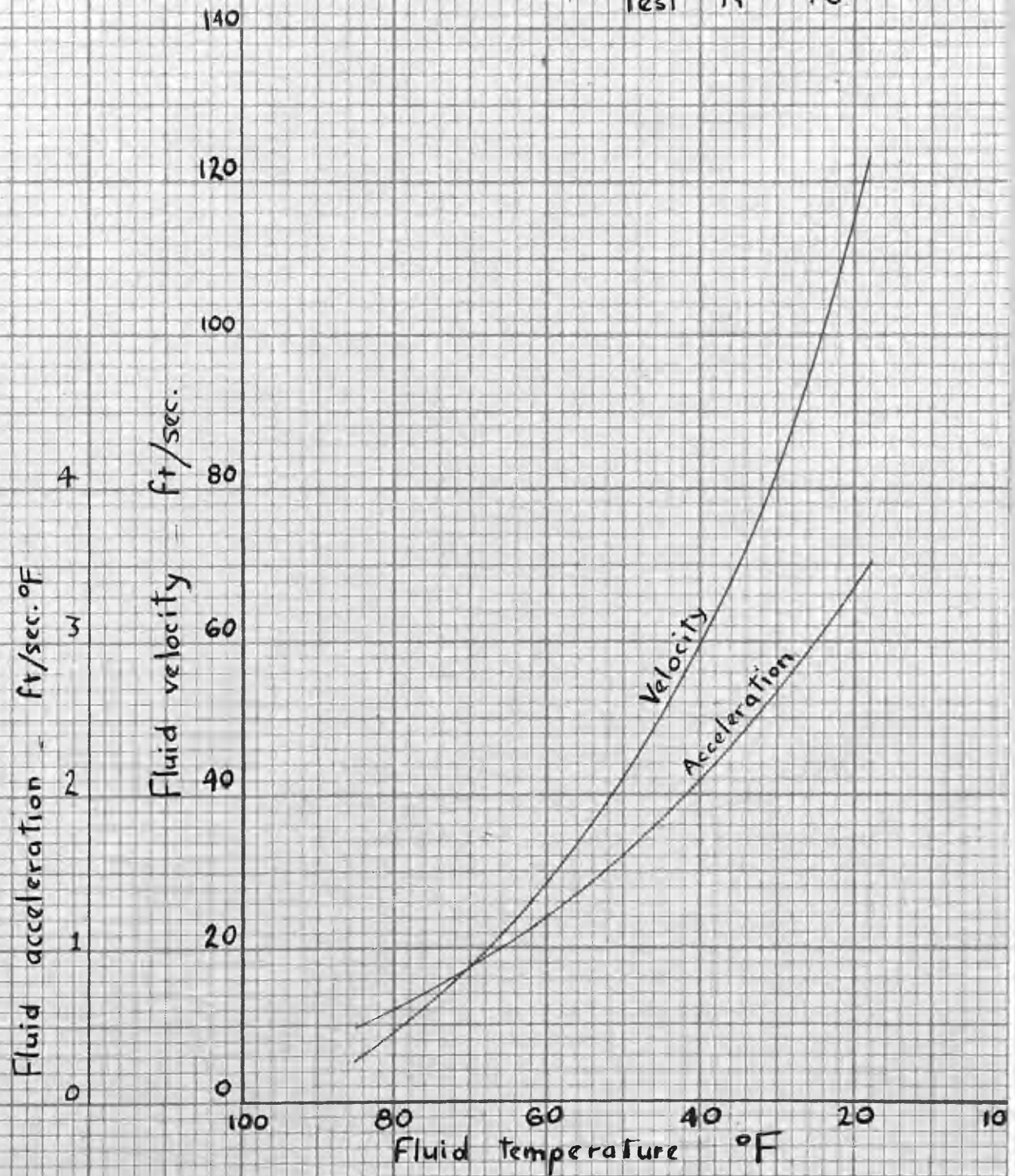

GRAPH A9·3 Fluid velocity and acceleration to a base of fluid Temperature.